Cold Spray Deposition of WC-Co Cermets

Miguel Pereira de Magalhaes e Couto

CIÈNCIA I TECNOLOGIA DELS MATERIALS

Cold Spray Deposition of WC-Co Cermets

by

Miguel Pereira de Magalhães e Couto

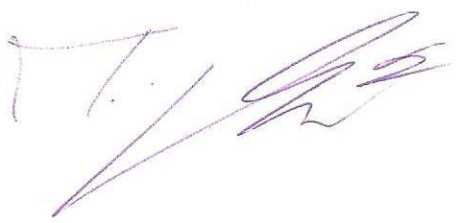

Dr. Sergi Dosta

Centre de Projecció Tèrmica, Universitat de Barcelona, C/Martí i Franquès, 1 08028, Barcelona

INDEX

LIST OF TABLES

List of Figures

ACKNOWLEDGEMENTS

I would like to thank Dr. Sergi Dosta for his expertise, guidelines and support in the development of this Thesis. I want to express my complete gratitude to Prof. Josep Maria Guilemany and the *Centre de Projecció Tèrmica* for these three years of scholarship and providing me this chance. Special thanks also go to the EU Manunet project "Intelligent Production Systems for Nano Coatings Through Thermal Spray" with reference number RDNETll-2-000101. I would also like to thank Dra. Irene García-Cano, Dr. Amadeu Concustell, Dra. Núria Cinca and Dr. Marc Torrell for sharing with me their know-how in thermal spray processes. I also feel obliged to thank all my colleagues that accompanied and helped me in all these years of Thesis: Dr. Marc Gardon, Victor Gómez, Victor Crespo and all the others who walked along with me.

0 MOTIVATION

Firstly, the main objective of this research work was to provide a new deposition method to obtain WC-Co cermets. This new technology produced new coatings without any decomposition of the initial powder's microstructure and thus improvement of the present WC-Co applications in the large industry.

Spraying of wear-resistant WC-Co cermets has always been one of the main applications of conventional thermal spraying techniques such as High-Velocity Oxy-Fuel (HVOF). The demands of industry in terms of production and the constant need and search for better mechanical and electrochemical properties lead to the main objective and motivation of this Thesis: producing better and new WC-Co coatings onto several substrates using a novel deposition technique, Cold Gas Spray (CGS).

The fact that before the publication of the first paper that was born out of this research work no one had previously successfully deposited such material by CGS was also one of the main motivation points. For this reason the reader will find, among the integrity of the document, research papers that were published during these years of doctoral program and accomplish the main objectives of this Thesis entitled "Cold Spray Deposition of WC-Co cermets".

1 SUMMARY

The main subject of this Thesis is the production of hard, wear and corrosion resistant cermets tungsten carbide and cobalt cermets (WC-Co) with different contents in cobalt matrix, onto low carbon steels and aluminum alloy Al7075-T6 substrates, by means of Cold Gas Spray (CGS). The current state of the art for the deposition of WC-Co uses High Velocity Oxy-Fuel (HVOF) as the main technique. Understanding both techniques was also one of the keys points in this work.

A deep theoretical approach about the CGS process, in which no melting of the particles occurs, was made at first to gain a better comprehension about the behaviour of the powder particles when sprayed onto different substrates and therefore being able to produce good quality coatings.

The starting purpose of this doctoral Thesis was to produce WC-25, 17 and 12%Co coatings onto low carbon steel and Al7075-T6 substrates. Until the day, using nitrogen as the process gas, such coatings could not be produced with enough adhesion, thickness and wear and corrosion properties. These are the main characteristics sought by the industry in these coatings. In the end of this doctorate WC-Co coatings were obtained with excellent mechanical and electrochemical properties, adhesion to both low carbon steel and Al7075-T6 substrates. Besides, these properties were increased and improved when compared to the same WC-Co coatings obtained by HVOF conventional deposition technique.

Initial problems such as flowability of the powders, bad adherence to the substrate, poor coating quality and extremely low deposition efficiencies were resolved during the period of the Thesis.

Also, and taking advantage of the novel coatings and excellent properties obtained using the referred feedstock powders and substrates, the knowledge was transferred to the industry as a trade secret.

The following lists the Thesis corresponding publications, congress presentations and trade secrets.

1.1 Publications:

[1P] S. Dosta, M. Couto, J.M. Guilemany, "Cold spray deposition of a WC-25Co cermet onto Al7075-T6 and carbon steel substrates", *Acta Materialia* (2013)

[2P] M. Couto, S. Dosta, M. Torrell, J. Fernández, J.M. Guilemany, "Cold spray deposition of WC–17 and 12Co cermets onto aluminum", *Surface & Coatings Technology* (2013)

[3P] M. Couto, S. Dosta, M. Torrell, J. Fernández, J.M. Guilemany, "Comparison of the mechanical and electrochemical properties of WC-25Co coatings obtained by high-velocity oxy-fuel and cold gas spraying", *Journal of Thermal Spray Technology* (2014)

[4P] M. Couto, S. Dosta, J.M. Guilemany, "Comparison of the mechanical and electrochemical properties of WC-17 and 12Co coatings onto Al7075-T6 obtained by high velocity oxy-fuel and cold gas spraying", *Surface & Coatings Technology* (2014)

1.2 Congresses:

[1C] M. Couto, "Cold Spray deposition of a WC-25Co cermet onto Al7075-T6 and carbon steel substrates", *XII Congreso Nacional de Materiales – IBEROMAT XII* (2012), Oral presentation

[2C] M. Couto, “Cold Spray deposition of a WC-25Co cermet onto Al7075-T6 and carbon steel substrates”, *International Thermal Spray Conference* (2014), Oral presentation

[3C] M. Couto, “Cold Spray deposition of a WC-25Co cermet onto Al7075-T6 and carbon steel substrates”, *Young Professionals ITSC 2014* (2014), Invited oral presentation

[4C] M. Couto, “Obtención de recubrimientos de cermets de WC-Co por Cold Gas Spraying”, *XIII Congreso Nacional de Materiales* (2014), Oral presentation

1.3 Trade secrets:

[1T] M. Couto, S. Dosta, J. Putzier, I. G. Cano, J. M. Guilemany, “WC-25/17/12Co cermet coatings obtained by Cold Gas Spray”, Protected technology: 10th of July 2014. Protocol number: 922

2 THESIS SCHEDULE AND OBJECTIVES

The main goal of this Thesis was to successfully produce WC-25, 17 and 12Co cermets onto two different substrates by Cold Gas Spray using nitrogen as a process gas and compare their mechanical, tribological and electrochemical properties with the same cermets produced by HVOF. A secondary goal was to increase their properties using the novel CGS technique and therefore apply the knowledge to real life applications, especially in wear and corrosion resistant parts to help increase their life at work. The third goal was to generate enough knowledge and to transfer it to the industry. To accomplish these goals, the following key points were achieved:

- Understanding the state-of-the art of WC-Co coatings obtained by Cold Gas Spray and High Velocity Oxy-Fuel, the processes' advantages and limitations, and determine new opportunities for producing WC-Co coatings by CGS;

- Study the mechanisms of bonding of WC-Co cermet particles, with different contents in ductile matrix, onto different types of substrates in order to achieve good quality coatings;

- Build-up WC-Co coatings by CGS and study their microstructure before and after deposition;

- Optimize spraying CGS spraying conditions for all the feedstock WC-Co powders;

- Measure CGS coatings' mechanical and electrochemical properties;

- Produce HVOF WC-Co coatings using the same feedstock powders without avoiding tensile residual stresses nonexistent in CGS;

- Measure HVOF coatings' mechanical and electrochemical properties and compare them with the previously obtained CGS coatings;

- Improve CGS coatings' properties when compared to HVOF;

- Transfer the optimum CGS spraying conditions for WC-25, 17 and 12Co feedstock powders onto low carbon steel and Al7075-T6 substrates;

- Test the obtained coatings in industry applications for wear and corrosion resistance improvement.

3 RELATION OF PAPERS

Results and partial discussion chapter of this Thesis is presented as a compilation of papers. Below are exposed, for each paper, the main reasons that confirm the quality of the publications:

Paper 1: S. Dosta, M. Couto, J.M. Guilemany, "Cold spray deposition of a WC-25Co cermet onto Al7075-T6 and carbon steel substrates", Acta *Materialia* (2013)

Starting target of this Thesis was to obtain what never before was accomplished using nitrogen as a CGS process gas. It was fundamental to obtain WC-25Co coatings onto both low carbon steel and Al7075-T6 substrates because, in theory, these were the easier cermets to deposit since they had a higher content in ductile matrix. After the optimization of the spraying conditions WC-25Co were successfully produced and their properties found to be rather when compared to conventional WC-Co cermets produced by HVOF. This novelty was appreciated and sent to one of the best rated journals of the Materials Science field.

Paper 2: M. Couto, S. Dosta, M. Torrell, J. Fernández, J.M. Guilemany, "Cold spray deposition of WC–17 and 12Co cermets onto aluminum", *Surface & Coatings Technology* (2013)

After having successfully deposited WC-25Co cermets by CGS, the goal was to lower the content in Co matrix in order to increase their tribological and

electrochemical properties therefore achieving equal or higher properties than those given by HVOF's WC-12Co coatings. This step allowed to have a broad information about the three chosen cermet powders and provided a wide characterization information about them.

Paper 3: M. Couto, S. Dosta, J. Fernández, J.M. Guilemany, "Comparison of the mechanical and electrochemical properties of WC-25Co coatings obtained by high-velocity oxy-fuel and cold gas spraying", *Journal of Thermal Spray Technology* (2014)

Based on the first results obtained after spraying WC-25Co by CGS another study was made using the same cermet powders and spraying it using the most used conventional thermal spray technique, HVOF. With its optimization came the mechanical and electrochemical testing and hence the inevitable comparison between CGS and HVOF results.

Paper 4: M. Couto, S. Dosta, J.M. Guilemany, "Comparison of the mechanical and electrochemical properties of WC-17 and 12Co coatings onto Al7075-T6 obtained by high velocity oxy-fuel and cold gas spraying", *Surface & Coatings Technology* (2014)

This work focused on obtaining WC-17 and 12Co cermets by HVOF, plus a bibliographic research about previously - and with widely published results – deposited WC-12Co and compare them with the results obtained during this Thesis. With the publication of this work the goals of the Thesis were achieved and surpassed.

4 INTRODUCTION

As engineering applications become more demanding the requirements for composite coatings increase as well. These coatings protect the substrate to retain its mechanical properties while increasing the resistance to wear and corrosion. In this Thesis special focus was given to coatings obtained onto low carbon steel and an aluminum alloy, Al7075-T6.

4.1 Low carbon steels

Low carbon steels are, of all the families of steels, those produced in the greatest quantities and contain up to 0.30wt%C. This family of steels are also unresponsive to heat treatments and their microstructures consist of ferrite and pearlite constituents. As a consequence, these alloys are relatively soft and weak but have outstanding ductility and toughness, they are machinable and are the less expensive to produce (Ref 1). Typical applications include automotive body components, structural shapes such as I-beams, and sheets used in pipelines, buildings, bridges and tin cans. These applications require materials that are serviceable under a wide variety of conditions and that are especially adaptable to low-cost techniques of mass production into articles having good appearance. Therefore, these products must incorporate, in various degrees and combinations, ease of fabrication, adequate strength, excellent finishing characteristics to provide

attractive appearance after fabrication, and compatibility with other materials and with various coatings and processes (Ref 1-4). In Table 1 some properties and chemical composition of the 0.20wt%C low-carbon steel are shown.

Table 1. Mechanical properties and chemical composition of the 1020 low carbon steel (Ref 4).

AISI No.	Tensile Strength, MPa	Yield Strength, MPa	Elongation, %	Hardness, HV	Composition, wt%	
1020	448.2	330.9	36	143	0.20C	0.45Mn

4.2 Aluminum

Aluminium has an attractive combination of properties such as low density, high strength, corrosion resistance, durability, ductility conductivity and ease of fabrication making it one of the fastest growing base/alloying metals for a variety of applications. It contributes to vehicle light-weighting and subsequent energy savings, its strength and corrosion-resistance guarantee durability, and its formability allow flexibility of design and ease of handling. Aluminium is widely used in car industry, trains, ships and aerospace industry (Ref 2, 3). Al7075-T6 is an aluminum alloy with zinc as primary alloying element. It is strong, has good fatigue strength and average machinability, but has less resistance to corrosion than many other Al alloys. T6 temper has tensile strength of approximately 510–572 MPa and yield strength 434–503 MPa. This temper is achieved by homogenizing the cast 7075 at 450ºC for several hours, and then aging at 120ºC for 24 hours. This yields the peak strength of the 7075 alloy because of the dispersed eta and eta' precipitates within grains and along grain boundaries.

4.3 WC-Co composites deposition

Hardmetals, or cemented carbides, are a group of hard composites, very resistant to wear and degradation, in which hard carbide particles are “cemented” by a

ductile and tough binder matrix, via liquid-phase sintering. These composite properties are achieved by combining both the toughness and plasticity of the metallic Co binder and the high hardness and strength of the covalent WC carbide. In matters of consumption and applicability the WC-Co group is regarded as the most important cermet, accounted with a quote of more than 80% in cutting applications and wear-resistant parts, especially for the heavy machinery industry (Ref 5). The cutting tool and wear part applications arise because of their unique combination of mechanical, physical and chemical properties.

Tungsten carbides are commercially one of the oldest and most successful powder metallurgy products and WC coatings have been widely used for their exceptional hardness, wear, erosion and corrosion resistance. Matrices of ductile metals, such as cobalt, greatly improve its toughness so that brittle fracture can be avoided, and even more, it allows the sintering of dense compacts at reasonable temperatures (Ref 6). WC-Co cermets are the most important wear-resistant coating materials that are nowadays employed for deposition techniques. Their high strength (two to three times that of steel), excellent thermal conductivity, low thermal expansion, and excellent adhesion, make them the ideal coating material (Ref 5).

As further, these cermet properties can be controlled by composition and microstructure, in order to improve certain behaviors for specific applications. For example, the hardness of the cermet will decrease with decreasing Co content and increasing particle size of WC, at some cost of rupture strength and fracture toughness (Ref 6).

The excellent properties mentioned above, there has been a reported concern on the particle size of the WC-Co powders that are used today. It is well known that nanocrystalline materials show greater mechanical properties compared to the conventional ones; the same happens when it comes to WC-Co particle size. A consequence of the smaller grain size is an improved performance, in terms of surface hardness and wear-resistance properties, as a direct consequence of the high density of grain boundaries, defects, and diffusion mechanisms that become available when a nanocrystalline size is achieved (Ref 7). For that same reason, better coating adhesion results will be expected (this subject will be further discussed). In the following table a mechanical properties' comparison, of a

submicron and a fine/medium grain sized WC-6Co grade (%wt), is made to prove this point.

When using these powders by conventional thermal spraying techniques there are some undesired decarburization and oxidation effects due to the high flame temperatures. When the temperature of a certain region of the spraying powder particles exceeds the melting temperature of the WC-Co pseudo-binary eutectic (~ 1350ºC) there is a rapid dissolution of the core of the WC particles in the liquid Co matrix. This provokes an increase in the amount of enriched in W and C liquid Co. Besides this enrichment of liquid Co there is a fast diffusion the carbon through the liquid Co and gasifies at the particle surface by the oxidative reaction $2C + O_2 \rightarrow 2CO$. During the subsequent cool-down from the superheated state, the Co liquid becomes supersaturated resulting in the formation of W_2C and W phases, depending on the extent of decarburization, and when cooling goes below the eutectic temperature precipitation of etc carbide phases may occur due to a reduction in solid solubility with decreasing temperature (Ref 8). This mechanism takes place during the solidification of the Co-rich matrix leading to the precipitation of the W_2C phase in the boundaries of the WC. As a consequence of these degradation reactions, some C is dissolved in the matrix while some C diffuses and reacts with the oxygen in the surface to form CO/CO_2, thus losing part of the C from the original powder. The retained C in the matrix with some W present in the liquid enriches the Co matrix to create amorphous regions (Ref 9, 10).

This is the other mechanism of formation of W_2C where the degradation reactions that take place during thermal spraying when WC grain decomposes have been described (Ref 9, 10) as:

$$2WC + O_2 \leftrightarrow W_2C + CO_2 \qquad \text{(Eq 1)}$$

or

$$2WC \leftrightarrow W_2C + C \qquad \text{(Eq 2)}$$

Also some elemental metallic W can be formed depending on the degree of decarburization, causing it to precipitate near the splat boundaries where a depletion of C due to its reaction with oxygen exists:

$$W_2(CO) \leftrightarrow 2W + CO \qquad \text{(Eq 3)}$$

These reactions take place mainly in WC grains that interact with oxygen. In addition, WC grains can be degraded in an oxygen-free atmosphere, especially those that are in the core of the particles:

$$W_2C + {}^{1}/_{2}\, W_2(CO) \qquad \text{(Eq 4)}$$

Depending on the degree of decarburization, the precipitation of ŋ-phases can take place as follows:

$$4Co + 4WC + O_2 \leftrightarrow 2Co_2W_4C + 2CO \qquad \text{(Eq 5)}$$

$$3Co + 3WC + O_2 \leftrightarrow Co_3W_3C + 2CO \qquad \text{(Eq 6)}$$

$$12Co + 12WC + 5O_2 \leftrightarrow 2Co_6W_6C + 10CO \qquad \text{(Eq 7)}$$

Table 2. Mechanical properties comparison between two different grain-sized WC-6Co grade cermets (Ref 5).

Grade (a)	Hardness HV_{30}	Transverse rupture strength, MPa	Elastic modulus, MPa	Fracture toughness, MPa.√m	Thermal expansion coefficient, $10^{-6}.K^{-1}$
WC-6Co/S*	1800	3000	630	10.8	6.2
WC-6Co/M*	1580	2000	630	9.6	5,5

(a) S*: submicron grain size; M*: fine/medium grain size.

4.4 Conventional thermal spray deposition techniques

Presently there are three main combustion deposition techniques, with its variants, of WC-Co cermet, them being Plasma Spraying, High Velocity Oxide Fuel and Cold Spraying. Limitations associated with the formation of brittle phases plus the decarburization observed when heated at high temperatures were the main

precursor in the search and development of new and more efficient deposition processes, such as Cold Spraying.

a. Plasma spray techniques

Plasma spray is one of the mostly used electrical thermal spray processes where a partially ionized conductive gas, known as 'plasma', is used to melt and propel powdered feedstock material onto the substrate. To create the plasma jet, inert plasma-forming gas, usually argon or nitrogen with minor additions of helium or hydrogen is injected into the annular space between two cylindrical electrodes, and a high amperage direct current (DC) arc is then struck between the electrodes. The arc partially ionizes the gas to form a high-temperature, electrically conductive plasma, which expands and escapes through the open end of the plasma spray gun to form a very hot, high-velocity, plasma jet. This process can produce enough plasma jet temperatures to melt even the most refractory metals or ceramics. For this reason, the plasma spray process is one of the most versatile of all spray processes, able to deposit an exceptionally wide range of materials. There are two main Plasma Spray processes: Conventional Plasma (APS) and Vacuum Plasma (VPS) (Ref 11).

The conventional process ought to be the Atmospheric Plasma Spray for its relative lower cost when compared to the Vacuum Plasma Spray process. The main advantages of the Plasma Spray processes is the capacity to achieve plasma temperatures ranging from 6000 to 15000ºC, values above the melting point of every known material, and effectively deposit a wide range of materials. The Vacuum Plasma, or Low-Pressure Plasma, Spray uses low-pressures in the range of 0.01 to 0.05MPa) inside the chamber before ionizing the gas. Afterwards, and considering the pressure is very low, the plasma becomes larger in diameter and length and will be forced through a converting/diverging nozzle, resulting in a higher gas speed than those achieved with the APS process. In order to constantly maintain the working chamber pressure, efficient pump systems have to be employed to remove the injected plasma gases. The main advantages of this process, when compared to the previously mentioned ones, would be the ability to produce denser, more adherent coatings with much lower oxide contents (due to the lack of oxygen inside the chamber) (Ref 11). Another advantage of the VPS technology is the option to clean the substrate surface especially from oxide layers

and preheat the substrate, both giving better adhesion (Ref 12). The better adhesion results can also be explained by the higher substrate temperatures since the cooling and convective heat transfer inside the chamber are reduced, therefore improving diffusion and reducing cooling residual tensions. On the other hand there are usually high investments and maintenance costs for achieving the vacuum conditions (Ref 12).

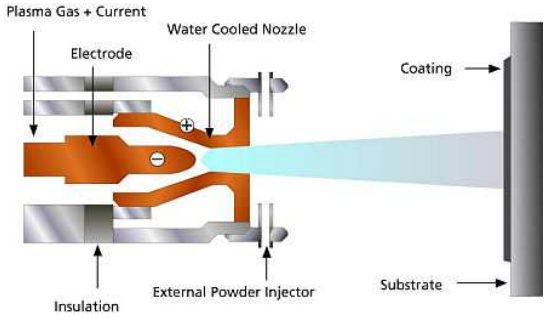

Figure 1. Schematic diagram of the plasma spray process (Ref 13).

b. High Velocity Air Fuel

HVAF (High Velocity Air Fuel) thermal spray technology is similar to HVOF (High Velocity Oxy-Fuel) in that a fuel source is combusted to allow the propellant to accelerate the coating powder particles. However, HVAF diverges from HVOF in that it uses air as the oxygen source, eliminating the need for compressed bottle oxygen. HVAF is considerably less expensive because it is based on combustion of fuel and compressed air. This technology can be easily used on-site and was invented in 1960 before HVOF. The lower temperature burn of HVAF heats the sprayed powder particles less, thus controlling the thermal alteration of the coating. HVAF has the flexibility to generate HVOF-like coatings and coatings similar to those produced using cold spray. Thus, since the flame temperature is lower in HVAF than HVOF a lower oxidation of the sprayed material occurs. HVAF coatings are similar to and generally comparable to coatings produced by HVOF and Cold Spray. HVAF is a "warm spray" process that is cooler than HVOF, but hotter than Cold Spray. HVAF guns utilize axial powder injection into an air-fuel jet with a temperature of about 1900°C. Therefore, the process is capable of effectively applying carbide-based materials, but since the air-fuel jet produces

considerably less oxides than high temperature oxy-fuel jets, the HVAF process can also apply metals with almost zero oxidation, similar to Cold Spray.

HVAF technology is well suited for tungsten carbide coatings on pump housings and axles for the oil and gas industries. HVAF is commonly used as a repair technology for the oil drilling and gas industries (Ref 12). Lower operating costs of the HVAF process in comparison with other high velocity systems makes this technology viable for thermal spraying applications for anti corrosion protection.

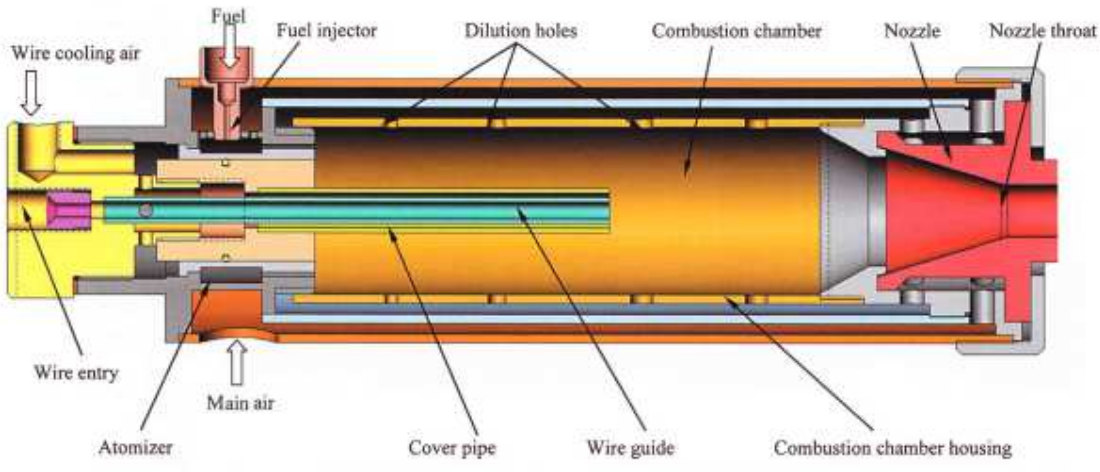

Figure 2. Schematic diagram of the HVAF thermal spraying gun (Ref 15).

The HVAF technique is a thermal spraying-based process that through the action of combustion will accelerate (into the 1000m/s to 1200m/s range) the coating material's powder particles. Such conditions will allow the formation of cermet coatings onto several substrates without the formation of virtually no oxides being this one of the main advantages. The particles are mostly solid upon impact on a substrate, which slows down diffusion of oxygen by several orders of magnitude compared to liquid metal. Allied with the compressive effect imparted to the substrate surface – due to the peening effect of the softened but not molten impinging particles - allow this process to produce dense and well-bonded coatings (Ref 15).

A HVAF combustion chamber is designed on the principles of a jet engine combustor working of liquid fuel and compressed air (Figure 3) which is supplied to the combustion zone in two stages: primary air for combustion and secondary

air for cooling of the flame. For this reason the design of the HVAF chamber is more complex than the HVOF chamber because the compressed air fed into the thermal spraying gun should provide stable, efficient combustion and, at the same time, cooling of the thermal gun parts. Combustion of fuel, mostly liquid fuels, takes place inside the combustion chamber after which gases expand in the *de Laval* nozzle.

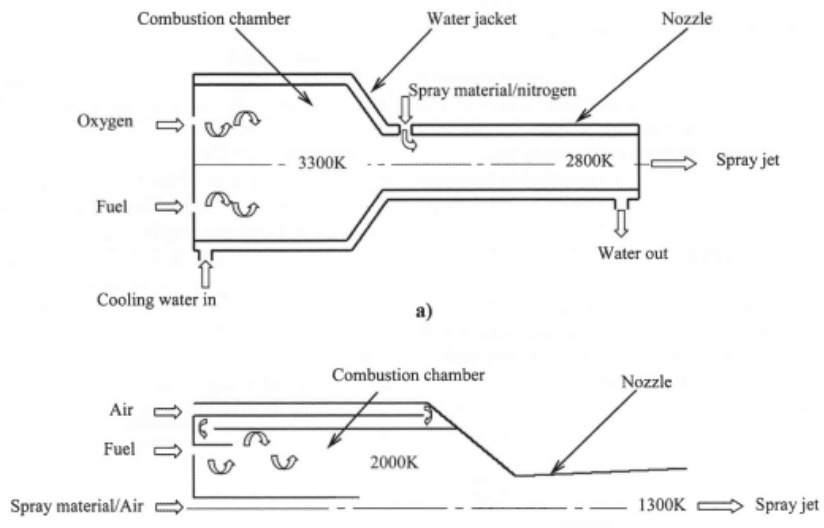

Figure 3. Schematics of a) HVOF burner; b) HVAF thermal spraying gun (half cross-section) (Ref 15).

In the following table are indicated and compared some of the systems parameters concerning the discussed Thermal Spray techniques.

Table 3. Comparison of thermal spray processes (Ref 12).

Process	Flame or exit plasma temperature (ºC)	Particle impact velocity (m/s)	Relative adhesive strength (a)	Oxide content (%)	Relative process costs (a)
APS	5500	240	6	0,5-1	5
VPS	8300	240-610	9	ppm values	10
HVAF	1900	1000-1200	9	ppm values	2
HVOF	3100	610-1060	8	0,2	5

low (1) to high (10)

c. High Velocity Oxygen Fuel

The High Velocity Oxygen Fuel, commonly known as HVOF, is one of the most versatile conventional chemical thermal spray deposition techniques. In this process an explosive high-volume mixture of gases (hydrogen, propylene, propane, acetylene and kerosene), oxygen and powder (borne by a carrier gas and fed into the nozzle), is fed into a combustion chamber. A spark plug will then generate combustion at very high combustion chamber pressures exceeding 241 kPa and heat inputs of nominally 527 MJ; the resulting heated gas will exit through a converging-diverging nozzle therefore generating a supersonic gas jet (check point 4 for a deeper insight on the *de Laval* nozzle) - the sheer volume of gas flow, coupled with the high temperature of combustion, creates gas velocities in the range of 1525 to 1825 m/s (Ref 12, 16). As the exiting gas jet expands through the nozzle and achieves supersonic velocities it will cool as thermal energy is converted to kinetic energy; the high pressure and velocity wave will heat and accelerate the powder particles – in this stage velocities of the order of 450-1000m/s are achieved - forcing them to travel down the barrel toward the substrate (Ref 17). Depending on the process parameters such as the spray device, spray material and operating conditions different particle velocities and adhesion efficiencies are obtained.

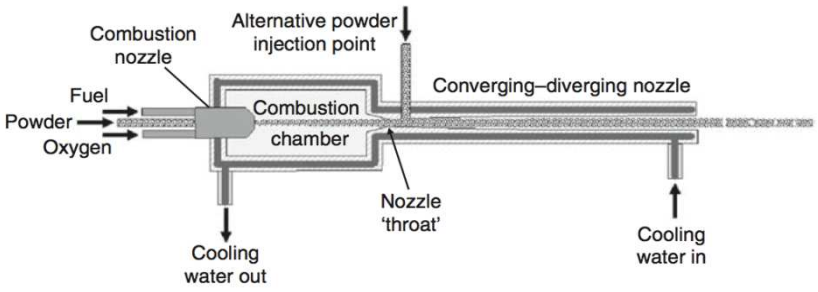

Figure 4. Schematic diagram of a HVOF spray gun (Ref 11).

The high gas velocity generated by HVOF will increase particle velocity, with a corresponding increase in coating density and adhesion with very little porosity (between 0.5 and 1.0%) and also create a more favorable compressive stress state caused by the peening effect of these high-velocity particles impacting the

substrate's surface. Lower average particle temperatures, compared to plasma spray, reduce the degree of particle melting and oxidation (Ref 12, 17).

The lower jet temperatures and higher particle velocities of HVOF make it a preferred process for applications such as spraying dense cemented carbide wear-resistant coatings, where the lower process temperatures prevent decarburization and the high impact velocities produce a relatively pore-free coating with a favorable residual stress state that makes it less prone to cracking.

b.1. Advantages

The main advantage of the conventional thermal spray deposition processes is the ability to deposit a wide range of materials that have a stable molten phase. Even some materials that do not melt can be co-deposited with another sprayable material thus creating a composite material coating – this is another advantage of these processes. Besides being able to deposit a wide range of materials it is also possible to deposit on an even wider range of substrates, even to temperature-sensitive materials because the thermal energy in a single droplet of molten spray material is quite limited therefore avoiding excessive heat build-up in the substrate. Some particle heating occurs on impact from the conversion of kinetic energy into thermal energy, which further aids in producing dense coatings. This process also offers the possibility to rapidly and economically coat very large surfaces meaning that it offers very high deposition rates (the material is deposited as 10-100μm molten droplets) (Ref 16).

The process effluents are relatively easy to control and dispose of in an environmentally friendly manner.

b.2. Limitations

The presence of porosity is one of the greatest limitations of traditional thermal spray processes because it can dramatically affect the coating's mechanical properties and if intended to protect the underlying substrate material from exposure to liquid or gaseous species that may cause corrosion and other problems. Porosity values vary according to the specific spray process, material

and deposition conditions. Usually, higher velocity processes can produce coatings with less porosity, typically of the order of 3-8%vol. (Ref 16).

Another drawback associated with this family of processes would be the undesirable presence of oxides in the spray-deposited material, meaning that the use of oxygen in this process requires special protection measures. These defects and impurities in the sprayed material's microstructure can degrade the mechanical, electrical and thermal properties of the coating as compared with the same material in conventionally processed form. Also, as these require heating to allow deposition of the powder particles it can result in the vaporization of more volatile species in a complex metal alloy causing a change in the chemical composition of the deposited material. Processes such as HVOF, that minimize heating of the spraying material result in lower oxide concentrations and minimal changes in alloy chemistry (Ref 16).

Residual stress is also a limitation of most thermal spray processes. The residual tensile stresses appear whenever each molten droplet solidifies and then cools to room temperature, undergoing in thermal contraction in direct proportion to the temperature change and the thermal coefficient of expansion for that material. Every time a new layer of coating material is deposited, the underlying and already solidified material, which is at a lower temperature, will result in a state of residual tensile stress, increasing as subsequent layers of material are added. Additionally, the steadily increasing residual tensile stress will limit the maximum thickness of thermal spray coatings and can sometimes crack or separate the coating from the substrate material. Coatings sprayed by HVOF processes, which tend to have less residual tensile stress because of the peening effect of the high-velocity impacting powder particles, may be in a state of compressive residual stress therefore superposing coating cracking and separating problems (Ref 16).

In virtually all thermal spray processes the deposition is limited to surfaces that are directly accessible to the spray stream.

c. Cold Gas Spray

The cold spray process as a deposition technology was developed by a group of Russian scientists of the Russian Academy of Science in the mid-80s. This group,

led by Professor Anatolii Papyrin, could deposit a wide variety of materials such as pure metals, metallic alloys, polymers and composites onto various substrate materials obtaining very high coating deposition rates using this novel deposition process. While studying models subjected to a supersonic two-phase flow (gas + particles) in a wind tunnel it was verified that it would be possible to deposit a wide range of materials on various substrates without the use of temperature to melt and deposit the spraying materials, as it was usually done on the most common thermal deposition processes (Ref 16).

Unlike the conventional deposition techniques, which require both kinetic (particle velocity) and thermal (temperature) energy in order to promote coating formation onto a substrate, the cold spray process simply uses the kinetic energy of the powder particles for the coating formation. The kinetic energy of the impinging particles is sufficient to produce plastic deformation and high interfacial pressures and temperatures meaning it is, almost entirely, a solid-state process. Furthermore, because cold spray is a low-temperature process, i.e., does not use thermal energy, it produces less porous coatings with less oxidation and higher hardness.

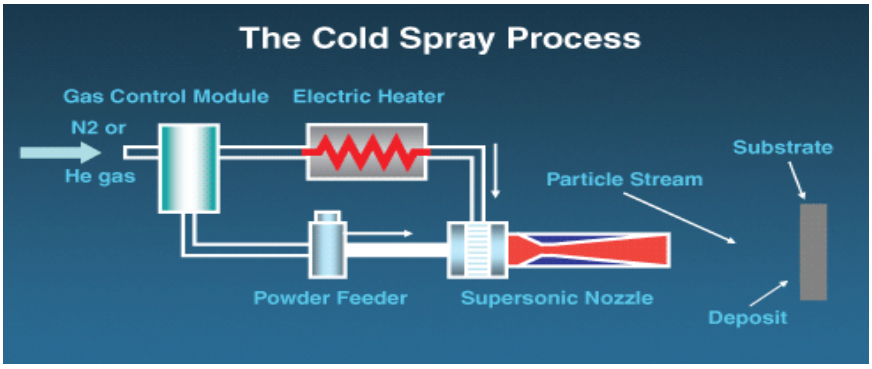

Figure 5. Schematic diagram of the cold spray process (Ref 16).

In the cold spray process it is necessary to produce a high-velocity stream of gas in order to give the powder particles enough kinetic energy to allow deposition onto the substrate. The metal powder particles which range in particle size from 5 to 50μm are fed centrally, by a separate gas stream typically introduced into the high-pressure side of a *de Laval* converging-diverging nozzle (Figure 6) where a

preheated gas (usually air, He, N_2, or mixture depending on the deposition material and gas temperature) in the range of 300-800ºC is compressed and will expand to supersonic velocity while decreasing in pressure and temperature. Such velocities can be reached due to the changes of geometry and Mach ($M = {}^{v_s}\!/\!_{v}$, where v_s is the gas exit speed and v is the speed of the sound in the medium) inside the nozzle. In the convergent part of the nozzle there is a subsonic flow where the gas is compressed, representing a subsonic Mach velocity (M < 1); at the throat, where the cross sectional area is minimum, the gas velocity becomes transonic (M = 1) and as the nozzle's cross sectional area increases the gas expands and its flow reaches supersonic velocities (M > 1) (Ref 17). This can be seen on the depicted diagram in Figure 6. It has to be noted that the gas is heated not to heat or soften spray particles, but instead to achieve higher sonic flow velocities, which ultimately result in higher particle impact velocities.

Since the contact time of the injected particles with the hot gas is short and the gas cools as it expands, it is considered that the particles temperature remains below its melting temperature. The term "cold spray" has been used to describe this process due to the gas stream's temperature (Ref 16, 18).

Table 4. Typical range of gas-jet parameters for cold spray coating (Ref 11).

Gas-jet parameters for cold spraying	
Stagnation jet pressure (MPa)	1-6
Stagnation jet temperature (ºC)	0-1100
Gas flow rate (m^3/min)	1-2
Powder feed rate (kg/h)	2-8
Power consumption (kW)	5-25
Particle size (μm)	5-50
Operating gases: nitrogen, helium, and their mixtures	

There are several parameters that can influence the quality of the deposition being the critical velocity the most important one. The critical velocity is the minimum

value of velocity that an individual particle must attain in order to deposit after impact with the substrate; if a particle fails to attain such velocity then it will bounce off the surface and erode it. In the cold spray process the particles are accelerated to velocities in the range of 500-1200m/s, and if enough to achieve a critical velocity the solid particles will plastically deform and flow out upon impact, creating hydrodynamic flow instability at the interface between the incoming particle and the substrate, resulting in bonding (Ref 16).

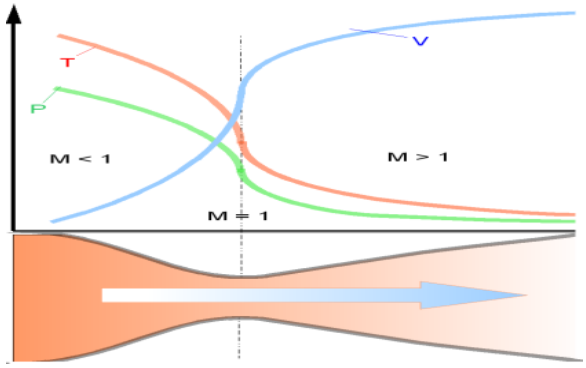

Figure 6. Diagram of a *de Laval* nozzle showing approximate flow velocity (v), together with the effect on temperature (T) and pressure (P) (Ref 17).

c.1. Advantages

Since cold spray is a solid-state process and does not require high temperatures to promote adhesion between the coating and the substrate material there are a large number of advantages associated with this process when compared to conventional thermal spray processes. This can be a very important advantage if a low porosity and low oxide content coating is desired. As so, these are two of the greatest advantages when producing coatings with cold spray: low porosity and low oxide content. Low porosity results from the fact that cold spray is, as stated before, a solid-state process so there is no melt and splashing of the powder particles onto the substrate; in addition, there will be a peening effect resulting from the impact of particles present in the outer high-velocity jet stream which tend to close any small pores and gaps in the underlying coating material which will also result in a very high density. As for oxidation of the metal powder during deposition, since it is processed at low temperatures, any reactions of metals with

oxygen is greatly reduced or eliminated. Moreover, as these two “defects” are reduced there will be an improvement of mechanical, electrical and thermal properties. In cold spray it is possible to obtain ductile coatings, after performing a post-deposition heat treatment to anneal it, since they’re oxide and porosity free (Ref 16).

In cold spray chemistry, phase composition and crystal (grain) structure of the feedstock powder are preserved in the final coating; this means that the initial particle material’s properties are retained and the final product will show the exact same properties as the one’s evidenced by the bulk material’s powder. Low temperature is once again the main precursor of these advantages because it prevents vaporization of more volatile elements in the deposition process (maintaining the powder’s chemistry), also the melting and solidification processes are inhibited so the phase composition and crystal structure remain unaltered. This can be an amazing advantage if someone wishes to work with nanocrystalline powders since their unique properties won’t be changed by thermal grain growth (Ref 16).

High density, phase purity and homogeneous microstructure of cold spray coatings also promote exceptional corrosion characteristics.

Since the cold spray particles are deposited at relatively low temperatures there is little temperature-drive dimensional change (thermal contraction). Adding the peening effect to this results it is expected that cold spray coatings are typically in a state of compressive residual stress that will prevent cracking and coating separation. This can also be a plus as thicker coatings can be obtained in this state of favourable residual stress. This process also shows very high bond strength over many substrates (metals, alloys, composites, etc.), even more it is possible to work with highly dissimilar materials since cold spray does not heat and melt the coating material and the formation of weak interfaces is avoided. Furthermore, in this process, there is a minimum thermal input to the substrate (the one received by the enthalpy of the impacting particles), which allows working on substrates made of temperature-sensitive materials (Ref 16).

It is also possible to deposit coating materials in highly localized areas without the need for costly masking operations. Moreover, this process has an elevated deposition rate due to its narrow and well-defined spray beam.

Considering all the previous advantages and high feeding powder rates it is also expected high deposition efficiency (DE) values for most materials.

The absence of high-temperature gas jets, radiation and explosive gases will increase operational safety.

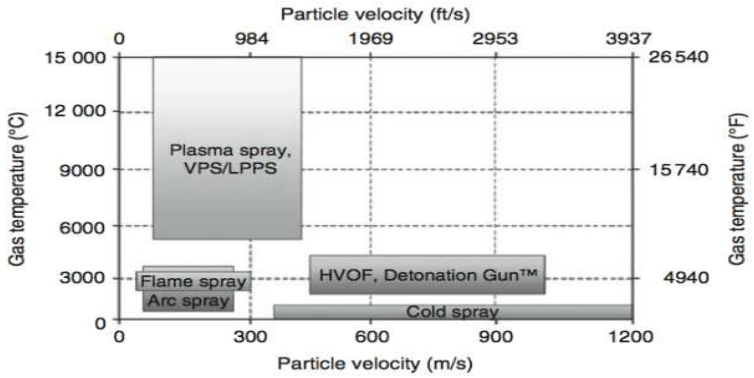

Figure 7. Comparisons of process temperature and particle velocity ranges for several common thermal spray processes and cold spray (Ref 16).

c.2. Limitations

The cold spray process, unlike traditional thermal spray processes, is essentially limited to depositing materials that exhibit good ductility to produce quality bonds between the coating and the substrate material. The fact that it is a solid-state process and the powder particles do not melt before impact, these should have at least a limited ductility in order to deform and create the hydrodynamic shear instability that bonds the particles with the underlying material. At the same time, the substrate material should be hard enough to allow the ductile particles to deform upon impact. So, in cold spray, harder and more brittle materials can't be used as coating material, and softer materials can't be used as substrates; although this is very limitative, composites that have a ductile matrix such as WC-Co can be deposited. Furthermore, this extensive plastic deformation suffered by the particles impinging on the substrate will provide a work hardening effect on the coating and result in very low ductility in the as-sprayed condition – for some applications it can be an issue while in other, such as wear resistant components, it can be an advantage (Ref 16).

Another drawback of cold spray is that it consumes much more process gas than the traditional thermal deposition techniques, in the order of 1-2m^3/min. If to this we add that some deposition materials such as titanium, which have high individual particle critical velocity, require the use of very expensive gases (He) to achieve the necessary impact velocity and coating quality then it can turn into a costly process and become a huge drawback (Ref 16). A solution could be using higher pre-heating temperatures (~800ºC) of the nitrogen in order to achieve superior existing jet velocities hence providing the minimal velocity (v_c) for deposition materials that require higher values of critical velocity.

Since the cold spray process's gun produces a very thin and well-defined beam it makes the process not suitable for coating very large surface areas. As in other processes, this is also a line-of-sight process hence spraying complex shapes and internal surfaces is somewhat difficult without using extensive robot planning and programming (Ref 16).

Although cold spray offers a wide range of advantages, such as low level of porosity and oxidation, it won't replace the traditional thermal spray processes mainly due to its limitation in coating/substrate materials compatibility.

c.3. Process parameters

The cold spray process will be influenced by several parameters (critical velocity; particle, gas and substrate temperature; powder size; etc.). Controlling these parameters will allow understanding the nature of the cold spray phenomenon and control the basic coating properties. One of the most important characteristics of the process is the deposition efficiency, which is defined as the ratio of the mass gain of the substrate during its exposure to the flow with the proper set of parameters and the decrease/consume in powder mass in the feeder during the same time (Ref 20). The relative deposition efficiency, RDE, is used to estimate the weight gains of coatings of several samples, through measuring its weights before and after deposition.

$$RDE = {W_c}/{W_{c\max}} \cdot 100$$

Figure 8. Relative deposition efficiency, where Wc is the coating weight at a certain standoff distance and Wc_{max} is the maximum weight among the coatings deposited at different standoff distances (Ref 21).

c.4. Particle velocity

The particle velocity prior to impact is one of the most important parameters in the cold spray process. There is a critical velocity value that depends both on particle and substrate nature and properties, below which no particle adhesion to the surface is possible. Particles hitting the substrate will either adhere (by plastic deformation) to it or bounce back (and erode the substrate surface). Optimizing this parameter will reduce the manufacturing costs by increasing the deposition efficiency. For a given material, there exists a critical velocity resulting in a transition from erosion of the substrate to deposition of the particle. Only those particles achieving a velocity higher than the critical one can be deposited to produce a coating.

It is important to have a narrow distribution window of particle size due to the effects of erosion/adhesion. As explained before, when a particle (usually the larger ones within a distribution window) does not achieve its critical velocity it will hit the surface of the substrate and bounce back eroding it hence reducing the deposition efficiency of the process. The velocity distribution was combined with the measured deposition efficiency and the particle size distribution, to give the size and velocity of the largest particle that would bond successfully to the substrate (Ref 16, 20-26). Erosion can also appear when the particle velocity is too high thus exceeding the deposition efficiency saturation point and causing a large-impact dynamics phenomenon. Brittle materials would cause erosion for any velocity at temperatures below their melting point. This is depicted on Figure 9.

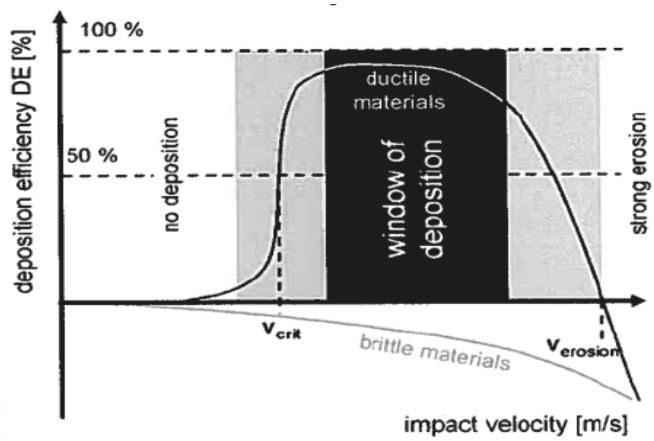

Figure 9. "Window of deposition" depicting a correlation between particle velocity and deposition efficiency for a constant impact temperature (Ref 24).

As particle velocity is higher than the critical one, the deposition efficiency increases with increasing the impact velocity. A further increase of velocity leads to an increase in deposition efficiency until it reaches the saturation level of almost 100% deposition efficiency. After reaching this limit the deposition efficiency will decrease with an increase in particle velocity due to the phenomenon discussed before. At the velocity where deposition efficiency is 0%, erosion velocity is defined – being usually two to three times higher than critical velocity (Ref 14, 22).

Based on an analysis and correlation of material properties and the critical velocity – or an interplay between kinetic energy, material strength and heat generation due to plastic deformation - Schmidt *et al.* (Ref 22) defined that critical velocity could be as:

$$v_{crit} = \sqrt{A\sigma/\rho + Bc_p\left(T_m - T\right)}$$

Figure 10. Critical velocity, where σ is the temperature-dependent flow stress, ρ is the density, C_p is the heat capacity, T_m is the melting temperature, T is the mean temperature of particles upon impact, and A and B are fitting constants (Ref 24).

Moreover, the particle velocity increases with the decrease of particle size and a higher velocity can be obtained for a particle of lower density under the same gas

conditions, or by incorporation of the materials into a ductile matrix (cermets, for example) (Ref 16).

c.5. Particle, gas and substrate temperature

Particle velocity is influenced by several parameters being the particle, gas and substrate temperature three of the most important; so, controlling the temperature of these parameters will allow for a greater deposition efficiency of the process. Thus, the coating quality can be further improved by increasing the initial temperatures of the particles and substrates.

If one wants to increase particle velocity increasing the gas temperature will result in higher particle velocities and lower critical velocity values. Generally, the purpose of increasing the gas temperature is not to heat the particles temperature but rather to increase the gas velocity. Also, using a smaller molecular weight gas such as helium will provide higher gas velocities as it is stated by the equation:

$$v = \sqrt{(\gamma RT / M_w)}$$

Figure 11. Equation for the speed of sound, where γ is the ratio of specific heats (1.4 for air, 1.66 for He), R is the gas constant, T is the gas temperature, and M_w is the molecular weight of the gas (Ref 16).

Altering the particle and substrate temperature will affect the physical and mechanical properties of the particle at the substrate in a way that will generally result in a reduced mechanical performance. Since particles at higher temperature need less kinetic energy to heat particle surface areas by plastic deformation, increasing the particle temperature should allow one to decrease the particle velocity necessary to achieve the same deposition efficiency for the coating. Additionally an increase in particle temperature improves the particle-particle adhesion. Moreover, heat conduction will be less effective due to lower temperature gradients, which leave more time for diffusion and bonding (Ref 16, 25). Figure 12 shows how critical velocity varies with temperature.

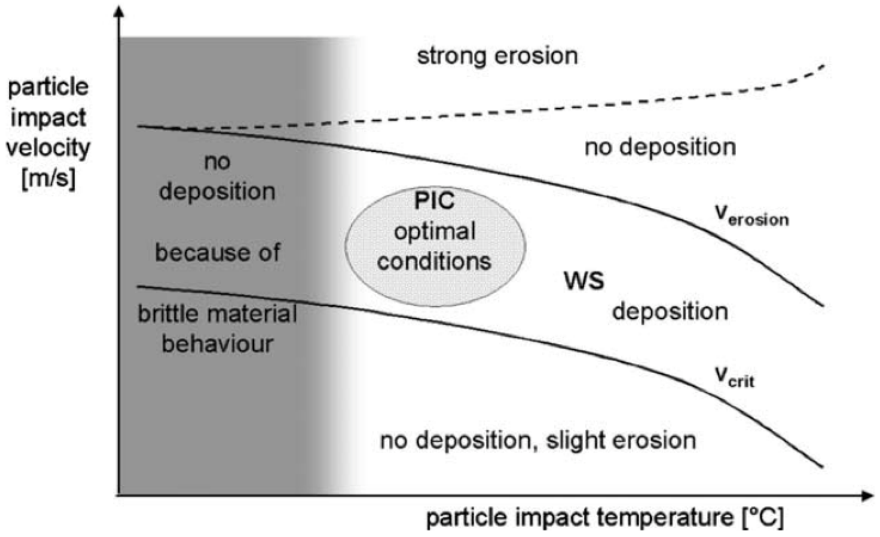

Figure 12. Particle velocity over particle temperature (Ref 25).

c.6. Powder size, morphology and density

Using materials with a finer grain structure means an increased amount of grain boundaries thus impeding dislocation motion and improving properties like hardness, toughness and even sliding and abrasion resistance. When compared to conventional materials, nanocrystalline materials are typically characterized by a significant increase of mechanical properties. For these reasons, the use of nanostructured feedstocks can produce these improvements in microstructure and bonding of the final coating (Ref 26).

For materials with a smaller particle size distribution a higher particle velocity is expected. This is due to the fact that the gas/particle momentum transfer or particle acceleration imparted by the gas is proportional to 1/d, based on Newton's law (acceleration and deceleration of the particles are considered to be action of the drag force acting on a particle which is proportional to the particle drag coefficient; an increasing drag coefficient leads to an increased drag force acting on the particle and thus to a higher particle velocity). Consequently, a smaller particle size will result in higher acceleration and particle impact velocity (Ref 27). This means that a lower gas/particle temperature is needed, avoiding possible effects of

oxidation of the small grain sized powder particles, resulting in better coating quality and characteristics.

Since one is relying on the coupling of the high-velocity gas stream to accelerate the particles, the particle morphology will determine the deposition efficiency. Long aspect shapes do not present a large cross-sectional area to promote drag effects. This type of particle geometry will tend to orientate into a direction that will present a reduced cross-section perpendicular to the gas flow reducing the drag coupling and consequently the final particle velocity.

The particle density is another factor to consider. Particles with a high density, such as tungsten, will accelerate more slowly than particles with a lower density such as aluminum. The very-high-density materials may also require higher velocity powder carrier gas flows, such as those provided by helium, to maintain particle suspension in the gas flow for the journey to the nozzle (Ref 16).

c.7. Powder feeding rate

Loading of the powder particles can also influence the properties of the coating. Varying the mass flow rate at which the powder particles are fed into the carrier gas stream can affect the coating's thickness.

Excessive powder feeding rate may saturate the gas stream flow resulting in a reduction in particle impact velocity due to a reduced gas/particle momentum transfer, while insufficient particle mass flow rate may lead to reduced coating thickness or coatings with high porosity. Increasing the powder feed rate increases the coating's thickness linearly until a maximum powder feed rate is reached for which there are too many particles impacting the surface of the substrate resulting in excessive residual stress causing the coating to peel - as a result of the higher powder mass flow rate, too many particles impact the substrate over a given surface area per unit time resulting in an increase in residual stresses in the coating (shot peening effect) (Ref 28).

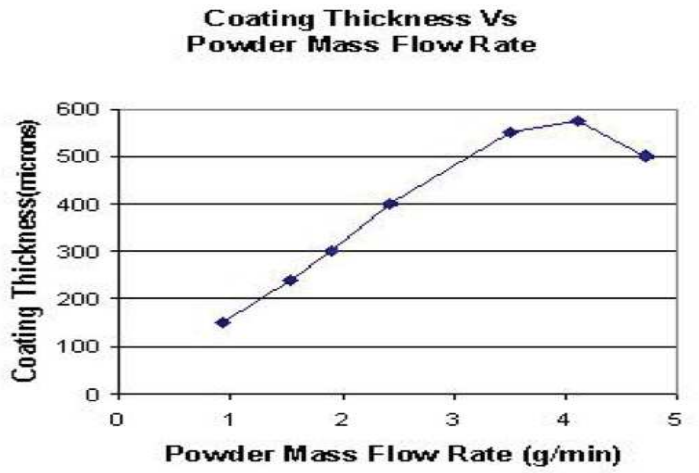

Figure 13. Example of a chart depicting the coating thickness as a function of the powder mass flow rate for copper (Ref 28).

c.8. Spraying angle

The deposition efficiency will also be affected by the spray angle and, since the particles deformation depends mainly on its, velocity this variable is considered to influence the coating characteristics and deposition behaviour.

The particle impact velocity is decomposed into a normal and a tangential velocity component, relative to the substrate surface:

$$V_n = V_p \sin\theta$$

$$V_t = V_p \cos\theta$$

Figure 14. Normal and tangential velocity component, here Vp is the particle impact velocity, Vn the normal component and Vt the tangential component of Vp, θ the spray angle. between the nozzle and the substrate (Ref 29).

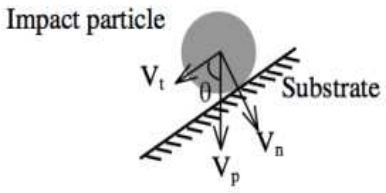

Figure 15. Decomposition of particle impact velocity at spray angle of θ (Ref 29).

Supposing that the tangential velocity component is negligible, the deposition efficiency will be solely affected by the normal velocity component. When particles are sprayed at an off-normal angle relative to the substrate surface, the normal component of the particle velocity will be inferior compared with that at the normal angle. With the decrease in the spray angle, the normal component of the velocity will be decreased until a point where its velocity is below the critical velocity thus not being able to deposit on the substrate. Also the flow direction of the depositing particles, which usually deposit perpendicular to the particles approaching direction, will be altered hence significantly influencing the layering directions of the spray particles and the coating's microstructure (Ref 28, 29).

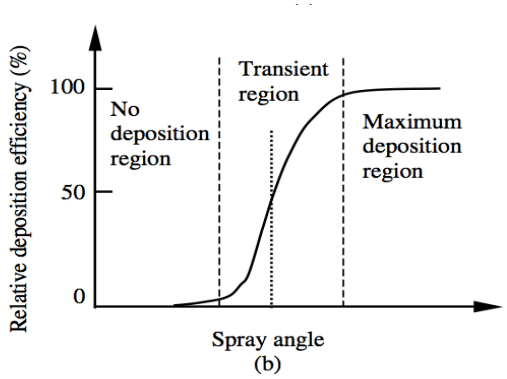

Figure 16. Dependency of relative deposition efficiency on spray angle (Ref 29).

As it can be observed in Figure 16 three typical angle ranges exist: maximum deposition angle range, transient region angle range (both depend on the particle mean velocity and velocity distribution) and no deposition angle range. At the maximum deposition angle range – this being 90º - the relative deposition efficiency reaches 100%; the angle range in which the relative deposition efficiency decreases from 100% to zero is defined as the transient angle range, being quite broad for the particles presenting a wider velocity distribution and narrower for the smaller ones (Ref 28, 29).

c.9. Nozzle-substrate standoff distance

The nozzle-substrate standoff distance is also one of the most important parameters in the cold spray deposition process. It is known that at short standoff

distances the impact velocity of small particles is reduced as a consequence of the bow shock formed at the substrate hence affecting the deposition efficiency of the process. The bow shock (Figure 17) is defined as a shockwave occurring as a result of a supersonic flow on the substrate; as gas molecules in the primary jet-flow impact with the substrate there is a general change in molecular energy which is transmitted to other regions of the flow by pressure waves travelling at the speed of sound thus forming a normal shockwave. The bow shock will enclose a region of high-density, low-velocity fluid that will affect the velocity and trajectory of the incoming primary jet's particles. As across the bow shock and the stagnation bubble there will be some negative drag forces decelerating the particles the deposition efficiency will be reduced if their velocity falls below the critical velocity; not only the bow shock will prevent the small momentum and sized particles to maintain their velocity to the substrate, but also larger particles with velocities only slightly above theirs critical velocity value (Ref 30).

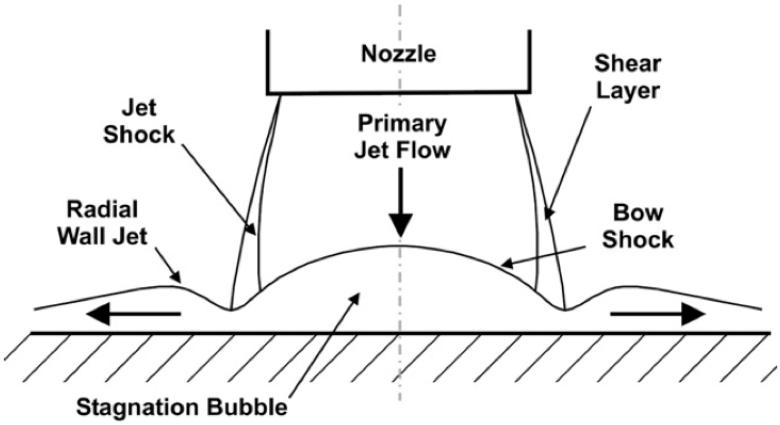

Figure 17. Schematic diagram of the supersonic impingement zone at the substrate (Ref 30).

Therefore in order to achieve optimum performance this parameter should be controlled, using diagrams such as the one depicted in Figure 18, where three distinct regions can be seen. At the first region, where the standoff distance is smaller, the presence of the bow shock adversely affects deposition performance, and is limited by the length of the nozzle's supersonic potential core; at the medium standoff region, where the bow shock has disappeared and, if the gas

velocity remains above the particle velocity (positive drag force), the deposition efficiency continues to increase until 100%; and at the large standoff region, where the gas velocity has fallen below the particle velocity (negative drag force), and the particles begin to decelerate hence decreasing the deposition efficiency as the standoff distance is increased. For optimal deposition the standoff distance should be set within Region 2 (Ref 30).

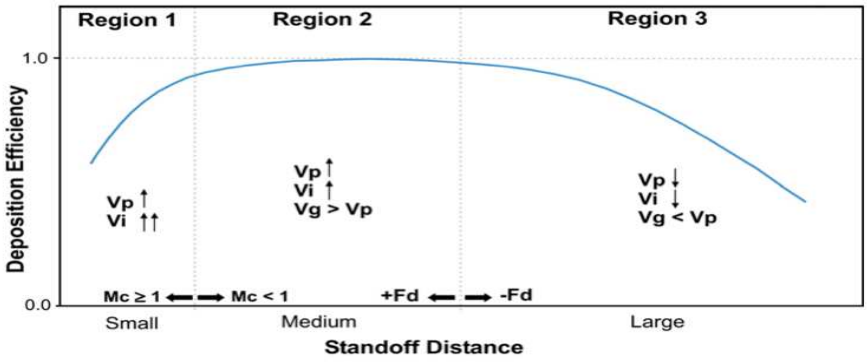

Figure 18. The effect of standoff distance on deposition efficiency. Here Fd is the drag force, Mc is the centreline Mach number, Vg is the gas velocity, Vi is the particle impact velocity and Vp is the in-flight particle velocity (Ref 30).

Besides the decrease of the deposition efficiency with the standoff distance, also the coating thickness decreases with the standoff's distance increase (Ref 21).

In cold spray the selection of a too short standoff distance could compromise the coating's oxide content because at shorter distances the previously deposited coating/substrate will be exposed to a higher gas temperature. Therefore, the selection of standoff distance should be careful with compromising the deposition efficiency and possible oxidation for temperature susceptive materials (Ref 21).

c.10. Substrate roughness and thickness

Studies show that the use of different grit sizes leads to changes in the mass deposited on the substrate (deposition efficiency) but have no significant effect on the coating microstructure. Both substrate preparation and substrate thickness showed to have effect on the final coating's characteristics hence making them cold

spray process parameters. Since one of the suggested bonding mechanisms is associated to mechanical interlocking it is possible to assume that an increased substrate roughness would further enhance bonding as it presents a greater array of recesses in which the particles can be lodged and then be subjected to additional compaction as successive particles impact on the substrate. Larger recesses also allow larger particles to come into better contact with the substrate. For surfaces with low roughness, the first particles to impact have fewer chances to bond because they have little surface area with which to bond, resulting in weaker bond strengths. All considered, a larger surface roughness area appears to be beneficial for the deposition efficiency of the process, although affecting it only for the first few layers of particles impinging on the substrate. A thinner substrate won't affect negatively the deposition efficiency or resulting microstructure meaning that this process can also be used for very thin substrates (Ref 31).

c.11. Bonding mechanism

In the cold spray process, bonding of the coating to the substrate occurs when the impact velocity of the powder particles equals or exceeds its critical velocity value, happening a localized deformation and adiabatic shear instability at the same time. The adhesion of the particles to the substrate in this process is due solely to their kinetic energy upon impact even though the actual mechanism by which the solid particles deform and bond during cold spray is still not well understood (Ref 16). During cold spray deposition there are two very different stages. During the initial stage, a thin film of particle material (monolayer) is deposited on the substrate. This stage is characterized by a direct interaction of particles with the substrate and depends very much on the degree of surface preparation and on the properties of the substrate material. The initial stage includes the time of surface activation, i.e., the incubation time, during which erosion instead of deposition can occur. In the second stage a coating layer of finite thickness is build up. In this stage particles interact with a surface formed by particles themselves (Ref 32).

It is know that the substrate, or the deposited material (depending if it has already been deposited a layer of coating material), and the powder particles undergo an extensive localized deformation during impact therefore providing the necessary

conditions for particle/substrate and particle/deposited material bonding, by means of a clean contact surface and high pressures. Localized deformation is known to cause disruption of the thin oxide films (as oxides tend to be more brittle than metals fracturing these oxide shells becomes a necessary part of coating formation) on the surface and enabling an intimate contact between the particles and the substrate/deposited material. This hypothesis is supported by such findings: (1) a wide range of ductile materials can be cold sprayed while non-ductile materials can be deposited only if they are co-cold sprayed with a ductile (matrix) material – plastic and localized deformation; (2) the mean deposition particle velocity should exceed a minimum critical velocity value to achieve deposition, which suggests that sufficient kinetic energy must be available – plastic deformation/disruption and cleaning of the surface films (Ref 16).

Moreover there are a number of phenomena that are frequently responsible for inter-phase bonding such as interfacial melting, atomic inter-diffusion and plastic deformation which are now believed not to play a significant role in the bonding mechanism of cold spray. This conclusion was elaborated based on the following (Ref 16):

The average kinetic energy of the particles is significantly lower than the energy required to melt the particle/substrate interfacial region meaning that the particle/substrate bonding is a solid-state process;

Provided very short particle/substrate contact times, atomic inter-diffusion is not expected to play a significant role in particle/substrate bonding. This can be readily proven as follows: the metal-to-metal inter-diffusion coefficient at temperatures near the melting point is of the order of 10^{-15} to 10^{-13} m^2/s, and for a typical particle/substrate contact time of 40 ns, the atomic inter-diffusion distance is between 0.004 and 0.1 nm. Since this distance is only a fraction of the inter-atomic distance, atomic diffusion at the particle/substrate interface should be excluded as a dominant particle/substrate bonding mechanism under the dynamic cold-spray deposition conditions.

So it is possible to conclude that the temperatures that are achieved in the interfacial region will be neither enough to produce interfacial melting nor to significantly promote atomic inter-diffusion, plus, adhesion is an atomic length-

scale phenomenon and its occurrence is controlled by the presence of clean surfaces and high contact pressures (Ref 16).

As mentioned before, in order for efficient adhesion to take place at the particle/substrate contact surfaces, such surfaces must be clean and subjected to high contact pressure plus, and all of the particle's kinetic energy must be transformed into heat and strain energy to the coating and substrate. A phenomenon known as adiabatic shear instability and the localization of the plastic flow into interfacial jets will ensure cleanliness of the surfaces during cold spray; thus high particle velocities will ensure the necessary high levels of particle/substrate contact pressure. At the highly strained interfaces, oxide shells are broken and the heated surfaces are pressed together and are thus bonded. In cold spraying, in particular, ductility is needed to obtain sufficient flattening of particles in order to build up a dense coating (Ref 25). This and the resultant plastic-flow localization are the phenomena that are believed to play a major role in the particle/substrate bonding during cold spraying.

Adiabatic shearing, occurring at strain-rates above 10^3 s^{-1}, is expressed as a much critical thermo-plastic material instability, i.e., by the balance between only the two strain-rate hardening and thermal softening terms. This meaning that, under adiabatic conditions, the plastic strain energy dissipated as heat increases the temperature causing thermal material softening and consequently decreasing the rate of strain hardening (Ref 33, 34). It has also been suggested that the dissipation of kinetic energy into heat is strain rate dependent, i.e., the fraction of plastic work dissipated into heat would be larger for higher strain rates. This would further support the assumption of adiabatic heating in cold gas sprayed particles (Ref 33).

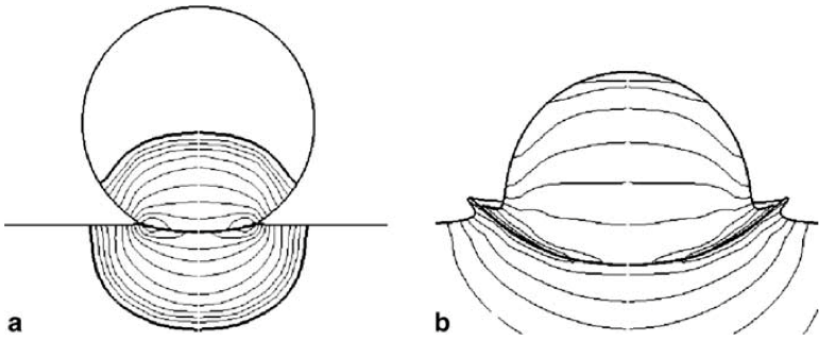

Figure 19. Pressure field during impact (a), jetting (b) (Ref 25).

When a particle first impacts, a strong pressure field propagates spherically - Figure 19 (a) – into the particle and the substrate from the point of first contact. This is followed by generation of a shear load, due to a pressure gradient at the gap between the colliding interfaces, accelerating the material laterally and thereby causing localized shear straining. Adiabatic shear instabilities phenomenon will appear when the impact pressure and the respective deformation are high enough thus occurring thermal softening of the material meaning that the latter process is locally dominant over strain and strain-hardening, which leads to a discontinuous jump in strain and temperature and consequently an immediate breakdown of stress. Also, in this region, the viscous flow will generate an out-flowing material jet with material temperatures close to the melting temperature – Figure 19 (b) (Ref 25). The coating build-up is not a simple one-particle impact, but rather a series of multiple impacts that transfer the incoming particle's kinetic energy to the substrate initially and then to the coating. A multistep process has been suggested consisting of substrate cratering and first-layer build-up, followed by particle deformation and realignment, metallurgical bonding and void reduction (Figure 20). When the deposition process is about to end it should be expected to have a not as well compacted last layer of coating as the first and medium ones, since the last particles that arrive and conform the last layer will not be impacted by any other particles and be subjected to the previously discussed mechanisms.

It is also suggested that an interfacial instability-based mechanism, by which interfacial mixing/interlocking occur, may also contribute to particle/substrate bonding. Interfacial instability can arise when two fluids are moving at different velocities in a direction parallel to their interface. When an interface is subjected to a perturbation, then as one fluid flows around the other a centrifugal force is generated thus raising a change in pressure, which may promote amplification of the interfacial perturbations. These instabilities may then lead to the formation of interfacial roll-ups and vortices which may enhance the overall strength of interfacial bonding in at least three ways: (1) by significantly increasing the interfacial area available for adhesion; (2) by producing a fine length-scale mixing of the two materials; (3) by creating mechanical interlocking between the two materials. Also a particle length-scale, rivet-like mechanism may also be operative and its onset may be linked with the minimum critical particle velocity (Ref 16, 33, 35).

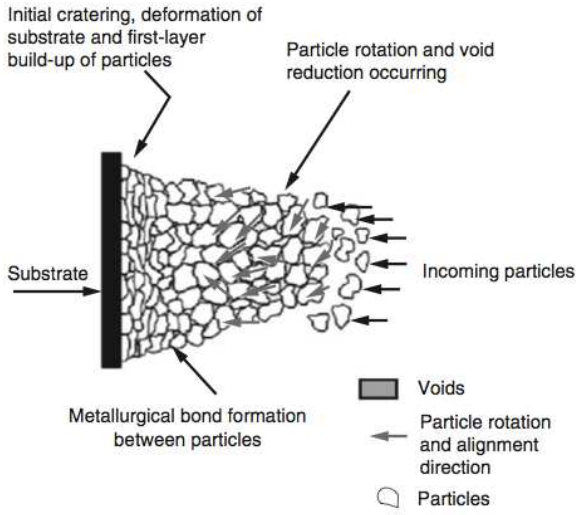

Figure 20. Multi-stage coating formation using the cold spray process (Ref 16).

5 EXPERIMENTAL PROCEDURE

5.1 Technologies

Cold Gas Spray and High Velocity Oxy-Fuel were used as main technologies to produce coatings in this Thesis.

Cold Gas Spray

The CGS equipment was a KINETICS® 4000 (Cold Gas Technology, Ampfing, Germany), with a maximum operating pressure of 40bar, temperature of 800°C and it used nitrogen as the process gas. Besides, KINETICS® 4000 has the possibility of using a pre-chamber of 120mm in length connected to the nozzle of the gun where the feedstock powders are heated up for a longer time.

As explained previously, CGS is a process that is affected by several parameters. During this Thesis and after deep theoretical studying, gas pressure and distance were chosen as the main variable parameters. For this reason a factorial design of experiments was made for each one of the three different studied powders, in order to optimize the spraying conditions.

Factorial design of experiments

An experimental design is a plan for assigning experimental units to treatment levels and the statistical analysis associated with the plan. It identifies the independent, dependent and nuisance variables of the studied process and tell us the way in which randomization and statistical aspects of an experiment are to be carried out; the main goal of an experimental design is to establish causal connections between the independent and dependent variables and to extract the maximum amount of information with the minimum expenditure of resources (Ref 37, 38). As said, in the experimental design there are three types of variables:

- Controllable factor: this factor can be manipulated and which handling will affect the response variable. Its handling helps to draw conclusions.

- Uncontrollable factor: this factor cannot be manipulated and can affect the response variable so one has to predict its influence on this.

- Response variable: both controllable and uncontrollable factors act on this variable and which is used to draw conclusions and therefore the main variable to study.

These variables and factors can be either dependent or independent in order to inter-relate between them and eliminate some parameters of the studied process. Factorial design is a type of experimental design in which the experiment will have two or more factors to be studied at two or more levels so this means that, those experimental units take on all possible combinations of these levels across all such factors. Most factorial experiments each factor has only two levels.

Considering all the different process parameters by gathering and analyzing experimental data to improve the spraying performance, a structured data table that contained substantially important data about structured variation/interactions, was generated, allowing a greater understanding of the process from fewer experiments (Ref 37). After defining the fixed and variable parameters, a total of 3 levels for each factor (variable parameter) were selected.

The 3^k factorial design comprised k factors of three levels each: low, medium and high. Of all the 3^k factorial designs, 3^2 of them correlated only two factors from the three levels; this means that there were a total of $3^2 = 9$ possible treatment combinations. Distance values ranged from 10 to 40mm and gas pressure from 30 to 40bar.

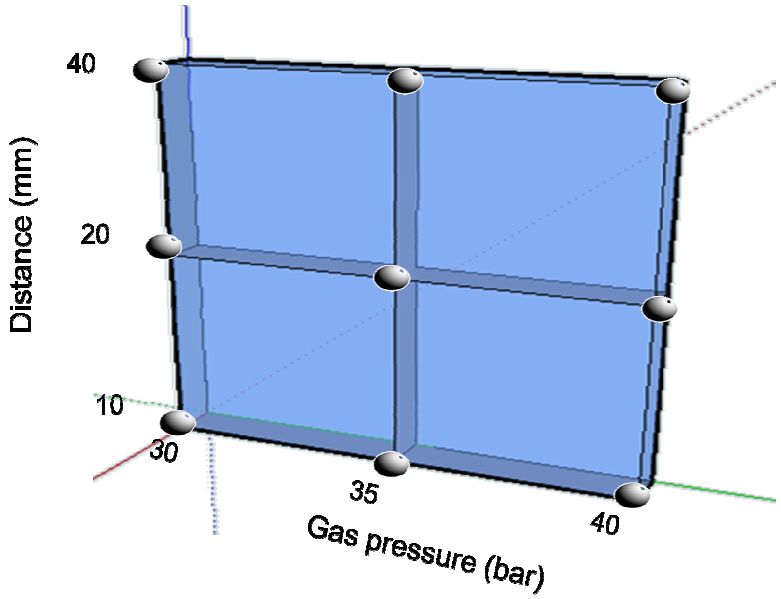

Figure 21. Example of a 3^2 factorial design table, where it correlates 2 different variable spraying parameters: distance (mm) and gas pressure (bar).

5.2 HVOF

The HVOF equipment used was a Sulzer (Winterthur, Switzerland) DJH with two different heads: DJH 2700 for propylene and DJH 2600 for hydrogen.

5.3 Characterization techniques

- Microscopy: Optical Microscopy (DMI-M Leica), Scanning Electron Microscopy (JSM-5310, Jeol – ProX, Phenom) and Field-Emission Scanning Electron Microscopy (401s, Hitachi) were used for the observation of feedstock powders, substrates and coated pieces. Previous metallographic preparation was done following the standard ASTM E3-95;

- Energy Dispersive Spectroscopy (EDS): Common point and scanning analysis (Xflash detector X5010, Bruker) were carried out in powders and coatings;

- X-Ray Diffraction (XRD): crystalline composition of different powders, substrates and coatings was analyzed by means of a diffractometer (X'Pert PRO MPD, PANalytical);

- Laser Scattering (LS): particle size distribution must be specially controlled and it was carried out using a Laser Diffraction Particle Size Analyser Beckman Coulter LS 13320;

- Hardness: this parameter has been evaluated by means of a Matsuzawa MTX-α Vickers equipment according to the ASTM E384-99 standard;

- Tensile Strength: coating adhesion has been evaluated following the ASTM C-633 standard with SERVOSIS ME-402/10 equipment;

- Roughness: roughness of the substrate must be especially controlled in TS processes and it was conducted in this study using a rugosimeter SJ-210 (Mitutoyo);

- Rubber-Wheel: abrasive wear tests were perfomed using a CM4 Ingeniería Mecánica OL-2000 following ASTM G65-00 standard;

- Ball-on-Disk: following ASTM G99-04 standard adhesive wear tests were performed using a CM4 Ingeniería Mecánica OPB;

- Confocal laser microscopy: to measure the lost volume and recreate the wear tracks of the coatings (Leica TSE-SE);

- Electrochemical resistance: was measured with a EG&G Parc-273 equipment;

- Salt fog spray: the resistance of the coatings to an aggressive corrosive environment was tested following ASTM B117-03 (Dycometal SSC-400);

- Grit-Blasting: corundum particles were propelled to substrates using a stream of compressed air (MAB-4, Mab Industrial, S.A.).

Further detailed information about the experimental procedure is found in Papers 1 – 4.

6 RESULTS AND PARTIAL DISCUSSION

6.1 Cold Gas Spray

a) Paper 1:

S. Dosta, M. Couto, J.M. Guilemany, Cold spray deposition of a WC-25Co cermet onto Al7075-T6 and carbon steel substrates, Acta Materialia, 2013

The following paper presents the first results obtained with the CGS technology. It was the first time ever that a WC-25Co powder was successfully sprayed by CGS onto low carbon steel and Al7075-T6 substrates using nitrogen as process gas. It was focused on obtaining excellent quality coatings by CGS and characterizes them as well as their mechanical and electrochemical properties.

Available online at www.sciencedirect.com

SciVerse ScienceDirect

Acta Materialia 61 (2013) 643–652

Acta MATERIALIA

www.elsevier.com/locate/actamat

Cold spray deposition of a WC-25Co cermet onto Al7075-T6 and carbon steel substrates

S. Dosta, M. Couto *, J.M. Guilemany

Thermal Spray Centre, CPT, Universitat de Barcelona, 08028 Barcelona, Spain

Received 21 June 2012; received in revised form 8 October 2012; accepted 11 October 2012
Available online 10 November 2012

Abstract

This work focussed on the deposition of wear-resistant and corrosion-resistant WC-25Co cermet powders on carbon steel and aluminium (Al7075-T6) substrates by cold gas spraying (CGS). The unique combination of mechanical, physical and chemical properties of WC-Co cermets has led to their widespread use for the manufacture of wear-resistant parts. X-ray diffraction tests were run on the powder and coatings to determine possible phase changes during the spraying process. The bonding strength of the coatings was measured by adhesion tests (ASTM C633-08). The sliding (ASTM G99-04) and abrasive (ASTM G65-00) wear resistance of the coatings were also studied. Corrosion resistance was determined by electrochemical measurements and salt fog spray tests (ASTM B117-03). CGS achieved thick, dense and hard WC-25Co coatings on both aluminium alloy Al7075-T6 and carbon steel substrates, with excellent tribological and electrochemical properties. We thus conclude that this method is very competitive compared with conventional thermal spraying techniques, giving thick, dense and hard coatings on both aluminium alloy Al7075-T6 and carbon steel substrates, with excellent tribological and electrochemical properties.

Keywords: Submicronic carbides; WC-25Co coatings; Cold spray; Wear resistance; Corrosion resistance

1. Introduction

WC-Co coatings are usually produced by conventional thermal spray techniques, such as high velocity oxy-fuel (HVOF) spraying, which use high temperatures to melt the powder particles and form a coating. However, this approach causes decarburization of the powder. Also, concern has been raised about reducing the particle size of the WC-Co powders currently used as spraying materials, despite knowledge that a reduction in particle size (from micrometric to submicrometric to nanometric) until a specific lower limit imparts improved performance in terms of hardness and wear resistance properties [1–5]. The effect of reducing the average particle size leads to a higher particle velocity and, consequently, a lower gas/particle temperature is required [6]. The drawback of using these powders in conventional thermal deposition techniques is that the process temperatures lead to undesirable effects in addition to decarburization, such as the formation of W_2C, W and/or fragile η phases [7–9]. Another deposition process known as warm spraying has been reported to successfully deposit WC-Co powders on carbon steel substrates, with scarce formation of the phases mentioned above. This process uses nitrogen to control the gas temperature, thereby allowing control of a wide range of temperatures used for deposition of the particles [4,5,10].

The cold spray technique is a solid-state deposition process where no melting of the powder particles occurs in a supersonic jet of compressed gas which deposits them on a substrate, where they deform and rapidly bond together, to build up a thick layer of material [11,12]. Although some experiments by Kim et al. reported cold spraying of WC-Co cermet powders using nitrogen as the carrier gas, this method has not been successfully tested to date [13,14]. The cold spray process is influenced by several parameters.

* Corresponding author.
E-mail address: mcouto@cptub.eu (M. Couto).

1359-6454/$36.00
http://dx.doi.org/10.1016/j.actamat.2012.10.011

The study of these allows researchers to gain an insight into the nature of the cold spray phenomenon and the way in which the basic coating properties can be controlled [12,13]. The main objective of this study was to determine the optimum spraying conditions for a submicron WC-25Co powder in order to obtain good quality coatings on aluminium alloy Al7075-T6 and carbon steel substrates. For this purpose we performed several mechanical and electrochemical tests to evaluate the quality of coatings achieved under a range of spraying conditions. The best results were then compared with those obtained by conventional thermal spraying techniques, namely HVOF spraying.

2. Experimental procedure

The studied powder was an experimental WC-Co cermet with 25 wt.% cobalt content obtained by agglomeration and sintering. This powder was processed and provided by Fujimi Inc. (Kiyosu, Japan). The powder was sprayed onto several samples of two distinct substrates of carbon steel and aluminium Al7075-T6 coupons: flat substrates ($100 \times 20 \times 5$ mm) and cylindrical substrates (diameter 25.4 mm, height 25.4 mm). The substrate was prepared by grinding using 240 grit SiC paper. The available cold spray equipment was a Kinetics® 4000/17 kW (Cold Gas Technology, Ampfing, Germany) with a maximum operating pressure of 40 bar and temperature of 800 °C, and limited to the use of nitrogen as the carrier gas. The powder was characterized by studying the microstructure by scanning electron microscopy (SEM) and field emission SEM (FE-SEM), the particle size distribution by laser diffraction (LS), the phase composition by X-ray diffraction (XRD) and the element composition by energy-dispersive spectroscopy (EDS). The coatings were also characterized by SEM and their phase composition by XRD. Vickers hardness tests were also performed to identify the best coatings obtained with the pre-experimental spraying parameters. Finally, mechanical and electrochemical tests were run on the selected optimum coatings to determine their properties and behaviour when tested under tensile load, abrasive and adhesive wear situations, and electrochemical corrosion and fog spraying conditions.

In order to optimize the spraying conditions an experimental design was produced to determine which factors (parameters) and interactions between them are most important when it comes to obtaining the final coating. Considering all the different process parameters by gathering and analysing experimental data in order to improve the spraying performance, a structured data table containing important data about structured variations/interactions was generated, allowing a greater understanding of the process from fewer experiments [15]. After defining the fixed and variable parameters, a total of three levels for each factor (variable parameter) were selected. The 3^k factorial design comprised k factors of three levels each: low, medium and high. Of the 3^k factorial designs 3^2 of them correlated only two factors from the three levels, meaning that there was a total of $3^2 = 9$ possible treatment combinations. Regarding the fixed process parameters, nitrogen was chosen as the process gas, 800 °C as the gas temperature, 90° as the spraying angle, and 250 mm s^{-1} as the gun speed. The chosen variable parameters were gas pressure, with values ranging from 30 to 40 bar, and distance values, ranging from 10 to 40 mm. These parameters were defined on the basis of previous results obtained at the Thermal Spray Centre of the University of Barcelona.

The quality of coating adhesion to the substrate is a major performance criterion. In order to determine the bonding strengths of the coatings adhesion tests were performed on two samples of each selected coating following the ASTM F1147 (2005) standard. A Servosis model ME-402/10 test apparatus was used at a velocity of 0.02 mm s^{-1}, which was controlled by position.

Two kinds of wear tests were performed to measure the wear resistance of the coatings. A sliding wear test was carried out using a ball on disk (BoD) method, following the ASTM G99-04 standard. A WC-12Co ball, a sample relative velocity of 131 r.p.m., a total test length of 1000 m and a force load of 25 N were the parameters selected for test purposes. Humidity and temperature were kept below 20% and 25 °C, respectively. Leica TCS-SE confocal equipment was used to measure the volume loss of the wear tracks and to recreate the wear path.

Dry abrasive tests (ASTM G65-00 standard) were carried out using a rubber wheel system with a rotation rate of 139 r.p.m., a load of 50 N, and a SiO_2 flux of between 250 and 310 g min^{-1} [8]. Material loss was measured by weighing the samples every 1 min during the first 5 min, and then every 5 min until the end of the test.

We evaluated the resistance of the samples to corrosion by performing electrochemical measurements in 80 ml of an aerated, unstirred 3.4% NaCl solution. The open-circuit potential (E_{OC} vs. time) and polarization curve (PC) were measured using EG&G Parc-273 equipment. Polarization experiments were carried out in the potential range −100 to +350 mV. All electrochemical experiments were performed at room temperature.

In addition a salt fog spray test was carried out, following the ASTM B117-03 standard, with a 5% NaCl solution at 35 °C, 15 mm^3 h^{-1} collected solution, and 1 bar.

3. Results and discussion

3.1. Structural characterization

3.1.1. Powder characterization

The powder had a micrometric particle size with submicron WC particles (measured by FE-SEM) and an average particle size of 32 ± 10 μm. The powder had a spheroid and relatively uniform morphology as well as a narrow particle size distribution (Fig. 1a). XRD analysis of the powder showed that no additional unusual phases of WC and Co, such as W_2C, W, Co_6W_6C and Co_3W_3C, were present.

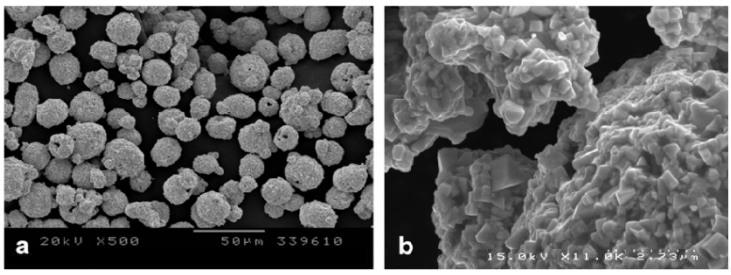

Fig. 1. (a) SEM and (b) FE-SEM micrographs of the free surface of the DTS-W775-32/10 powder at 500×, and a higher magnification image of a particle at 11,000× showing the submicron carbides.

The EDS cross-sectional analysis of the WC-Co powder also confirmed the sole presence of elemental W and Co.

3.1.2. Characterization of the coatings

Previous experiments using low temperatures (600 °C) and pressures below 30 bar (Fig. 2) and distances greater than 40 mm showed poor substrate coating adherence and inter-layer adherence as well as delamination and the presence of cracks in the final layers of the deposited material. Above 600 °C the initial particle temperature resulted in a softer material and a requirement for less kinetic energy (critical velocity) to heat the particle surface area by plastic deformation, thereby resulting in improved coating quality [16].

The mechanical and electrochemical properties of the coatings can be enhanced by the compressive effect of the impinging particles during spraying, thus allowing a non-porous coating without the presence of cracks.

After the first characterization and study of the coatings sprayed onto Al7075-T6 and carbon steel substrates the optimum spraying conditions were chosen from the previously defined testing conditions. These test conditions varied from 600 to 800 °C gas temperature, 30 to 40 bar gas pressure and 10 to 40 mm spraying distance. Since Al7075-T6 is more ductile than carbon steel the impacting particles interact differently with each substrate in the early stages of coating, thus optimization of the spraying parameters was studied for both two substrates.

Afterwards other defined optimum sets of conditions for each substrate were used in order to study their mechanical and electrochemical properties.

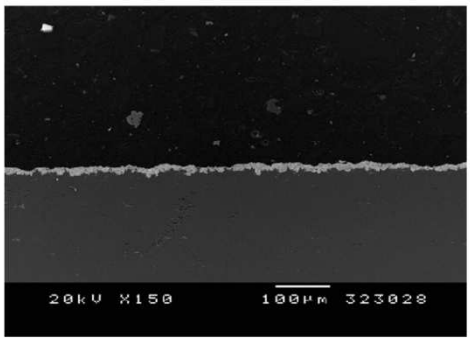

Fig. 2. Example of a WC-25Co coating on Al7075-T6 using the process conditions: nozzle substrate distance 40 mm, gas temperature 600 °C, pressure below 30 bar.

3.1.2.1. Coatings obtained on Al7075-T6 substrate. Several spraying conditions were tested from the variable parameters (gas pressure and distance) defined in the experimental design. Fig. 3 depicts representative cross-section SEM micrographs of coatings sprayed under distinct conditions onto Al7075-T6 substrate. At lower pressures and shorter spraying distances the coatings showed extensive delamination, cracking between layers and a lack of homogeneity (Fig. 3a). These conditions were insufficient to provide a homogeneous and dense (well-compressed) coating because of a lack of kinetic energy imparted in the particles when they hit the substrate. For a coating obtained while spraying at higher pressures and larger distances a very high density was achieved. When the gas pressure was raised to the maximum there was erosion of the coating their final layers, as shown in Fig. 3a. An intermediate set of spraying parameters, with a temperature pressure ratio of 22.9 and a spraying distance of 20 mm, produced a homogeneous and dense coating without any cracks or delamination, as shown in Fig. 3b and c, in which good bonding with the substrate can be seen. This finding can be explained by the critical velocity theory for particles, which states that when a particle reaches its critical velocity before impacting the substrate it will successfully adhere and bond to it or to already deposited particles, in addition to compressing the layer. The optimum coatings obtained on Al7075-T6 substrates had average thicknesses of 211 ± 24 µm and Vickers hardness values of 848 ± 55 HV_{300}. In previous studies with a WC-12Co powder sprayed onto an aluminium alloy substrate by HVOF spraying Magnani et al. [17] reported hardness values of 1094 ± 21 HV_{300} before delamination. A comparison of these observations with our results indicates that the CGS technique improves the quality of coatings, considering that a decrease in the Co matrix content will provide greater hardness. Furthermore, during spraying with the

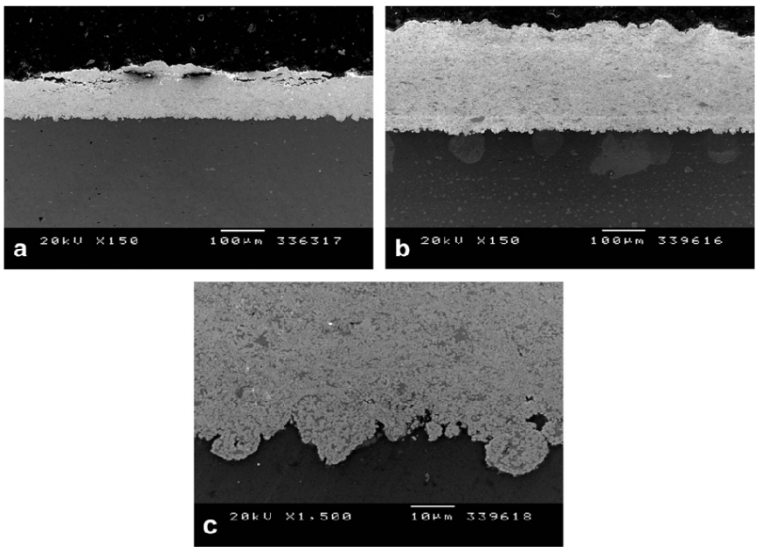

Fig. 3. SEM micrographs of selected coatings on the Al7075-T6 substrate. (a) A coating showing evidence of significant erosion due to a high gas pressure. (b, c) Micrographs of coating A1.

CGS technique particles are not decarburized nor do they form fragile η phases, implying that the bulk properties of the powder are retained. In contrast, in HVOF spraying a hardening effect caused by the W_2C and η phases formed as a result of the high flame temperatures provide a false hardness indicator. The deposition efficiency of the process was approximately 24%.

To facilitate discussion of the results the samples coated on Al7075-T6 using the optimum spraying conditions will be referred to as A1.

3.1.2.2. Coatings obtained on carbon steel substrate. At the maximum temperature and pressure of the system the coatings showed neither erosion of the final layers nor cracking/delamination (Fig. 4b). However, they did show a high density, with very little visual evidence of porosity. Furthermore, the high magnification SEM micrograph of the coating depicted in Fig. 4c shows excellent bonding between the substrate and the initial layers of sprayed powder, with well-distributed and embedded WC particles in the Co matrix. These results were achieved with a temperature pressure ratio of 20 and spraying distance of 10 mm. As carbon steel is harder than the Al7075-T6 substrate the first impacting particles showed greater deformation. Of note is the difference in adhesion of the first particles to impact on the different substrates studied (Figs. 3c and 4c). At lower pressures (Fig. 4a) the coatings were less homogeneous and deposition was less efficient. The increase in spraying distance had an inverse effect to that of raising the gas pressure as it decreased particle velocity, producing worse results. The optimum coatings sprayed onto the substrates had thicknesses of 263 ± 32 µm and hardness values of 981 ± 58 HV_{300}. In a study of HVOF spraying of a WC-17Co coating onto carbon steel substrates Liao et al. reported values of 1126 ± 30, which is harder than WC-25Co as a result of the higher content of a hard phase [18]. However, the CGS results proved competitive and noteworthy. Kitamura et al. presented HV_{200} values of approximately 675 ± 50 after depositing conventional WC-25Co powders onto stainless steel substrates [10]. These values are considerably lower than those achieved in the present study. The deposition efficiency of spraying the studied powder onto a carbon steel substrate was approximately 17%. XRD tests (Fig. 5) showed neither contamination of the powder nor the presence of fragile phases. To facilitate discussion of the results the samples coated on carbon steel using the optimum spraying conditions will be referred to as CS1.

To confirm the presence of the same phases as those present in the powder XRD tests (Fig. 5) were run on the coatings obtained on both the Al7075-T6 and carbon steel substrates. The W carbides in the particles did not decarburize, and no fragile or hard η phases were formed during spraying.

3.2. Adhesion tests

To measure the quality of the substrate coating interface bonding and inter-layer adhesion adhesion tests were performed on samples prepared under the same spraying conditions. Coatings CS1 had σ values of 74 ± 6 MPa. The mechanism of breakage was also determined. A phenomenon known as adiabatic shear instability and localization of the plastic flow in interfacial jets ensure cleanliness

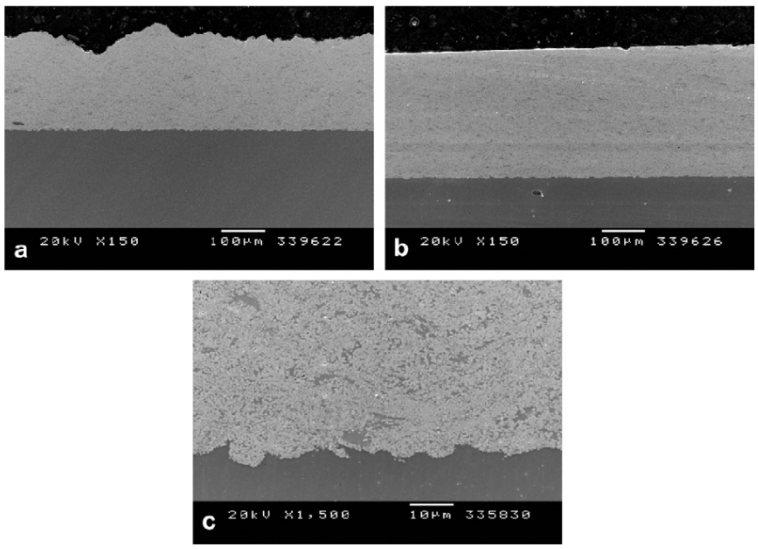

Fig. 4. SEM micrographs of selected coatings obtained on the carbon steel substrate. (a) Micrograph of a coating obtained at lower pressures. (b, c) Micrographs of coating CS1.

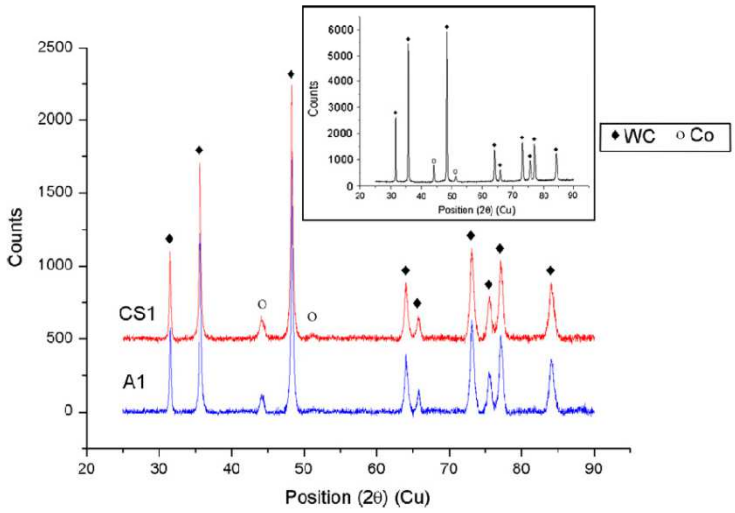

Fig. 5. XRD analysis of the optimum coatings (A1 and CS1) obtained on Al7075-T6 and carbon steel, and a comparison with XRD analysis of the experimental powder.

of the surfaces during cold spraying, thus high particle velocities will ensure the high particle/substrate contact pressures required. At highly strained interfaces oxide shells are broken and the heated surfaces pressed, thence the passivation layer of alumina present on the surface of the aluminium alloy substrate will not influence the adhesion quality. In cold spraying a certain degree of ductility of the particles and hardness of the substrate are needed to obtain sufficient localized plastic deformation, i.e. flattening of the particles, in order to build up a dense coating; the harder the substrate, the greater the flattening of the particles [16,19]. This and the adiabatic shear instabilities resulting from a high strain rate deformation upon impact are the phenomena believed to play a major role in particle/substrate bonding, influenced by the spraying conditions and powder characteristics, during cold spraying.

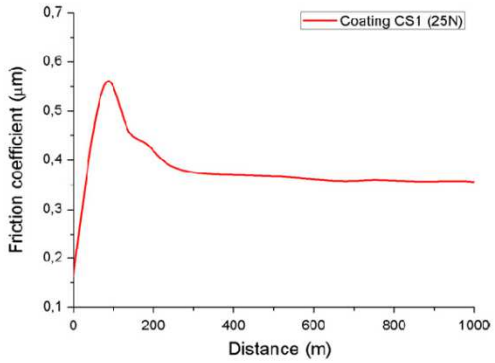

Fig. 6. Evolution of the friction coefficient for coating CS1 sprayed onto carbon steel substrate.

Adiabatic shear is expressed as a critical thermo-plastic material instability. This implies that under adiabatic conditions the plastic strain energy dissipated as heat increases the temperature, thus causing thermal material softening and, consequently, a decrease in the rate of strain hardening [16,19]. Assadi et al. proposed that the dissipation of kinetic energy as heat is strain rate dependent, i.e. the fraction of plastic work dissipated as heat would be larger for higher strain rates. This notion would further support the assumption of adiabatic heating in CGS. The coatings failed at the substrate coating interface meaning that interlayer bonding was stronger than that of the substrate coating interface.

3.3. Sliding tests (ball on disk)

Evolution of the coefficient of friction of coating CS1 is shown in Fig. 6. Coating CS1 shows a slightly higher friction wear resistance than coating A1. The wear resistance during testing CS1 proved to be quite high, with non-uniform material loss being observed. SEM characterization and EDS analysis showed that there was little material loss, which was occurring mainly by abrasion at the beginning of the test, pulling off some WC-Co particles from the coating. The wear mechanism seems to start with the extraction of carbides from the matrix, even though the binder phase acts as an excellent support for these. The carbides that are not removed maintain their wear resistance function, thus explaining the low wear rates observed. Fig. 7a shows slight wear of some parts of the wear track as well as displacement of entire particles during testing. The wear mechanism discussed is the same for coatings obtained on carbon steel and Al7075-T6, hence the depiction of a single wear track showing a representative area of the wear track produced after testing the CS1 coating. Satisfactory dispersion of the carbides provided excellent sliding wear behaviour. In previous studies of WC-Co coatings produced by HVOF spraying Shipway et al. reported that the sliding wear rate of sprayed coatings increases with an increase in decomposition products, especially W_2C [20], which are formed due to the high temperatures during spraying. The material applied by CGS technology did not undergo any phase changes or decomposition. Thus the wear rate of the coatings was not impaired. Coating CS1 displayed very uniform and constant behaviour throughout the test, with a final friction coefficient of 0.38 ± 0.03 for a test force load of 25 N. Debris was detected at the edges of the wear track, which may indicate the presence of W and Co lubricant oxides as a result of the high temperatures achieved during the process and may help explain the excellent behaviour and almost no material loss found. Patches of debris appeared along the wear path as dark areas. EDS analysis at specific points along the wear path confirmed the presence of oxides that could be responsible for the lubricant effect. Coating A1 had a higher sliding wear resistance than CS1, with a final friction coefficient of 0.41 ± 0.02 for a test force load of 25 N. The wear mechanism was the same as that acting during the sliding test on coating CS1. EDS analysis (Fig. 9) also showed the presence of lubricant oxides at the edge of the wear track. This observation is attributable to the debris pulled off during the test and the high temperatures reached. As both coatings resulted in a very small wear track profilometric measurements were performed using a confocal laser technique to quantify the material lost and to measure the path diameter. Fig. 8 shows the wear track reconstruction after test-

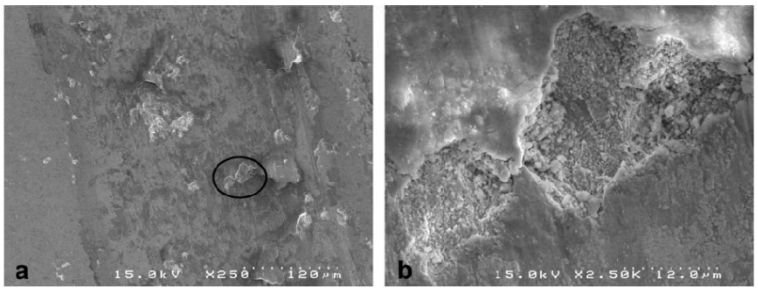

Fig. 7. FE-SEM micrograph of (a) a representative sliding wear area after testing, where a slightly more worn area can be seen, as well as (b) the ripping off of an entire particle in the close-up micrograph.

ing on coatings A1 and CS1. This approach allowed measurement of the volume lost and wear track diameter for each coating. Coating A1 had a volume loss of approximately 0.010 mm^3 and the test produced a 550 μm diameter wear track, while CS1 lost approximately 0.011 mm^3 and had a wear track diameter of 500 μm. Initially the test conditions were less severe in terms of force load, a force of load of 15 N was used, but no visible wear track was produced, thus making it impossible to measure the volume of coating material lost during the test or to study the sliding wear resistance of the coatings. However, the coefficient of friction results obtained from these tests were useful to compare them with those obtained under the same test conditions at 15 N and 1000 m by Guilemany et al. [7] for a WC-12Co conventional powder deposited on carbon steel by means of HVOF spraying. In that study the authors reported a coefficient of friction of 0.282 for the last 200 m of the BoD test [7]. Comparing this value with the coefficient of friction results of 0.32 ± 0.05 obtained for the coating deposited on a carbon steel substrate under

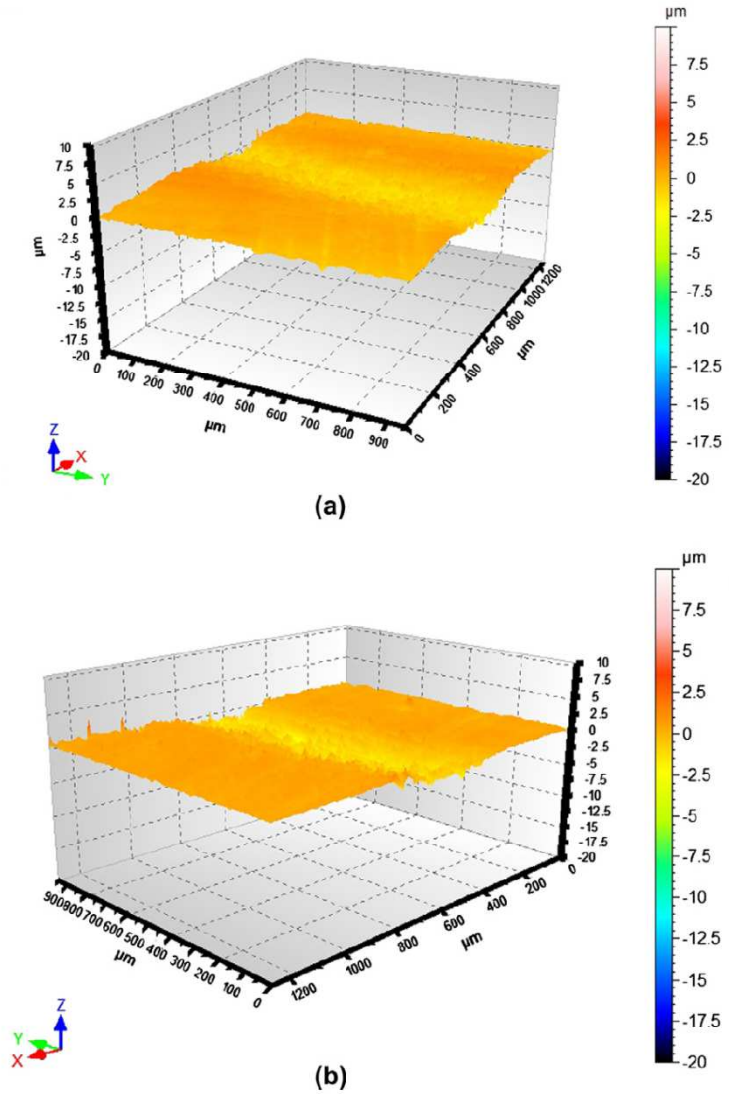

Fig. 8. Wear track reconstruction of coatings A1 and CS1, respectively, after a BoD test.

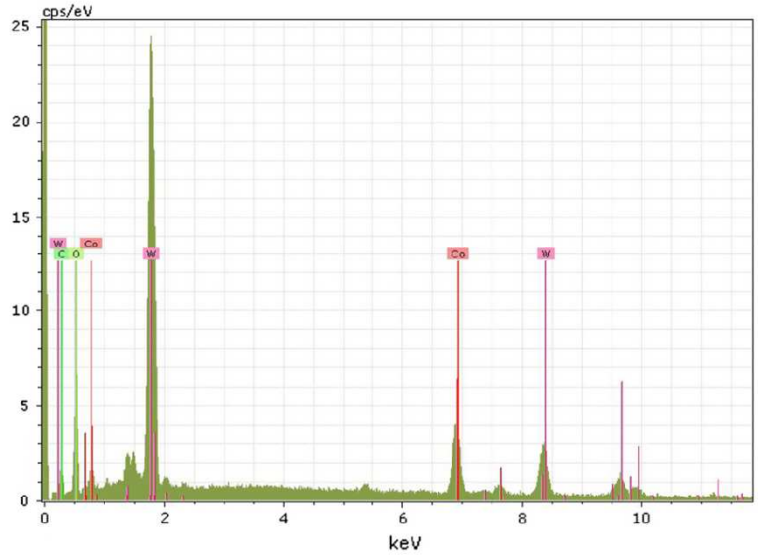

Fig. 9. EDS analysis performed at the wear track borders of A1 and CS1 coatings showing the presence of oxides.

the same test conditions it is apparent that similar behaviour can be obtained when spraying WC-25Co powder by CGS, without an adverse effect on the ductile Co matrix.

3.4. Abrasive tests (rubber wheel)

Samples of coatings A1 and CS1 were also tested using an abrasive rubber wheel, which resulted in wear rates of $2.75 \times 10^{-5} \pm 5.4 \times 10^{-7}$ and $2.87 \times 10^{-5} \pm 1.85 \times 10^{-6}$ - $mm^3\,N\,m^{-1}$ for the optimum coatings sprayed onto Al7075-T6 and carbon steel substrates, respectively. There was a substantial decrease in the wear rate during the first minutes of testing as a result of the high initial surface roughness values: $R_{a\ Al7075\text{-}T6\ substrate} = 9.1\ \mu m$ and $R_{a\ CS\ substrate} = 8.19\ \mu m$. Since the coatings exhibited similar average Vickers hardness values, $884 \pm 55\ HV_{300}$ for coating A1 and $981 \pm 58\ HV_{300}$ for CS1, and the composition of the powder was the same, the coatings were expected to behave in a similar manner when subjected to abrasive wear tests, as seen in Fig. 10. The good distribution of WC carbide particles in the metallic Co matrix and the homogeneous and sub-micrometric size of the carbide particles, without detrimental brittle phases, led to high abrasion resistance. Guilemany et al. reported abrasive wear rates of about 1.0×10^{-5} after 30 min testing for WC-12Co powders sprayed by a conventional HVOF spray method onto carbon steel substrates [7]. Although the wear rate obtained for the carbon steel substrate was higher after 30 min, it should again be noted that, unlike HVOF spraying, the CGS technique does not produce fragile or hard WC phases during deposition. As a result of this the HVOF approach achieves a harder coating surface and a slight

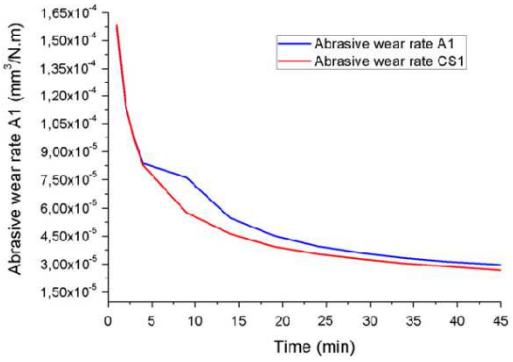

Fig. 10. Abrasive (rubber wheel) wear rates vs. time curves for the A1 and CS1 coatings.

improvement in wear rate, although the latter should be considered a "false" indicator because of these fragile and brittle phases. Furthermore, WC-12Co powder will have a higher hardness value and, consequently, a better wear behaviour than WC-25Co because of the increase in the hard WC phase. Thus WC-25Co coatings deposited by the CGS technique can compete with a WC-12Co coating produced by HVOF spraying in terms of abrasive wear resistance.

3.5. Electrochemical tests

Electrochemical tests in aerated and unstirred 3.5% NaCl solution were run to determine the resistance of the

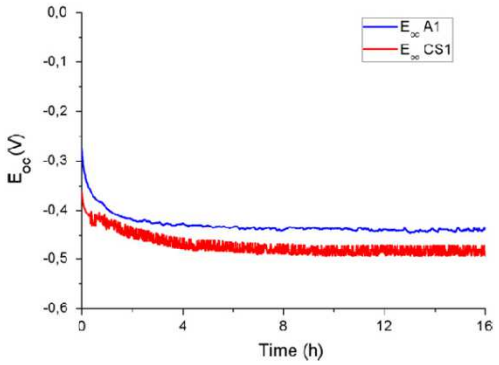

Fig. 11. Open-circuit potential (E_{oc}) vs. time (h) curves for coatings A1 and CS1.

coatings to corrosive conditions. The results are shown in Fig. 11. Initially the curves corresponding to coatings A1 and CS1 show a decrease in potential due to the dissolution of oxides in the coating surface and penetration of the electrolyte. The potentials after 16 h immersion were -0.439 ± 0.018 V for coating A1 and -0.481 ± 0.016 V for CS1.

On the basis of these results it can be concluded that the electrolyte had not reached the substrate coating interface after 16 h immersion, as seen in the E_{oc} vs. immersion time plot (Fig. 11). Since the electrical potential of Al7075-T6 was about -0.687 V and the test result for coating A1 after 16 h immersion was -0.439 ± 0.018 V it is apparent that the electrolyte did not reach the substrate and no oxides were formed on the surface of the test sample. Coating CS1 showed constant behaviour throughout the test. The same phenomenon was observed with the dissolution of oxides present in the surface of the coating at the beginning of the test, thus accounting for the steep decrease in potential. Coating CS1 resisted penetration of the electrolyte. Guilemany et al. [7,8] reported that a microstructured WC-12Co coating obtained by HVOF spraying onto carbon steel subjected to the same electrochemical test conditions for 18 h had a potential of -0.53 V. This result was closer to the -0.744 V value of carbon steel than the -0.481 ± 0.016 V value obtained after 16 h immersion in the present study. Although greater corrosion resistance is expected for a WC-12Co coating than WC-25Co, due to the lower Co content, the higher density of coating achieved by the CGS method prevented the electrolyte from attacking the Co matrix interface, thereby increasing the resistance of the coating to corrosion.

A salt fog spray test was carried out on samples using the same spraying conditions for coatings A1 and CS1 until the first signs of corrosion appeared. Both coatings remained unaltered for more than 500 h. This observation confirms that the coatings had similar corrosion resistances, confirming the results of the electrochemical tests.

4. Conclusions

- Dense, thick and well-bonded WC-Co coatings were achieved on both Al7075-T6 and carbon steel substrates.
- After spraying no microstructural changes, decarburization or formation of fragile η phases were observed, indicating that the bulk properties of the powder were maintained.
- For WC-Co deposition higher temperatures resulted in denser and thicker coatings on both substrates.
- Coatings showed highly satisfactory adhesive resistance, comparable with that achieved by HVOF spraying.
- The good distribution of WC particles in the Co matrix led to high abrasion and friction resistance of both coatings.
- After 16 h immersion the electrolyte did not reach the substrates of either coating. A salt fog spray test was also run and after 500 h neither sample showed signs of pitting corrosion.
- CGS technology can clearly compete with conventional deposition techniques when used to spray WC-25Co powders. This cold spraying technique allows thick, dense and hard WC-25Co coatings to be deposited on Al7075-T6 and carbon steel substrates in a short time and with excellent tribological and electrochemical properties.

Acknowledgements

The authors wish to thank the University of Barcelona for financial support for this research and the Generalitat de Catalunya for funding Project 2009 SGR-00390. Thanks also go to Fujimi Inc. for providing the WC-Co powder.

References

[1] McCandlish LE, Kevorkian V, Jia K, Fischer TE. In: Proceedings of the international conference and exhibition on powder metallurgy and particulate materials. Toronto; 1994. p. 329–37.
[2] Yandouzi M, Sansoucy E, Richer P, Jodoin B, Ajdelsztajn L. In: Proceedings of the the international thermal spray conference. Materials Park, OH: ASM International; 2007. p. 660.
[3] Guilemany JM, Paco JM, Nutting J, Miguel JR. Metall Mater Trans A 1999;30A:1913–21.
[4] Chivavibul P, Watanabe M, Kuroda S, Kawakita J, Komatsu M, Sato K, et al. J Therm Spray Technol 2008;17:750–6.
[5] Chivavibul P, Watanabe M, Kuroda S, Kawakita J, Komatsu M, Sato K, et al. J Therm Spray Technol 2009;19(1/2):81–8.
[6] Jodoin B, Ajdelsztajn L, Sansoucy E, Zúñiga A, Richer P. Surf Coat Technol 2006;201(6):3422–9.
[7] Guilemany JM, Dosta S, Miguel JR. Surf Coat Technol 2006;201:1180–90.
[8] Guilemany JM, Dosta S, Nin J, Miguel JR. J Therm Spray Technol 2005;14(3):405–13.
[9] Dosta S, Miguel JR, Guileman JM. Mater Sci Forum 2008;587(588):1024–8.
[10] Kitamura J, Sato K, Watanabe M, Chivavibul P, Komatsu M, Sakaki K, et al.. Mechanical properties of WC-Co coatings prepared by Cold and Warm Spray processes. In: Paper presented at ITSC 2011, Hamburg, Germany; 2011.

[11] Champagne VK. The cold spray materials deposition process: fundamentals and applications. Boca Raton, FL: CRC Press; 2007.
[12] Cinca N, Barbosa M, Dosta S, Guilemany JM. Surf Coat Technol 2010;205:1096–102.
[13] Kim H, Lee C, Hwang S. Surf Coat Technol 2005;191:335–40.
[14] Kim H, Lee C, Hwang S. Mater Sci Eng A 2005;391:243–8.
[15] Douglas M. Diseño y Análisis de Experimentos: Editorial Limusa SA de CV; 2005.
[16] Schmidt T, Gärtner F, Assadi H. Acta Mater 2006;54:729–42.
[17] Magnani M, Suegama PH, Espallargas N, Dosta S, Guilemany JM. Surf Coat Technol 2008;202:4746–57.
[18] Liao H, Normand B, Coddet C. Surf Coat Technol 2000;124:235–42.
[19] Assadi H, Gartner F, Stoltenhoff T, Kreye H. Acta Mater 2003;51:4379–94.
[20] Stewart DA, Shipway PH, McCartney DG. Abrasive wear behavior of conventional and nanocomposite HVOF-sprayed WC-Co coatings. Wear 1999;225–229:789–98.

b) Paper 2:

M. Couto, S. Dosta, M. Torrell, J. Fernández, J.M. Guilemany, *Cold spray deposition of WC-17 and 12Co cermets onto aluminum*, Surface and Coatings Technology, 2013

After the publication of the first research work, emphasis was made on achieving equally excellent coatings onto Al7075-T6 substrates but, in this case, lowering their contents in cobalt matrix in order to achieve even higher mechanical and tribological properties. A different set of experimental designs was done for each of the powders. This represented the accomplishment of one of the objectives of this Thesis.

Surface & Coatings Technology 235 (2013) 54–61

Contents lists available at ScienceDirect

Surface & Coatings Technology

journal homepage: www.elsevier.com/locate/surfcoat

Cold spray deposition of WC–17 and 12Co cermets onto aluminum

M. Couto *, S. Dosta, M. Torrell, J. Fernández, J.M. Guilemany

Thermal Spray Centre. CPT. Universitat de Barcelona. 08028. Spain

ARTICLE INFO

Article history:
Received 3 April 2013
Accepted in revised form 4 July 2013
Available online 12 July 2013

Keywords:
Submicronic carbides
WC–17/12Co coatings
Cold spray
Wear/corrosion resistance
Aluminum Al7075-T6 substrates

ABSTRACT

The objective of this study was to deposit two wear- and corrosion-resistant WC cermet powders with distinct cobalt content (WC–17Co and WC–12Co) onto Al7075-T6 substrates using the Cold Gas Spraying (CGS) technique. WC–Co cermets show excellent mechanical and chemical properties and are thus extensively used in many industries. The addition of more ductile Co binder to the composite facilitates deposition by CGS while conferring proprieties that differ to those achieved with a WC–Co cermet with a lower content of ductile binder. XRD tests were run on the powder and coatings to identify all the present phases and determine the possible phase changes during spraying. The bonding strength of the coatings was measured by adherence tests (ASTM C633-08); the sliding (ASTM G99-04) and abrasive (ASTM G65-00) wear resistances of the coatings were also studied. Corrosion resistance was determined by electrochemical measurements. Such results were compared to the ones produced by conventional thermal spraying techniques. CGS yielded the deposition of dense and hard WC–17/12Co coatings with satisfactory tribological and electrochemical properties on aluminum alloy Al7075-T6.

1. Introduction

This study follows on from a line of research based on the deposition of distinct WC–Co cermets onto carbon steel and aluminum Al7075-T6 substrates using a solid-state deposition technique called Cold Gas Spraying (CGS). Previously published results on the deposition of a WC–25Co cermet with submicronic carbides using CGS show that this technology can compete with conventional deposition techniques since it allows the deposition of thick, dense and hard WC–25Co coatings with excellent mechanical and electrochemical properties on Al7075-T6 and carbon steel substrates [1]. In the present study two WC–Co cermets differing in their content of ductile Co binder (17 and 12Co) were coated onto Al7075-T6 aluminum substrates by CGS. The distinct microstructure of these powders affects their final mechanical and electrochemical properties. A decrease in Co content provides greater coating hardness while the fracture toughness shows the opposite behavior [2]. WC–Co coatings are usually produced by conventional thermal spray techniques, such as High Velocity Oxy-Fuel (HVOF), which use high temperatures to melt the powder particles and form a coating. However, this approach causes decarburization of the powder. Also, it is known that a reduction in particle size (from micrometric to submicrometric to nanometric) until a specific lower limit allows improved performance in terms of hardness and wear resistance [3–7], and concern has been raised about reducing the particle size of the WC–Co powders currently used as spraying material. A decrease in the average particle size leads to a higher particle velocity and, consequently, a lower gas/particle temperature is required [8]. The drawback of using these powders in conventional thermal deposition techniques is that, due to decarburization, the process temperatures give rise to undesirable effects, such as the formation of W_2C, W and/or fragile η phases [9–11].

CGS is a solid-state deposition process that does not involve melting the powder particles in a supersonic jet of compressed gas, which deposits them onto a substrate, where they deform and rapidly bond to form a thick layer of material [1,12,13]. Previous experiments at the *Thermal Spray Centre* successfully tested the deposition of WC–Co cermets by CGS using nitrogen as carrier gas [1]. CGS is influenced by several parameters. The effect of attaching a pre-chamber to the nozzle was also tested in order to determine its influence on the deposition of the studied WC–Co cermets. As air temperature in the pre-chamber increases particle velocity and particle and substrate temperatures also increase [1]. The study of these parameters allows researchers to gain insight into the nature of the cold spray phenomenon and the way in which basic coating properties can be controlled [14,15].

The results of a previous study using CGS to deposit a WC–25Co cermet onto Al7075-T6 and carbon steel substrates using low temperatures (600 °C), pressures below 30 bar and spray distances greater than 40 mm, showed poor substrate coating and interlayer adherence, thus resulting in poor coating quality [1]. That same paper demonstrated that in order to deposit that same WC–25Co powder, higher temperatures were required to ensure that the powder particles achieved enough velocity (kinetic energy) and temperature to soften the material and the particle surface areas by plastic deformation, thereby successfully achieving particle adherence to either substrate. Given these observations, the present study considered only the

* Corresponding author. Tel.: +34 674997014.
E-mail address: mcouto@cptub.eu (M. Couto).

0257-8972/$ – see front matter © 2013 Elsevier B.V. All rights reserved.
http://dx.doi.org/10.1016/j.surfcoat.2013.07.011

maximum operating temperature of 800 °C as it was already proven that lower temperatures do not yield satisfactory results. For this same reason, the effect of using a pre-chamber was also tested. In Cold Gas Spraying, as mentioned, higher particle temperatures will increase the ductility of the impinging particles allowing those to successfully bond to a substrate surface. Even though the system uses a pre heating module to increase the particles temperature, the cooling of the gas in the *de Laval* nozzle during the expansion will rapidly cool down the smaller particles meaning that those will not achieve enough temperature to allow bonding. The use of a pre-chamber pre-heats the particles and limits this cooling of the smaller particles by increasing the time of the particles in the hot gas by injection into an elongated pre-chamber.

The present study aimed to determine the optimum spraying conditions for the deposition of submicronic WC–17Co and WC–12Co cermets onto Al7075-T6 substrates. For this purpose, tribological and electrochemical properties of the coatings achieved were measured by means of several tests. The best results were then compared with those obtained by a conventional thermal spraying technique, namely HVOF.

2. Experimental procedure

The powders used were two experimental WC–Co cermets with a 17 and 12 wt.% cobalt content (17 and 12Co) obtained by agglomeration and sintering. This powder was processed and provided by Fujimi Inc., (Kiyosu, Japan). The powders were sprayed onto several samples of aluminum Al7075-T6 coupons: flat (100 × 20 × 5 mm), and cylindrical (= 25.4 mm, height 25.4 mm) substrates. These were prepared by grinding using 240 grit *SiC* paper. The cold spray equipment comprised was a KINETICS® 4000/17 kW (Cold Gas Technology, Ampfing, Germany) with a maximum operating pressure of 40 bar, and temperature of 800 °C, limited to the use of nitrogen as the carrier gas. The microstructure of the powders was characterized by Scanning Electron Microscopy (SEM) and Field Emission SEM (FE-SEM); particle size distribution by Laser Diffraction (LS); and phase composition by X-ray diffraction (XRD). Afterwards, the coatings were also characterized by SEM and their phase composition by XRD. Vickers hardness tests with a load of 300 gF were also performed to identify the optimum coatings obtained from the pre-experimented spraying parameters. Finally, mechanical and electrochemical tests were run on the selected optimum coatings to determine their properties and behavior when tested by tensile loads, abrasive and adhesive wear conditions, and electrochemical corrosion conditions.

In order to optimize the spraying conditions, an experimental design was made to determine which factors (parameters) and interactions between them are most important when it comes to obtaining the final coating. Experimental data on all the process parameters were gathered and analyzed to improve spraying performance, and a structured data table comprising substantially relevant information about structured variation/interactions was generated, thereby allowing a greater understanding of the process from fewer experiments [16]. After defining the fixed and variable parameters, a total of three levels for each factor (variable parameter) were selected. The 3^k factorial design comprised k factors of three levels each: low, medium and high. Of all the 3^k factorial designs, 3^2 of them correlated only two factors from the three levels; this means that there were a total of $3^2 = 9$ possible combinations. The fixed process parameters were as follows: nitrogen was the process gas; 800 °C the gas temperature; 90° the spraying angle; four gun passes; and 250 mm/s gun speed. These were chosen based on previous experiments developed where temperatures below 800 °C and gas pressures below 30 bar produced poor substrate–coating adherence and inter-layer adherence as well as delamination and the presence of cracks in the final layers of the deposited material [1].

The chosen variable parameters were gas pressure, with values ranging from 25 to 35 bar, and distance, with values ranging from 10 to 30 mm. Also the effect of a pre-chamber attached to the nozzle was tested, thus implying that two different 3^2 experimental designs were made.

The quality of coating adherence to the substrate is a major performance criterion. In order to determine the bonding strengths of the coatings, adherence tests were performed on two samples, grinded using 120 grit *SiC* paper, of each selected coating following the ASTM F1147 (2005) standard. For this purpose, a testing apparatus Servosis ME-402/10 model with a velocity of 0.02 mm/s, which was controlled by position, was used. Afterwards, the mechanism of breakage was determined by EDS analysis using a SEM technique; using this kind of analysis it was possible to determine whether the coatings had failed either at the substrate–coating interface or through the inter-layer interfaces.

Two kinds of wear tests were performed to measure the wear resistance of the coatings. A sliding wear test was carried out using a ball-on-disk (BoD) method, following the ASTM G99-04 standard. For test purposes, the following parameters were selected: a WC–12Co counterpart ball; a sample relative velocity of 131 rpm with a total testing distance of 1000 m for a radius of 14 mm; and a force load of 25 N. Humidity and temperature were kept below 20% and 25 °C, respectively. Leica TSC-SPE confocal equipment was used to measure the volume loss of the wear tracks and to recreate the wear path.

Dry abrasive tests (ASTM G65-00 standard) were carried out using a rubber wheel system with a rotation of 139 rpm, a load of 50 N, and a SiO_2 flux of between 250 and 310 g/min [9]. Material loss was measured by weighing the samples every minute during the first 10 min, and then every 5 min until the end of the test.

The resistance of the samples to corrosion was evaluated by performing electrochemical measurements in 80 ml of an aerated and unstirred 3.4% NaCl solution. The open-circuit potential (E_{OC} vs. time) was measured using EG&G Parc-273 equipment. Polarization experiments were carried out in a potential range of −100 to +350 mV. All electrochemical experiments were performed at room temperature.

3. Results and discussion

3.1. Structural characterization of WC–17co and WC–12Co powders

The powders had a micrometric particle size with submicronic WC particles (measured by FE-SEM) and an average particle size of −32 + 10 μm. Powders presented a spheroid and relatively uniform morphology as well as a narrow particle size distribution (Figs. 1a and 2a). The XRD analysis of the powder showed that no other strange phases of WC and Co such as W_2C, W, Co_6W_6C and Co_3W_3C were present. The EDS cross-sectional analysis of the WC–Co powder confirmed the presence of WC and Co.

3.2. Structural characterization of the coatings

3.2.1. Characterization of the WC–17co coatings on AL7075-T6

After the first characterization and examination of the coatings on the Al7075-T6 substrate, the optimum spraying conditions were chosen from the previously defined testing conditions. These conditions were the following: gas temperature of 800 °C, gas pressure of 25 to 35 bar and spraying distance between 10 and 30 mm, with and without the use of a pre-chamber attached to the spraying gun.

Analysis of the pre-experiment results showed that for all the gas pressures and the spraying distances equal to or higher than 20 mm the process produced coatings with very poor quality, and the last layers sprayed were observed to rebound off the substrate (Fig. 3).

After characterization of the coating samples obtained in the pre-experiment, it was determined that the maximum spraying pressure and shortest spraying distance for the DTS-W774-32/10 WC–17Co cermet deposition produced coatings with severe delamination, especially

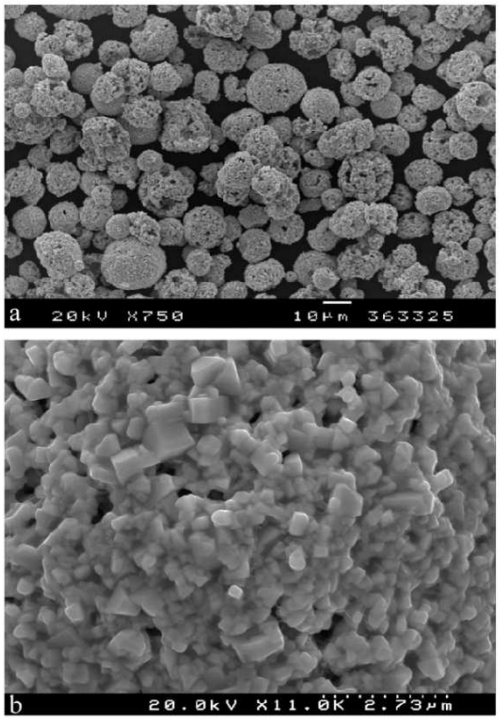

Fig. 1. SEM (a) and FE-SEM (b) micrograph of the free surface of the DTS-W774-32/10 WC–17Co powder at 750×, and close-up of a particle at 11,000× showing the submicronic carbides.

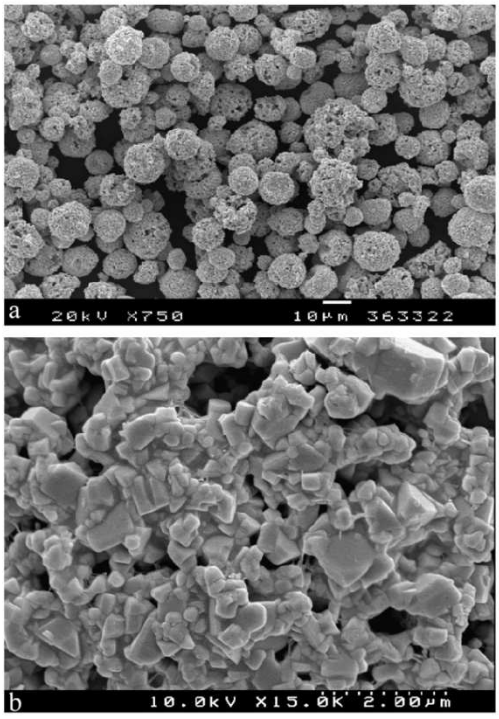

Fig. 2. SEM (a) and FE-SEM (b) micrograph of the free surface of the DTS-W773-32/10 WC–12Co powder at 750×, and close-up of a particle at 15,000× showing the submicronic carbides.

in the last layer of material deposited (Fig. 4a). This effect is attributed to the extreme kinetic energy that the impinging particles achieve before hitting those deposited previously. The compression effect of the last sprayed particles had a negative impact on the quality of the coating.

The same effect occurred, although on a minor scale, when spraying the same powder using the shortest spraying distance and the lowest spraying pressure (Fig. 4b). The coatings were not as irregular as those achieved using the maximum spraying pressure but still presented some delamination. Since the effect of lowering the gas pressure did not produce a coating of acceptable quality, as interlayer delamination was noted for the four gun passes in the pre-experiment, an alternative method was devised to obtain coatings onto Al7075-T6 without delamination. The same conditions were tested; however, to prevent interlayer delamination, a lower gun speed was used (100 mm/s) and with only one gun pass. Finally, an intermediate gas pressure and the shortest spraying distance produced the best quality coatings for the WC–17Co cermet powder. Afterwards, the effect of the pre-chamber was studied using the optimum spraying conditions.

Fig. 5 shows the representative cross-section SEM micrographs of the optimum coating obtained in the pre-experiment. The use of the pre-chamber conferred excessive energy to the impinging particles and instead of producing a thicker coating with higher deposition efficiency, it produced a delaminated coating (Fig. 5a). Given these observations, the optimum spraying conditions were kept without using the pre-chamber.

The optimum spraying conditions produced a relatively uniform, pore-free coating, with an average thickness of 129 ± 5 µm, without fissures caused by delamination. This coating showed good adherence to the substrate (Fig. 5b) and an average HV_{300} of 1223 ± 59. The process showed a deposition efficiency of 11.9%.

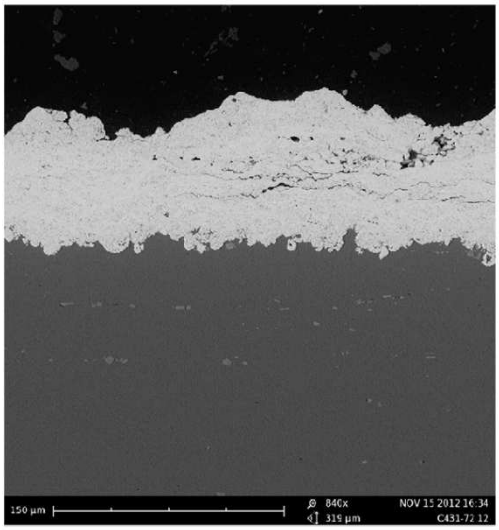

Fig. 3. SEM micrographs of a representative coating obtained onto Al7075-T6 with a spraying distance equal or higher than 20 mm where delamination and poor adherence can be seen resulting in a poor quality coating.

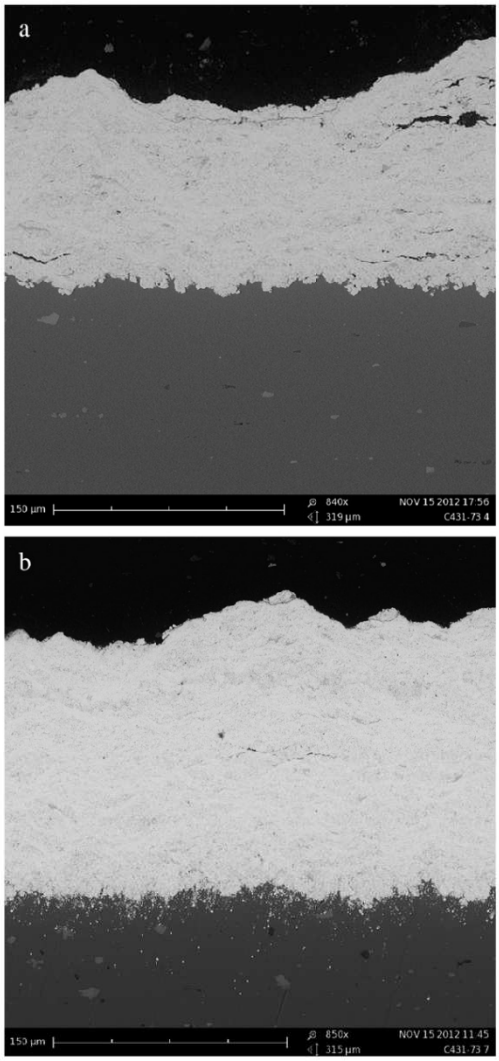

Fig. 4. SEM micrographs of DTS-W774-32/10 WC–17Co cermet coatings on Al7075-T6 achieved with the maximum spraying pressure and shortest spraying distance (Fig. 4a) and minimum spraying pressure and shortest spraying distance (Fig. 4b). Images show a poor quality coating with delamination and irregularity.

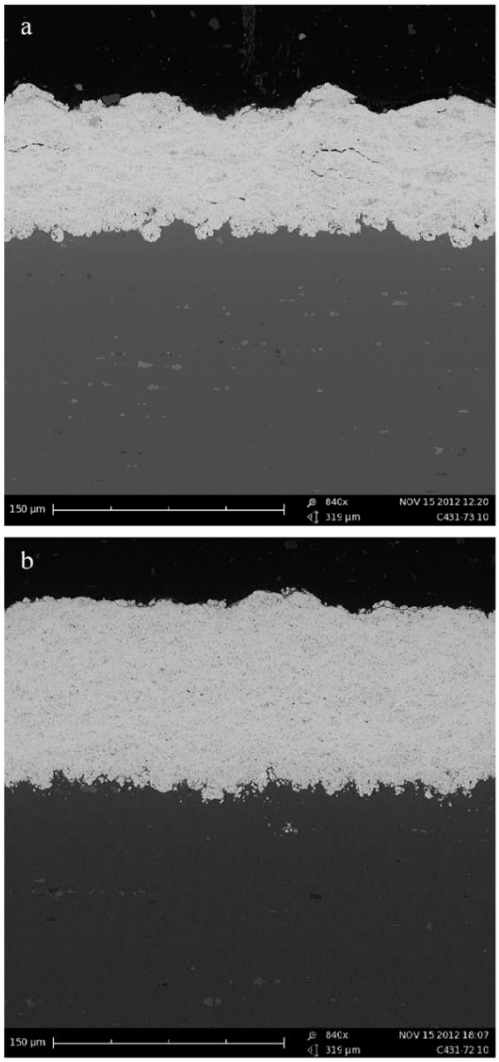

Fig. 5. Effect of a pre-chamber attached to the gun on the final quality of the coatings under the same optimum spraying conditions. DTS-W774-32/10 WC–17Co cermet coating on Al7075-T6 obtained with a pre-chamber (a) and without (b).

Afterwards, more samples of the defined optimum set of conditions were sprayed to study their mechanical and electrochemical properties.

3.2.2. Characterization of the WC–12Co coatings obtained on AL7075-T6

The same pre-experimental design was followed to determine the optimum spraying conditions for the DTS-W773-32/10 WC-12Co cermet powder. The pre-experiment results for the WC–17Co powder were consistent with those obtained after the characterization of the pre-experimental samples for the WC–12Co powder. These observations imply that for all the spraying distances equal to or higher than 20 mm and for all the gas pressures tested, the coatings produced did not show an acceptable final quality or satisfactory interlayer adherence to allow mechanical and electrochemical testing. In the following paragraphs only the results obtained with one gun pass will be discussed since at higher gun speeds and more gun passes (4) the results were unsatisfactory.

The coating samples obtained in the pre-experiment were characterized and it was determined that for the spraying of the DTS-W773-32/10 WC–12Co cermet the maximum spraying pressure and shortest spraying distance (as for the spraying of the WC–17Co presented in point 3.1.2) produced coatings with severe delamination (Fig. 6a). It is well known that the use of CGS requires, in order to spraying any given materials, that both the substrate and the spraying material have certain characteristics. The particles of the raw powder must show a given degree of ductility, and the substrate should show some suitable mechanical properties, as for example, hardness, to obtain sufficient localized plastic deformation, i.e., flattening of particles, in order to build up a dense coating [17,18]. These requirements are needed because of

the extreme kinetic energy that the impinging particles achieve before arriving and hitting those previously deposited ones. Since the WC–12Co powder used in this study had lower ductile binder content than WC–17Co, and thus greater hardness, the particles had an eroding effect over the sprayed particles, therefore producing delamination and fissures. The compression effect of the last sprayed particles on the coating had a negative impact on the final quality of the coating.

When the shortest spraying distance and lowest spraying pressure were applied (Fig. 6b), the coatings produced did not present such severe delamination. Moreover, they showed a slightly better quality as a result of the lower energy of the hard WC–12Co cermet particles upon deposition. Like the ones obtained using maximum spraying pressure, these coatings still presented some delamination. Again, an intermediate gas pressure and the shortest spraying distance produced the best quality coatings for WC–12Co. Afterwards, the effect of a pre-chamber was studied using the optimum spraying conditions.

Fig. 7 shows the representative cross-section SEM micrographs of the optimum coating obtained in the pre-experiment with and without a pre-chamber (Fig. 7a and b, respectively). The use of a pre-chamber produced a much more uniform coating without delamination. In this case, all the particles were well compressed and adhered to the substrate. Furthermore, higher deposition efficiency values were achieved using this chamber. These values are due to the longer time that the powder particles are exposed to the gas temperature before being sprayed. Greater exposure gives them a higher acceleration and a greater degree of ductility, thus a higher number of particles finally adhered to the substrate, without detriment to the

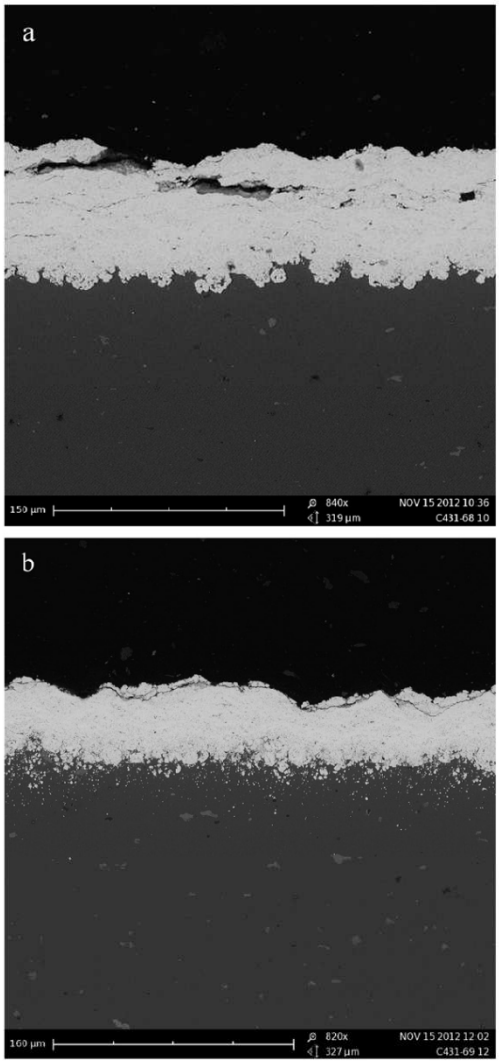

Fig. 6. SEM micrographs of DTS-W773-32/10 WC–12Co cermet coatings on Al7075-T6 achieved using the defined spraying conditions. Images show a poor quality coating with delamination and irregularity.

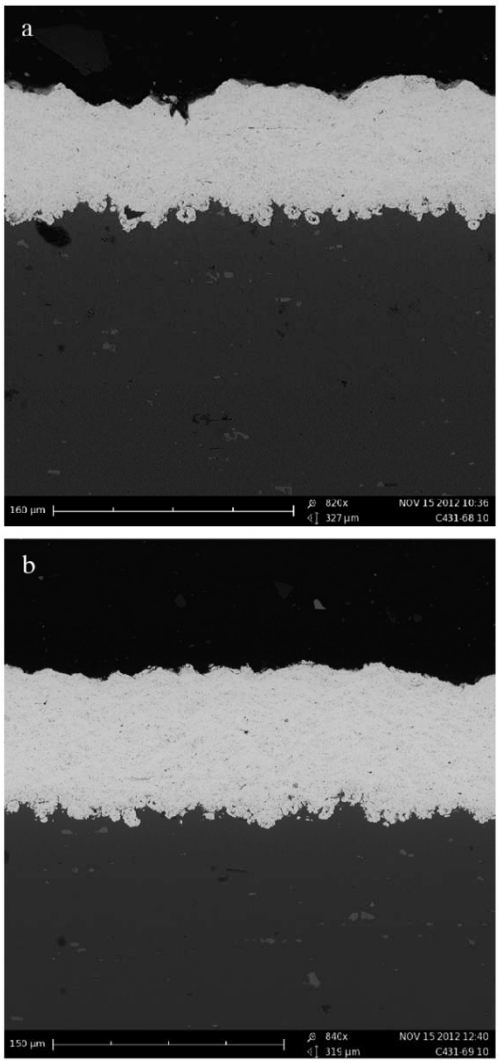

Fig. 7. Effect of a pre-chamber attached to the gun on the final quality of the coatings under the same optimum spraying conditions. DTS-W773-32/10 WC–12Co cermet coating on Al7075-T6 obtained without a pre- chamber (a) and with one (b).

quality of the coating. The optimum spraying conditions were defined including the use of the pre-chamber.

The optimum spraying conditions produced a relatively uniform, pore-free coating, with an average thickness of 93 ± 8 μm, without fissures caused by delamination. The coating showed good adherence to the substrate (Fig. 7b) and an average HV_{300} of 1419 ± 93. The process showed a deposition efficiency of 14.2%.

Fig. 8 shows the XRD result of a representative analysis made on one of the optimum coatings obtained, and supports the sentences that no strange or fragile phases are formed during the process with Cold Gas Spraying. Also shown is a comparative with an XRD analysis of the WC–17Co powder. Both coatings and powders evidenced the same final qualitative XRD results and for this reason only a representative sample of results is depicted here to corroborate the facts described in the previous sentence.

3.3. Adherence tests

The optimum coatings' bonding interface quality was tested by performing adherence tests on samples prepared according to the defined spraying conditions. Coatings WC–17Co had σ_{max} values of 26 ± 10 MPa while the optimum WC–12Co coatings obtained had σ_{max} values of 19 ± 1 MPa. In cold spraying, a certain degree of ductility of the particles and hardness of the substrate are needed to obtain sufficient localized plastic deformation to build up a dense coating. This and the adiabatic shear instabilities resulting from high strain rate deformation upon impact are the phenomena believed to play a major role in particle/substrate bonding—influenced by spraying conditions and powder characteristics—during cold spraying [1,17,18]. For this reason WC–17Co coatings were expected, and confirmed, to perform better under such tensile tests with its adherence results being better when compared to WC–12Co. The coatings failed through the substrate–coating interface in both cases, meaning that the interlayer bonding was stronger than that of the substrate–coating interface.

3.4. Sliding tests (ball-on-disk)

A comparison of the adhesive wear resistance of the WC–17Co and WC–12Co coatings was made. The latter evidenced a higher friction wear resistance than WC–17Co. The wear resistance during testing on the two coatings was higher when compared to previous results tested on WC–25Co coatings obtained by CGS [1], with different material loss mechanisms acting during the testing. To study the wear mechanisms that acted on the coatings, the latter were subjected to FE-SEM characterization. For WC–12Co samples, material loss occurred mainly as a result of the ripping off of some WC–Co particles from the coating (observed in Fig. 9); these particles were probably not well adhered and were therefore pulled away from the coating by the counter-ball. Since there is a small amount of ductile metallic binder, the wear resistant WC carbide particles provided a higher adhesion wear resistance than those coatings with a higher Co content in their microstructure. Analysis of the wear track by FE-SEM showed a small number of particles ripped off and an almost unaltered coating. These observations imply that under the conditions of 25 N and 1000 m the system barely produced a wear effect over the optimum WC–12Co coatings. These coatings showed a friction coefficient of 0.41 ± 0.01 and a volume loss of approximately 0.0038 mm^3 (measured by profilometric measurements using a Confocal Laser technique).

The WC–17Co coatings showed a different wear mechanism, as depicted in Fig. 10. It appears that during testing, particles were pulled off the coating, and micro fusions of these to the coating occurred, thus explaining the *beaching* effect observed in Fig. 8. These coatings evidenced a slightly higher friction coefficient (0.47 ± 0.03) than WC–12Co ones and a volume loss of approximately 0.0086 mm^3.

Comparing these results with those obtained in a previous study by S. Dosta et al. on WC–25Co coatings deposited onto Al7075-T6 and carbon steel substrates, it was concluded that WC–25Co provides the lowest friction coefficients, followed by WC–12Co, and finally WC–17Co, which registered the highest value for this parameter. Nevertheless, and despite the observation that WC–12Co and WC–17Co have higher friction coefficients than WC–25Co, the first evidenced a lower material loss, i.e., a higher wear adhesive resistance [1].

3.5. Abrasive tests (rubber-wheel)

After 45 min of rubber-wheel abrasive testing on several samples of optimum WC–17Co and WC–12Co coatings these finished with abrasive wear rates of $1.3 \times 10^{-5} \pm 2.4 \times 10^{-6}$ and $8.7 \times 10^{-6} \pm 7 \times 10^{-7}$ $mm^3/N \cdot mm$, respectively (Fig. 11). The increase in Vickers hardness and decrease in ductile binder/increase in wear-resistant WC of the WC–12Co coatings compared to the WC–17Co ones caused the latter to have a slightly lower abrasive resistance and higher wear rate than the former. Also, as the powders presented an excellent WC carbide particle distribution in the ductile binder, without brittle or fragile phases, a very high abrasion resistance was achieved when tested under the specified conditions. J.M. Guilemany et al. reported abrasive wear rates of about 1.0×10^{-5} $mm^3/N \cdot mm$, after 30 min of testing for WC–12Co powders

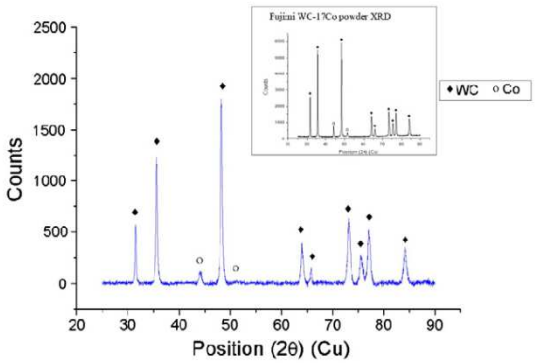

Fig. 8. Representative XRD analysis of the optimum WC–17Co coatings obtained after CGS spraying onto Al7075-T6, and a comparison with XRD analysis of the WC–17Co powder.

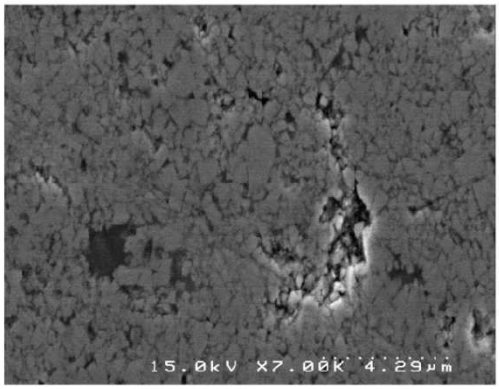

Fig. 9. FE-SEM micrograph of representative sliding wear area after testing on a representative WC–12Co coating, where an almost unaltered wear track can be seen as well as the ripping off of some particles.

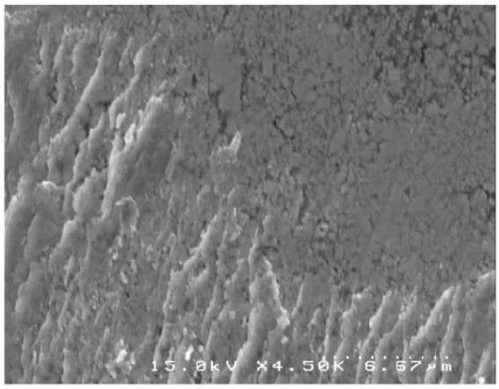

Fig. 10. FE-SEM micrograph of representative sliding wear area after testing on a representative WC–17Co coating, where the ripping off and fusion of particles, alongside an unaltered part of the wear track can be seen.

sprayed by a conventional Diamond Jet Hybrid DJH 2700 HVOF equipment onto carbon steel substrates [9]. In the present study, after 30 min of testing for a WC–12Co coating on Al7075-T6, the wear rate was 1.1×10^{-5} mm^3/N·mm, which is virtually the same as the rate obtained by HVOF. Although CGS and HVOF present the same wear rates under the same testing conditions for a WC–12Co coating, HVOF does not have some of the advantages of CGS, namely the absence of brittle and fragile phases caused by decarburization/oxidation and the maintenance of the raw powder microstructure. CGS can therefore produce equally acceptable abrasive-resistant WC–12Co coatings without detriment to ductile binder and without the appearance of strange powder phases.

3.6. Electrochemical tests

In order to measure the electrochemical resistance of the optimum WC–17Co and WC–12Co coatings on Al7075-T6 to corrosive conditions, samples of these coatings were put in aerated and unstirred 3.4% NaCl solution for 24 h. Both coatings presented a steep decrease in potential during approximately the first 4 h of testing (Fig. 12). This decrease was due to the dissolution of oxides on the surface of the coatings during the stabilization of the electrochemical potential and also to penetration of the electrolyte. After 24 h of testing, the open circuit potential of the samples of the optimum WC–17Co coatings on Al7075-T6 substrate was -0.394 ± 0.009 V, while WC–12Co coatings registered -0.387 ± 0.001 V. The WC/Co interface is a preferable path for the electrolyte to enter and corrode the coatings, meaning that the lower ductile binder content the less available ways for corrosion to take place and higher the corrosion resistance. Both coatings showed constant behavior, followed by stabilization after 16 h of testing, and in neither case did the electrolyte reach the substrate, i.e., the WC–Co powders sprayed on Al7075-T6 successfully prevented the electrolyte from reaching the substrate and hence protected it from extreme corrosive conditions. This conclusion was drawn after subjecting Al7075-T6 substrate samples to the same electrochemical testing conditions. In this case, after 24 h, the Eoc was -0.687 V, which is considerably more negative than the open circuit potentials obtained for the WC–17Co and WC–12Co coatings.

S. Dosta et al. [1] reported Eoc values of -0.439 ± 0.018 V after stabilization of testing for a WC–25Co cermet powder sprayed onto Al7075-T6. As expected, and described in the previous paragraph, the decrease in ductile binder was accompanied by a slight increase in electrochemical resistance. A comparison of the results of a WC–25Co, WC–17Co and WC–12Co sprayed onto Al7075-T6, after their stabilization, showed that WC–12Co (-0.387 ± 0.004 V) showed greater protective performance than WC–17Co (-0.394 ± 0.009 V), which, on the other hand, showed a slight increase in corrosion resistance towards electrochemical corrosion than WC–25Co (-0.439 ± 0.018 V).

In CGS there is a compressive effect of the particles during spraying. This effect produces less porous coatings, and hence fewer paths for the electrolyte to penetrate and reach the substrate than those seen in conventional thermal spraying techniques such as HVOF. This observation is confirmed by comparing the work of J.M. Guilemany et al. on a WC–12Co coating on carbon steel under the same testing conditions. Those authors achieved an Eoc of -0.53 V, which contrasts with an Eoc of -0.387 ± 0.004 V for WC–12Co in the present study.

4. Conclusions

- Dense, thick and well-bonded WC–17Co and WC–12Co coatings were achieved on Al7075-T6 substrates.
- After spraying, no microstructural changes, decarburization, or formation of fragile η phases were observed, meaning that the bulk properties of the powder were maintained.

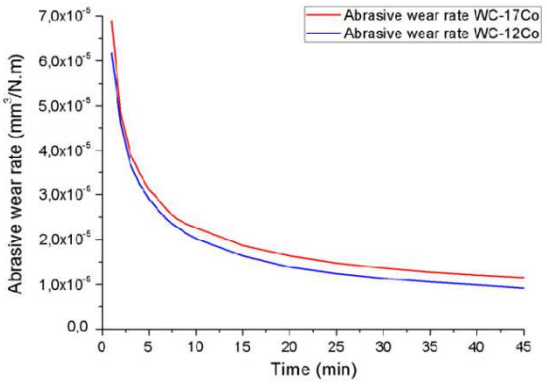

Fig. 11. Abrasive (rubber-wheel) wear rates versus time of the average result obtained for WC–17Co and WC–12Co coatings.

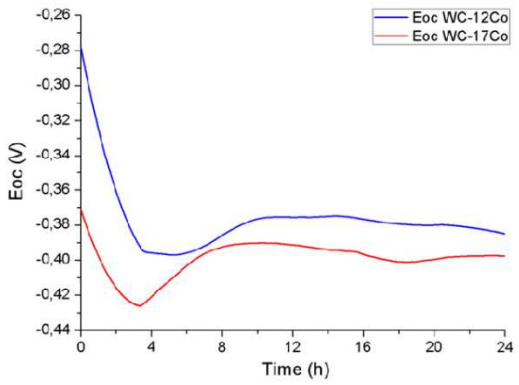

Fig. 12. Open-circuit potential (Eoc) vs. time (h) curve of the average result obtained for WC–17Co and WC–12Co coatings.

- Spraying distances equal or higher than 20 mm will result in poor quality results while spraying WC-17/12Co powders onto Al7075-T6.
- For the deposition of WC–Co, higher temperatures resulted in denser and thicker coatings on both coatings; in the case of WC–12Co using a pre-chamber provides better results.
- WC–17Co coatings showed better adherence results (26 ± 10 MPa) than WC–12Co (19 ± 1 MPa).
- The uniform distribution of WC particles in the Co binder led to high abrasion and friction resistance for WC–12Co and WC–17Co coatings, with the former showing better adhesive and abrasive wear resistance than the latter.
- After 24 h of immersion, the electrolyte did not reach the substrates for either coating.
- CGS allows the deposition of thick, dense and hard WC–17/12Co coatings with excellent tribological and electrochemical properties onto Al7075-T6 substrates in a short time.
- Cold spray gas technology can clearly compete with conventional deposition techniques, such as HVOF, to spray the studied WC–Co powders.

Acknowledgments

The authors wish to thank the University of Barcelona for the financial support for this research and the Generalitat de Catalunya for funding Project 2009 SGR-00390. Thanks also go to Fujimi Inc. for providing the WC–Co powders.

References

[1] S. Dosta, M. Couto, J.M. Guilemany, Acta Mater. 61 (2) (2013) 643.
[2] M. Yandouzi, L. Ajdelsztajn, B. Jodoin, Surf. Coat. Technol. 202 (16) (2008) 3866.
[3] L.E. McCandlish, V. Kevorkian, K. Jia, T.E. Fischer, Proceedings of the International Conference and Exhibition on Powder Metallurgy and Particulate Materials, 1994, p. 329, (Toronto, Ontario; Canada).
[4] M. Yandouzi, E. Sansoucy, P. Richer, B. Jodoin, L. Ajdelsztajn, Proceedings of The International Thermal Spray Conference, ASM International(OH), Beijing, China, 2007.
[5] J.M. Guilemany, J.M. Paco, J. Nutting, J.R. Miguel, Metall. Mater. Trans. A 30A (1999) 1913.
[6] P. Chivavibul, M. Watanabe, S. Kuroda, J. Kawakita, M. Komatsu, K. Sato, J. Kitamura, J. Therm. Spray Tech. 17 (2008) 750.
[7] P. Chivavibul, M. Watanabe, S. Kuroda, J. Kawakita, M. Komatsu, K. Sato, J. Kitamura, J. Therm. Spray Tech. 19 (1–2) (2009) 81.
[8] B. Jodoin, L. Ajdelsztajn, E. Sansoucy, A. Zúñiga, P. Richer, Surf. Coat. Technol. 201 (6) (2006) 3422.
[9] J.M. Guilemany, S. Dosta, J.R. Miguel, Surf. Coat. Technol. 201 (2006) 1180.
[10] J.M. Guilemany, S. Dosta, J. Nin, J.R. Miguel, J. Therm. Spray Tech. 14 (3) (2005) 405.
[11] S. Dosta, J.R. Miguel, J.M. Guilemany, Mater. Sci. Forum 587–588 (2008) 1024.
[12] V.K. Champagne, The cold spray materials deposition process: fundamentals and applications, CRC, 2007.
[13] N. Cinca, M. Barbosa, S. Dosta, J.M. Guilemany, Surf. Coat. Technol. 205 (2010) 1096.
[14] H. Kim, C. Lee, S. Hwang, Surf. Coat. Technol. 191 (2005) 335.
[15] H. Kim, C. Lee, S. Hwang, Mater. Sci. Eng. A391 (2005) 243.
[16] Douglas M., Diseño y análisis de experimentos, Editorial Limusa S.A. De C.V, 2005.
[17] H. Assadi, F. Gartner, T. Stoltenhoff, H. Kreye, Acta Mater. 51 (2003) 4379.
[18] T. Schmidt, F. Gärtner, H. Assadi, Acta Mater. 54 (2006) 729.

6.2 Cold Gas Spray vs High Velocity Oxy-Fuel

c) Paper 3:

M. Couto, S. Dosta, J.M. Guilemany, Comparison of the mechanical and electrochemical properties of WC-25Co coatings obtained by high velocity oxy-fuel and cold gas spray, Journal of Thermal Spray Technology, 2014

This was the first approach to comparing the first results obtained with spraying WC-25, 17 and 12Co by CGS. The main concern was the different mechanical and electrochemical properties that each technology produced while spraying the same powders. HVOF WC-25Co coatings were optimized characterized and fully tested for comparison with CGS WC-25Co coatings. Fracture toughness tests were performed, and added to this research paper as a novelty, on both coatings to study the effect of decarburization in HVOF and the advantages of CGS when it comes to this.

JTTEE5
DOI: 10.1007/s11666-014-0123-0
1059-9630/$19.00 © ASM International

Comparison of the Mechanical and Electrochemical Properties of WC-25Co Coatings Obtained by High Velocity Oxy-Fuel and Cold Gas Spraying

M. Couto, S. Dosta, J. Fernández, and J. M. Guilemany

(Submitted October 31, 2013; in revised form June 2, 2014)

Cold gas spray (CGS) coatings were previously produced by spraying WC-25Co cermet powders onto Al7075-T6 and low-carbon steel substrates. Unlike conventional flame spray techniques (e.g., high-velocity oxy-fuel; HVOF), no melting of the powder occurs; the particles are deformed and bond together after being sprayed by a supersonic jet of compressed gas, thereby building up several layers and forming a coating. WC-Co cermets are used in wear-resistant parts, because of their combination of mechanical, physical, and chemical properties. XRD tests were previously run on the initial powder and the coatings to determine possible phase changes during spraying. The bonding strength of the coatings was measured by adhesion tests. Here, WC-25Co coatings were also deposited on the same substrates by HVOF spraying. The wear resistance and fracture toughness of the coatings obtained previously by CGS and the HVOF coatings obtained here were studied. Their corrosion resistance was determined by electrochemical measurements. It was possible to achieve thick, dense, and hard CGS coatings on Al7075-T6 and low-carbon steel substrates, with better or the same mechanical and electrochemical properties as those of the HVOF coatings; making the former a highly competitive method for producing WC-25Co coatings.

Keywords aluminum Al7075-T6 substrates, cold spray, low-carbon steel substrates, submicronic carbides, WC-25Co coatings, wear/corrosion resistance

1. Introduction

WC-Co coatings, which are highly resistant to sliding and abrasive wear, are conventionally produced by thermal spray techniques, such as high-velocity oxy-fuel (HVOF) spraying. HVOF is a high-temperature process (up to ~3000 °C) that, in order to deposit the material onto a substrate, uses chemical flame heat to melt the powder particles. Due to the high temperatures used in the process, there is decarburization and brittle phases form (Ref 1–3). To avoid this negative effect, cold gas spraying (CGS), a solid-state deposition process in which no melting of the powder particles occurs, has successfully been used to deposit WC-Co cermets onto Al7075-T6 and low-carbon steel substrates (Ref 4). The particles are sprayed onto the substrates in a supersonic jet of compressed gas. On impact, the particles deform and bond to the substrate, building up a layer of material (Ref 4–6). Warm spraying has also been reported to successfully deposit novel coatings with little or no formation of other phases. That process uses a nitrogen gas flow to control the gas temperature, thereby allowing a wider range of temperatures for particle treatment (Ref 7).

When brittle materials such as cobalt cermets (WC-Co) are under severe testing or working conditions, a brittle wear mechanism usually causes them to wear out. Erosive brittle wear is usually conditioned by the flow of particles to the surface or fracture resulting in brittle fracture and a loss of material from the surface by nucleation and the intersection of cracks. Under such conditions, materials possessing the highest fracture toughness (Kc), which is the most relevant material property, exhibit the best wear resistance (Ref 8, 9).

Due to the thermal-spraying deposition process, the resultant coatings have an anisotropic microstructure typically characterized by lamellae. Because of this microstructure, the cracks produced when tested under indentation develop parallel to the different layers of deposited material: this direction is the most favorable to decohesion. At very high indentation loads, transverse cracks are observed; since interlamellar cracks propagate in WC-Co coatings, only cracks parallel to the interface are considered valid in the analysis (Ref 8–10).

To measure the fracture toughness of brittle materials, the Vickers indentation technique is the most commonly used method because it can determine this property in a specific zone of a coating and therefore determine the fracture toughness as a function of the material microstructure (Ref 10).

Crack models used to predict fracture toughness are functions of the indenter, the crack geometries, and the indentation loads: the Palmqvist model is used for low

M. Couto, S. Dosta, J. Fernández, and **J.M. Guilemany**, Thermal Spray Centre (CPT), Facultad de Química, Universitat de Barcelona, Barcelona, Spain. Contact e-mail: sdosta@cptub.eu.

Journal of Thermal Spray Technology

Published online: 02 July 2014

indentation loads; the Half-Penny model for high indentation loads. Half-Penny (Eq 2) cracks are typically observed in brittle ceramics at high indentation loads (Ref 8–10).

The primary objectives of this work were to: (i) obtain coatings of WC-25Co cermets on Al7075-T6 and low-carbon steel substrates by HVOF and (ii) compare their properties with those previously reported for coatings of the same powder on the same substrates deposited by CGS (Ref 4). To this end, different mechanical and electrochemical tests were performed on the best coatings obtained by HVOF.

2. Experimental Procedure

The experimental WC-Co cermet powder studied contained 25 wt.% cobalt and was obtained by agglomeration and sintering; it was produced and provided by Fujimi Inc., (Kiyosu, Japan). The powder was sprayed onto several samples of Al7075-T6 aluminum: flat substrates (100 mm × 20 mm × 5 mm) and cylindrical substrates ($\varnothing = 25.4$ mm, height = 25.4 mm). To improve coating adhesion, the substrates used for CGS were prepared by grinding, using 240 grit SiC paper; while the substrates for HVOF spraying were prepared by grit-blasting, using Al_2O_3 particles. The powder was characterized by studying its microstructure using scanning electron microscopy (SEM) and field emission SEM (FE-SEM); and its phase composition via x-ray diffraction (XRD). The microstructure of the coatings was also characterized by SEM and their phase composition by XRD (Ref 11). Vickers hardness tests were performed at different loads. The elastic modulus was estimated using a Knoop indentation technique by performing 10 Knoop indentations at a load of 9.80 N. Finally, mechanical and electrochemical tests were run on selected coatings to determine their properties and behavior under tensile loads, abrasive wear, and electrochemical corrosion.

The HVOF coatings were sprayed using the following conditions: 225-mm spraying distance; 15 gun passes (layers); feed rate of 30 g/min; C_3H_6 flow of 40 FMR (flow meter readings) at 6.9 bar (77 slm); O_2 flow of 40 FMR at 10.3 bar (252 slm); air flow of 48 FMR at 6.9 bar (375 slm).

The CGS spraying conditions were set with a temperature-pressure ratio of 22.9 and a spraying distance of 20 mm for the Al7075-T6 substrates; and a temperature-pressure ratio of 20 and spraying distance of 10 mm for the low-carbon steel substrates (Ref 4).

In order to measure the fracture toughness, Vickers indentations were performed at 9.80 N on polished coating cross sections; the diagonals and crack lengths were measured using an optical microscope. An average of 10 indentations were made and the total crack length was estimated using Eq 1, where $2d_{\parallel}$ and $2d_{\perp}$ are the Vickers diagonals parallel and perpendicular to the coating surface that was produced in the indentation; and al and ar are the left and right crack lengths. To determine the fracture toughness, Eq 2 was used, where H_v and E are the Vickers hardness and elastic modulus, respectively (Ref 8):

$$c = (2d_{II} + 2d_{\perp})/4 + (a_l + a_r)/2 \quad \text{(Eq 1)}$$

$$K_c = 0.0711\left(H_v d^{1/2}\right)\left[E/H_v\right]^{2/5}\left[c/d\right]^{-3/2} \quad \text{(Eq 2)}$$

Equation 2 is only valid for a Half-Penny crack regime that occurs when $c/d \geq 2.5$, where d is the Vickers half-diagonal.

The quality of coating adhesion to the substrate is a major performance criterion. In order to determine the bonding strength of the coatings, adhesion tests were performed on two samples of each selected coating following the ASTM F1147 (2005) standard. Testing apparatus SERVOSIS ME-402/10 was used with a velocity of 0.02 mm/s, which was controlled by position.

Two kinds of wear tests were performed to measure the wear resistance of the coatings. A sliding wear test was carried out following a ball-on-disk (BoD) method and the ASTM G99-04 standard. A WC-12Co counterpart ball, a sample relative velocity of 131 rpm, with a total test of 1000 m, and a force load of 25 N for a radius of 14 mm were selected. Humidity and temperature were kept below 20% and 25 °C, respectively. Leica TCS-SE confocal equipment was used to measure the volume loss of the wear tracks and to recreate the wear path. Dry abrasive tests (ASTM G65-00 standard) were carried out using a rubber-wheel system with a rotation of 139 rpm, a load of 50 N, and a SiO_2 flux of between 250 and 310 g/min (Ref 3). Material loss was measured by weighing the samples every 1 min for the first 10 min and then every 5 min until the end of the test (45 min).

The resistance of the samples to corrosion was evaluated by performing electrochemical measurements in 80 ml of an aerated and unstirred 3.4% NaCl solution. The open-circuit potential (E_{OC} vs. time) and polarization curve were measured using EG&G Parc-273 equipment. Polarization experiments were carried out over a potential range of −100 to +350 mV. All electrochemical experiments were performed at room temperature.

3. Results and Discussion

3.1 Structural Characterization of WC-25Co Powder

The powder consisted of micrometric particles containing submicronic WC particles. The powder had a rather uniform spheroid morphology and a narrow particle size distribution of $-32 + 10$ μm (Fig. 1). XRD analysis of the powder showed only the presence of WC and Co without any W_2C, W, Co_6W_6C, or Co_3W_3C (Fig. 4).

3.2 Structural Characterization of the WC-25Co Coatings Obtained by CGS and HVOF Spraying

Figure 2 shows representative SEM cross-section micrographs of the coatings on Al7075-T6 and low-carbon

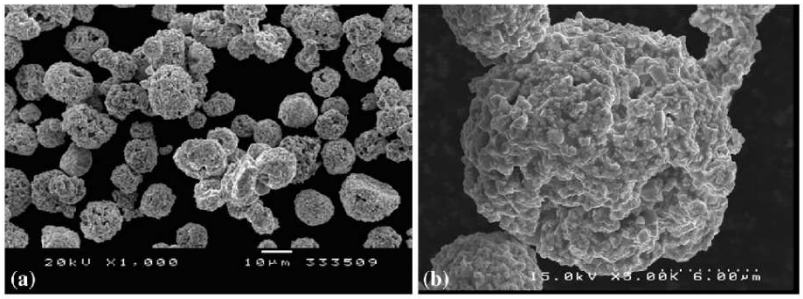

Fig. 1 SEM and FE-SEM micrographs of the free surface of the experimental WC-25Co cermet powder

steel, by HVOF (a and b) and CGS (c and d), using the experimental WC-25Co powder.

Figure 2 a and b shows the HVOF-sprayed WC-25Co powder on Al7075-T6 (Fig. 2a) and low-carbon steel substrates (Fig. 2b).

The coatings deposited by HVOF on the Al7075-T6 substrates presented uniform thickness and hardness with values of 163 ± 7 µm and 971 ± 134 HV_{300}, respectively, without any cracks or delamination. They exhibited good adhesion to the substrate. In a previous study dealing with a WC-25Co powder sprayed onto Al7075-T6 substrates by CGS (Ref 4), a coating thickness of 211 ± 24 µm and Vickers hardness of 848 ± 55 HV_{300} were reported (an example of a WC-25Co coating sprayed onto Al7075-T6 by CGS is shown in Fig. 2c). As discussed earlier, in CGS, there is no decarburization or formation of fragile η phases, i.e., the microstructure of the original material does not suffer any changes, whereas it does during HVOF spraying. Therefore, the coatings produced by HVOF suffer from decomposition of the WC-25Co powder during the spraying process and therefore hardening due to the presence of η phases. Besides increased hardness, these coatings will also be more brittle than those deposited by CGS due to the lower elemental ductile Co matrix content and the presence of fragile and hard Co_6W_6C or Co_3W_3C η phases. The temperatures during HVOF spraying cause a depletion of the ductile Co matrix resulting in more brittle coatings, as confirmed by the fracture toughness test results reported in section 3.3 below.

The coatings deposited on low-carbon steel substrates shown in Fig. 2b also presented uniform thickness, 126 ± 6 µm, and HV_{300} values of 991 ± 57, as well as good adhesion to the substrate. In the same study referred to in the previous paragraph, (Ref 4), for deposition of the same WC-25Co cermet powder deposited by CGS, uniform coatings that were well adhered to the substrate, without any cracks or inter-layer delamination, were reported with a thickness of 263 ± 32 µm and hardness of 981 ± 58 HV_{300} (Fig. 2d).

During the CGS process, the impinging particles have a compressive effect which allows the production of virtually non-porous coatings, as presented in (Ref 4).

The CGS deposition efficiency for the powder studied on the Al7075-T6 and low-carbon steel substrates was 24 and 17%, respectively. For the HVOF spraying performed in this study, the deposition efficiency was of 69 and 66%, respectively. Thus, one of the major disadvantages of the CGS process for the deposition of WC-25Co cermets is its low deposition efficiency. Since it is a solid-state deposition process, it is affected by several parameters that are different from those of conventional thermal-spraying processes. The particles are injected into a supersonic jet of compressed gas which deposits them onto a substrate, deforming them, and building up a layer of material (Ref 6, 10). The ductility of the powder and substrate, as well as the particle impact velocity, is the parameters that most affect the CGS process. In HVOF, the powder is heated due to the heat released by exothermic combustion in the mixing chamber, causing the powder particles to melt or partially melt; they are then flattened when they hit the substrate before they re-solidify. Thus, most of the sprayed material that arrives at the substrate adheres to it, or to the previously deposited material layers, in HVOF (Ref 1). Meanwhile in CGS, the particles that do not achieve a certain critical velocity will not adhere, since it is a solid-state deposition process that is entirely dependent on kinetic energy. However, if the particles achieve velocities that are too high, the substrate or previous layers of coating can be eroded by the impact resulting in a poor quality coating (Ref 6).

Careful observation of the micrographs revealed that some Al_2O_3 particles used for substrate preparation before HVOF deposition are found at the coating-substrate interface (marked with two arrows in Fig. 3a).

Bands of dissolution of the WC into the Co matrix can be seen in Fig. 3(a) at higher magnification. This means that there are few free carbides in the final coating, resulting in a decrease in some mechanical properties, for example, fracture toughness, as a direct consequence of the formation of hard Co_6W_6C and Co_3W_3C phases. Initially, WC grains partially dissolve in the liquid matrix. This decomposition leads to a hardened of the matrix holding the submicronic partially dissolved WC particles in place, surrounded by W_2C. This sub-carbide formation is due to carbon diffusion toward the surface of the grains

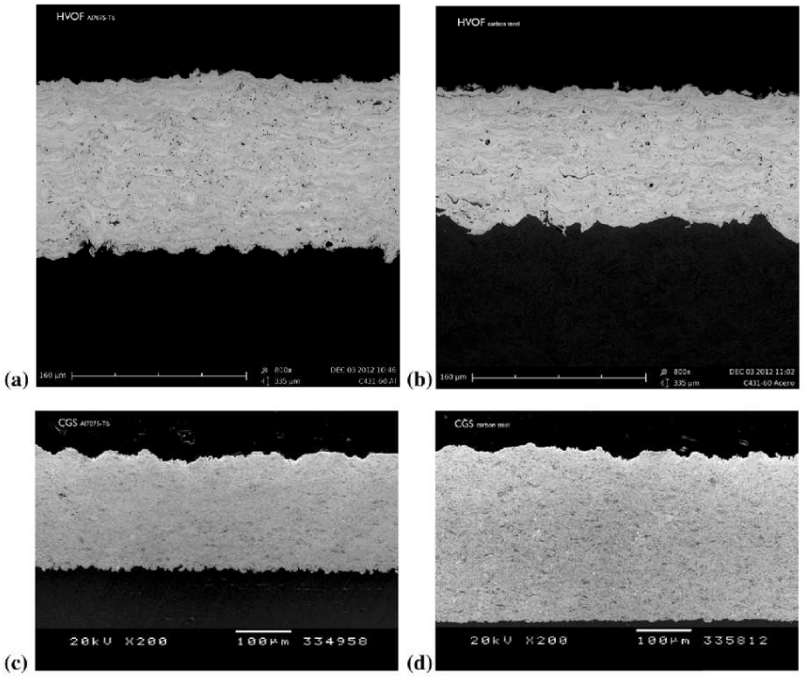

Fig. 2 SEM micrographs of the coatings obtained by HVOF (a and b) and CGS (c and d) on Al7075-T6 and low-carbon steel substrates, respectively

(Ref 2, 12). In Fig. 3(c), a clean interface can be seen, where no other particles that could alter the substrate/coating microstructure are present, as can the good adhesion of the CGS coating to the substrate. During CGS, there is no dissolution of the carbides into the matrix, thus the coating reflects the original properties of the powder (Fig. 3c and d). No cracking of the coatings and virtually no porosity can be seen in either figure.

Figure 4 shows XRD analysis; it reveals the sole presence of WC and Co in the final coatings. A1 and CS1 represent coatings obtained by CGS on the Al7075-T6 and low-carbon steel substrates, respectively. The results show that the substrate has no influence on the final phase composition of the WC-25Co CGS coatings. Table 1 shows a summary of the structural characterization of the obtained coatings.

XRD analysis of the HVOF coatings confirmed the presence of the brittle W_2C phase as well as the fragile Co_6W_6C or Co_3W_3C η phases (Fig. 5).

3.3 Fracture Toughness Tests

The results of the coating toughness predicted from the Half-Penny crack regime model are shown in Table 2. The WC-25Co coatings obtained by CGS showed the highest fracture toughness. Such an improvement in the fracture toughness of the CGS-sprayed coatings compared to those produced by the conventional HVOF technique can be attributed to the fact that during spraying the powder is not subjected to phase changes (Tables 2, 3, 4). Fragile η phases that drain the ductile-free metallic matrix in the microstructure and the brittle W_2C phase are not present in the CGS coatings. The cobalt present remains in the coatings and acts as a ductile element, thus improving the fracture toughness of these coatings. The compressive effect caused during CGS spraying corroborates the higher indentation fracture toughness of the CGS coatings. However, the fact that these coatings do not have W_2C phases seems the most significant factor in improving the fracture toughness, as indicated by Lima et al. (Ref 9).

3.4 Abrasive Wear Tests (Rubber-Wheel)

Testing the HVOF coatings on Al7075-T6 and low-carbon steel resulted in wear rates of $2.2 \times 10^{-5} \pm 1.5 \times 10^{-6}$ and $2.0 \times 10^{-5} \pm 7.0 \times 10^{-7}$ $mm^3/(N\ m)$, respectively. The results were expected to be similar considering that the substrates should have no effect (Fig. 5). The initial decrease in the wear rate is due to the initial roughness of the coatings ($Ra_{HVOF\ Al7075\text{-}T6} = 8.6$ µm and $Ra_{HVOF\ CS} = 7.8$ µm). Since the coating material, its hardness and the spraying parameters were the same for both substrates, the abrasive wear behavior was expected, and confirmed, to be very similar. Dosta et al. (Ref 4) reported abrasive wear rates of $2.75 \times 10^{-5} \pm 5.4 \times 10^{-7}$ and 2.87nbsp;$\times 10^{-5} \pm 1.85 \times 10^{-6}$ $mm^3/(N\ m)$ when spraying WC-Co via CGS onto Al7075-T6 and low-carbon

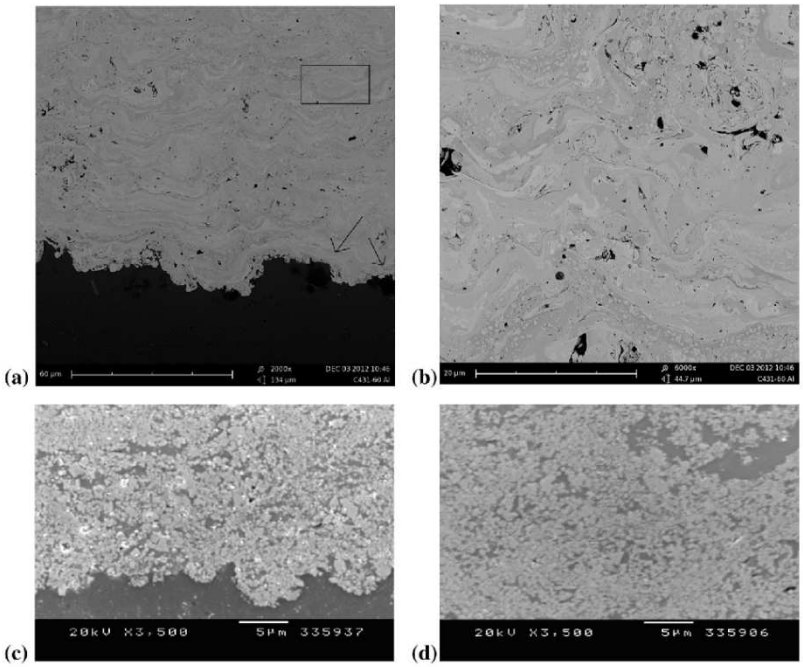

Fig. 3 SEM micrographs of WC-Co coating deposited on Al7075-T6 substrate: by HVOF spraying (a and b) where the dissolution of the Co matrix (indicated by the rectangle in a) can be seen; and by CGS (c and d), respectively

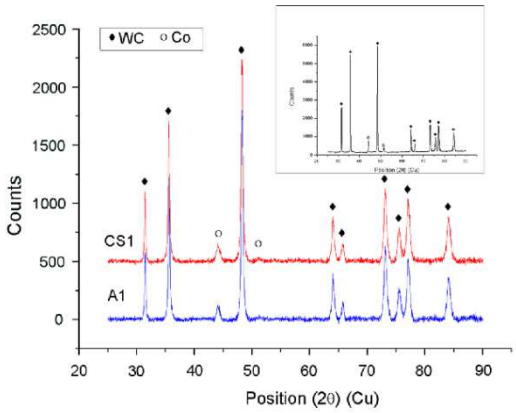

Fig. 4 XRD analysis of the CGS coatings and original powder

steel, respectively. These results show that with no depletion of the WC carbides and no hardness effect due to the production of brittle phases during deposition, CGS can produce coatings with approximately the same wear properties as those of HVOF coatings. Figure 6 shows the average results for the coatings obtained by both spraying techniques: the abrasive wear rate is of 2.1×10^{-5} mm^3 $\pm$ 1.1×10^{-6} for HVOF and 2.81×10^{-5} mm^3 $\pm$ 1.2×10^{-6} for CGS (Table 3).

Table 1 Summary of the structural characterization of coatings obtained by HVOF and CGS on Al7075-T6 and low-carbon steel substrates

	Thickness, μm	Hardness, HV_{300}	Deposition efficiency, %
HVOF Al7075-T6	163 ± 7	971 ± 134	69
CGS Al7075-T6	211 ± 24	848 ± 55	24
HVOF steel	126 ± 6	991 ± 57	66
CGS steel	263 ± 32	981 ± 58	17

3.5 Sliding Wear Tests (Ball-on-Disk)

The friction wear resistance of the HVOF coatings was tested under a load of 25 N and the best results compared with the best results for the CGS coatings (Table 4). The initial substrate roughness values were the same as those mentioned in section 3.4 above. The coatings produced by HVOF had a friction coefficient of 0.441 ± 0.09, a lost volume of approximately 0.05 mm^3, and produced a wear track of 840 μm; the wear track is reconstructed in Fig. 7. Meanwhile, the CGS coatings (Ref 4) had a friction coefficient of 0.380 ± 0.03, a lost volume of approximately 0.01 mm^3, and a wear track of 500 μm. In both cases, the wear resistance during testing proved to be high, with a slight improvement in the CGS coatings. In previous studies of HVOF WC-Co coatings, Shipway et al. reported that the wear rate of sprayed coatings increased with an

increase in decomposition products, especially W_2C (Ref 13), which were formed due to the high temperatures of the HVOF process. In CGS, this does not occur and the coatings, produced with no decomposition of the free WC carbides in the matrix, behaved better under the wear testing conditions. Figure 8(a) shows a representative sliding wear track on a CGS coating after testing to corroborate the statements in the text; at 50×, an arrow shows the sliding direction. Figure 8(b) and (c) depicts the same testing area at 150× and 3500×, respectively.

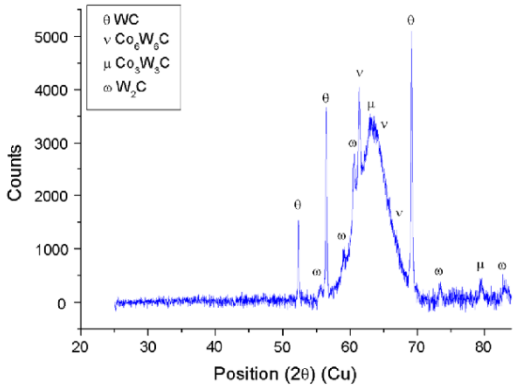

Fig. 5 XRD analysis of the HVOF coatings and original powder

Table 2 Fracture toughness of CGS and HVOF WC-25Co coatings

Coating	$K_{IC}(Mpam^{1/2})$
WC-25Co by HVOF	5.1 ± 0.2
WC-25Co by CGS	8.7 ± 1.6

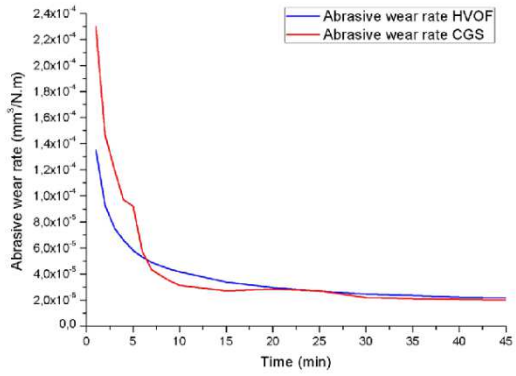

Fig. 6 Abrasive (rubber-wheel) wear rates vs. time (min) curves for HVOF and CGS coatings

3.6 Adhesion Tests

The quality of the substrate-coating interface bonding and inter-layer adhesion was measured by performing adhesion tests on samples prepared under the same spraying conditions. The initial substrate roughness values were the same as those mentioned above. The samples of the HVOF coatings on Al7075-T6 had a value of 27 ± 2 MPa. The mechanism of breakage was also determined and it was found that the coatings failed at the substrate-coating interface, meaning that inter-layer bonding was stronger than that of the substrate-coating interface. The CGS coatings sprayed onto Al7075-T6 exhibited much higher adhesion values than those of the HVOF coatings: 65 ± 4 MPa, with the tests ending in failure of the testing glue. These coating samples broke through the testing glue, meaning that the actual adhesion values are probably higher than those given. In CGS, a

Table 4 Summary of the BoD results for coatings obtained by HVOF and CGS

	Friction coefficient, μ	Lost volume, mm^3	Wear track, μm
HVOF	0.441 ± 0.09	0.05	840
CGS	0.380 ± 0.03	0.01	500

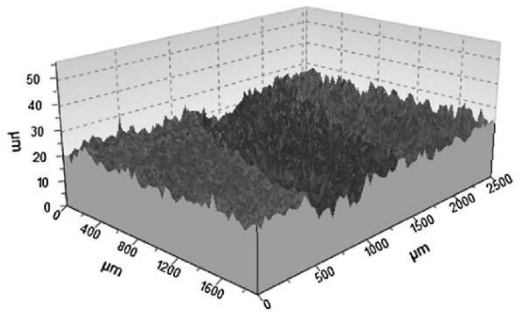

Fig. 7 Wear track reconstruction of the HVOF coating after testing

Table 3 Summary of the abrasive wear results for HVOF and CGS coatings on Al7075-T6 and low-carbon steel substrates

Technique/substrate	Al7075-T6, $mm^3/(N\ m)$	Steel, $mm^3/(N\ m)$
HVOF	$2.2 \times 10^{-5} \pm 1.5 \times 10^{-6}$	$2.75 \times 10^{-5} \pm 5.4 \times 10^{-7}$
CGS	$2.0 \times 10^{-5} \pm 7.0 \times 10$	$2.87 \times 10^{-5} \pm 1.85 \times 10^{-6}$

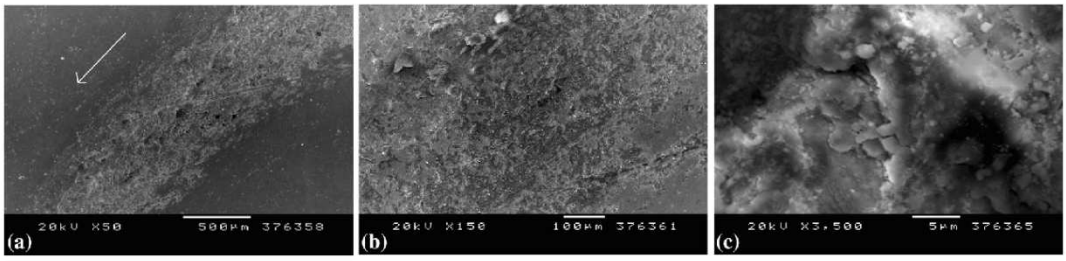

Fig. 8 SEM micrographs of the HVOF coating of a representative sliding wear area after testing at 50× (a), 150× (b), and 3500× (c)

Table 5 Summary of the electrochemical results after 24 h for HVOF and CGS coatings on Al7075-T6 and low-carbon steel substrates

Technique/substrate	Al7075-T6, V	Steel, V
HVOF	−0.573 ± 0.001	−0.568 ± 0.001
CGS	−0.439 ± 0	−0.481 ± 0.016

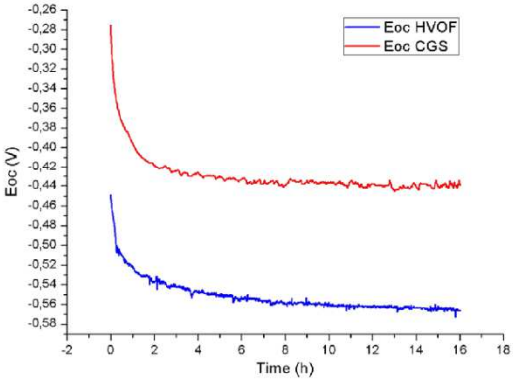

Fig. 9 Open-circuit potential (E_{oc}) vs. time (h) curves for HVOF and CGS coatings

certain degree of ductility of the particles and hardness of the substrate are needed to obtain sufficiently localized plastic deformation, i.e., the flattening of the particles, in order to build up a dense coating; the harder the substrate, the greater the flattening of the particles (Ref 4, 14, 15). The theory maintains that, in CGS, adherence values will be higher if the powders are sprayed onto low-carbon steel substrates than onto the more ductile Al7075-T6 substrates. Higher low-carbon steel adhesion values (74 ± 6 MPa) were observed by Dosta et al. (Ref 4).

3.7 Electrochemical Tests

Electrochemical tests were run to determine the resistance of the coatings to a corrosive environment. The initial decrease in the curve is a consequence of the dissolution of oxides at the surface of the coatings and initial penetration of the electrolyte (Ref 16). After 24 h of testing, the potential was −0.573 ± 0.001 V for the HVOF coatings deposited on Al7075-T6 and −0.568 ± 0.001 V for those on low-carbon steel (Table 5). The behavior was constant and the potential stabilized after 16 h of testing: the potential being approximately the same after 24 h. The electrolyte did not reach the substrate, meaning that both coatings, after 24 h, successfully protected the substrate from electrochemical corrosion. This was concluded after submitting the Al7075-T6 and low-carbon steel substrates to the same testing conditions: their open-circuit potentials were −0.687 and −0.744 V, respectively, after 24 h of testing, which were considerably more negative than those obtained after testing the HVOF-sprayed coatings. It should be noted that after 16 h of electrochemical testing under the same conditions, the CGS coating exhibited a potential of −0.439 ± 0 on the Al7075-T6 substrate and a potential of −0.481 ± 0.016 on the low-carbon steel substrate (Ref 4). This slight improvement in electrochemical corrosion resistance of the CGS coatings was attributed to the compressive effect of the particles during CGS, which produces less porous coatings and therefore fewer ways for the electrolyte to penetrate and reach the substrate. Figure 9 shows the average results of the best coatings obtained by both HVOF and CGS spraying techniques; the HVOF coatings deposited onto low-carbon steel substrates and the CGS coatings on Al7075-T6 substrates.

4. Conclusions

Although the CGS deposition of WC-Co coatings was less efficient than that of HVOF spraying:

- Dense, thick, and well-bonded WC-25Co coatings were obtained by CGS using N_2 as the process gas;
- Higher HV_{300} hardness values were obtained by HVOF, due to the formation of brittle W_2C and Co_xW_xC phases, with an associated depletion of the ductility provided by the Co matrix, due to the high decarburization and dissolution caused during the spraying process by the high temperatures of the HVOF flame;
- Microstructural changes, specifically the formation of W_2C and W, resulted from the HVOF process;

- The CGS deposition efficiency needs to be improved as it is considerably lower than that achieved using HVOF spraying: 24 versus 69% for Al7075-T6 and 17 versus 66% for low-carbon steel substrates;
- Rubber-Wheel tests produced abrasive wear rates in the magnitude of 10^{-5} both by CGS and HVOF spraying, demonstrating that the processes can produce equally wear-resistant coatings; while taking into account that CGS, as a solid-state deposition process, does not produce other brittle phases;
- CGS coatings showed 5 times higher friction wear resistance and a gain of 71% in fracture toughness, compared to HVOF coatings;
- HVOF coatings provided higher adhesion to the Al7075-T6 substrates (73.7 ± 6 MPa) than the CGS coatings (27 ± 2 MPa); and
- CGS produced compact and non-degraded coatings with less porosity than the HVOF coatings and therefore a slight improvement in the electrochemical resistance (~15% E_{oc} reduction).

Acknowledgments

The authors wish to thank the University of Barcelona for financial support for this research and the *Generalitat de Catalunya* for funding project 2009 SGR-00390. Our thanks also go to Fujimi Inc. for providing the WC-Co powder.

References

1. V.V. Sobolev, J.M. Guilemany, and J. Nutting, *High Velocity Oxy-Fuel Spraying*, Maney, London, 2004
2. J.M. Guilemany, S. Dosta, and J.R. Miguel, The Enhancement of the Properties of WC-Co HVOF Coatings Through the Use of Nanostructured and Microstructured Feedstock Powders, *Surf. Coat. Technol.*, 2006, **201**, p 1180-1190
3. J.M. Guilemany, S. Dosta, J. Nin, and J.R. Miguel, Study of the Properties of WC-Co Nanostructured Coatings Sprayed by High-Velocity Oxyfuel, *J. Therm. Spray Technol.*, 2005, **14**(3), p 405-413
4. S. Dosta, M. Couto, and J.M. Guilemany, Cold Spray Deposition of a WC-25Co Cermet Onto Al7075-T6 and Carbon Steel Substrates, *Acta Mater.*, 2013, **61**(2), p 643-652
5. M. Couto, S. Dosta, M. Torrell, J. Fernández, and J.M. Guilemany, Cold Spray Deposition of WC-17 and 12Co cermets onto aluminum, *Surf. Coat. Technol.*, 2013, **235**, p 54-61
6. V.K. Champagne, *The Cold Spray Materials Deposition Process: Fundamentals and Applications*, CRC Press, Boca Raton, 2007
7. J. Kawakita, H. Katanoda, M. Watanabe, K. Yokoyama, and S. Kuroda, Warm Spraying: An Improved Spray Process to Deposit Novel Coatings, *Surf. Coat. Technol.*, 2008, **202**, p 4369-4373
8. M.M. Lima, C. Godoy, P.J. Modesi, J.C. Avelar-Batista, A. Davison, and A. Matthews, Coating Fracture Toughness Determined by Vickers Indentation: An Important Parameter in Cavitation Erosion Resistance of WC-Co Thermally Sprayed Coatings, *Surf. Coat. Technol.*, 2004, **177-178**, p 489-496
9. M.M. Lima, C. Godoy, J.C. Avelar-Batista, and P.J. Modesi, Toughness Evaluation of HVOF WC-Co Coatings Using Non-linear Regression Analysis, *Mater. Sci. Eng.*, 2003, **A357**, p 337-345
10. E. López Cantera and B.G. Mellor, Fracture Toughness and Crack Morphologies in Eroded WC-Co-Cr Thermally Sprayed Coatings, *Mater. Lett.*, 1998, **37**, p 201-210
11. N. Cinca, M. Barbosa, S. Dosta, and J.M. Guilemany, Study of Ti Deposition Onto Al Alloy by Cold Gas Spraying, *Surf. Coat. Technol.*, 2010, **205**, p 1096-1102
12. C. Verdon, A. Karimi, J.L. Martin, and L. Pawlowski, A Study of High Velocity Oxy-fuel Thermally Sprayed Tungsten Carbide Based Coatings. Part I: Microstructures, *Mater. Sci. Eng.*, 1998, **A246**, p 11-24
13. D.A. Stewart, P.H. Shipway, and D.G. McCartney, Abrasive Wear Behavior of Conventional and Nanocomposite HVOF-Sprayed WC-Co Coatings, *Wear*, 1999, **225-229**, p 98-789
14. T. Schmidt, F. Gärtner, H. Assadi, and H. Kreye, Development of a Generalized Parameter Window for Cold Spray. Deposition, *Acta Mater.*, 2006, **54**, p 729-742
15. H. Assadi, F. Gärtner, T. Stoltenhoff, and H. Kreye, Bonding Mechanism in Cold Gas Spraying, *Acta Mater.*, 2003, **51**, p 4379-4394
16. R.G. Kelly, J.R. Scully, D.W. Shoesmith, and R.G. Buchheit, *Electrochemical Techniques in Corrosion Science and Engineering, Chapter 7*, Marcel Dekker Inc, New York, 2002

d) Paper 4:

M. Couto, S. Dosta, J.M. Guilemany, Comparison of the mechanical and electrochemical properties of WC-17 and 12Co coatings onto Al7075-T6 obtained by high velocity oxy-fuel and cold gas spraying, Surface and Coatings Technology, 2014

The satisfactory results of the first comparison of CGS and HVOF coatings led to the continuing efforts in this research line in which WC-17 and 12Co HVOF coatings were produced and compared with CGS WC-17 and 12Co coatings. With this research work, all of the Thesis' objectives were fulfilled with success.

ARTICLE IN PRESS
SCT-19354; No of Pages 10
Surface & Coatings Technology xxx (2014) xxx–xxx
Contents lists available at ScienceDirect
Surface & Coatings Technology
journal homepage: www.elsevier.com/locate/surfcoat

Comparison of the mechanical and electrochemical properties of WC-17 and 12Co coatings onto Al7075-T6 obtained by high velocity oxy-fuel and cold gas spraying

M. Couto, S. Dosta *, J.M. Guilemany

Thermal Spray Centre (CPT), Facultad de Química, Universitat de Barcelona, Spain

ARTICLE INFO

Article history:
Received 17 January 2014
Accepted in revised form 11 April 2014
Available online xxxx

Keywords:
Submicronic carbides
WC–17Co and WC–12Co coatings
Cold spray
Wear/corrosion resistance
Aluminum Al7075-T6 substrates

ABSTRACT

Cold Gas Spray (CGS) coatings were produced by spraying WC-17 and 12Co cermet powders with submicronic WC particles onto aluminum alloy (Al7075-T6) substrates. WC–Co cermets have been used for wear-resistant parts due to their combination of mechanical, physical and chemical properties. Conventionally WC–Co cermets are produced by other thermal spray techniques, i.e. High-Velocity Oxy-Fuel (HVOF). A study was made to compare the mechanical and electrochemical properties of WC-17 and 12Co coatings sprayed both by CGS and HVOF obtained in this work. It is known that with a decrease in cobalt content some mechanical properties, i.e., hardness and wear resistance, are increased while others such as fracture toughness suffer the opposite effect. XRD tests were run on the powder and coatings to determine possible phase changes during the spraying process. The abrasive wear resistance and adhesive wear resistance of both optimum coatings obtained by CGS and HVOF were measured and compared in this work. The corrosion resistance was determined by electrochemical measurements. CGS for obtaining WC-17 and 12Co coatings has been proven to be very competitive when compared to coatings deposited by HVOF, obtaining dense and hard coatings onto Al7075-T6 substrates with enhanced mechanical and electrochemical properties as those produced by HVOF.

1. Introduction

WC–Co coatings, which are highly resistant to wear, are usually produced by conventional thermal spraying techniques, such as high velocity oxy-fuel (HVOF). This is a high temperature process that, in order to deposit the material onto a substrate uses temperature to melt or heat up the powder particles. Due to the high temperatures used in this process, decarburization and formation of brittle phases happen [1–3]. To avoid this negative effect, cold gas spraying (CGS) was tested to successfully deposit WC–25Co cermets [4] and WC-17 and 12Co cermets [5] onto Al7075-T6 substrates. The distinct microstructure of these powders affects their final mechanical and electrochemical properties. A decrease in Co content provides greater coating hardness while the fracture toughness shows the opposite behavior [6]. CGS is a solid state process deposition where no melting of the powder particles, hence avoiding the mentioned undesirable decomposition effect in HVOF, occurs. The particles are sprayed onto the substrates in a supersonic jet of compressed gas where they deform and bond to them thus creating a thick layer of material [4–7]. Warm spraying has been reported to successfully deposit novel coatings with scarce formation of impurity phases. This process uses nitrogen to control the gas temperature allowing control of a wide range of temperatures used for deposition of the particles [8].

The main objective of this work was to obtain coatings of WC–17Co and WC–12Co cermets onto Al7075-T6 by HVOF and afterwards compare them with those obtained in a previous study published by M. Couto et al. where the authors deposited the same powder onto these substrates by CGS. To achieve this goal, different mechanical and electrochemical tests were performed on the best obtained coatings using HVOF.

2. Experimental procedure

The studied powders WC–Co cermets were obtained by agglomeration and sintering and had different contents in cobalt: 17 and 12 wt.%. These powders were processed and provided by Fujimi Inc. (Kiyosu, Japan). The powder was sprayed onto several samples of aluminum Al7075-T6 coupons: flat substrates (100 × 20 × 5 mm); and cylindrical substrates (Ø = 25.4 mm, height 25.4 mm). The substrates for CGS were prepared by grinding using a 240 grit SiC paper while the substrates for HVOF were prepared by grit-blasting using Al_2O_3 particles to improve deposition efficiency. The powders were characterized by studying their microstructure through Scanning Electron Microscopy (SEM) and Field Emission SEM (FE-SEM) and the phase composition by X-ray Diffraction (XRD). Afterwards, the coatings were also characterized by

* Corresponding author.
E-mail address: sdosta@cptub.eu (S. Dosta).

http://dx.doi.org/10.1016/j.surfcoat.2014.04.034
0257-8972/

SEM and their phase composition by XRD. Vickers hardness tests were also performed on the cross-section of each coating with a fixed load of 300 gf for 15 s.

Two kinds of wear tests were performed to measure the wear resistance of the coatings. A sliding wear test was carried out using a ball-on-disk (BoD) method, following the ASTM G99-04 standard. A WC–12Co counterpart ball, a sample relative velocity of 131 rpm, with a total testing of 1000 m and a force load of 25 N for a radius of 14 mm, were the parameters selected for test purposes. Humidity and temperature were kept below 20% and 25 °C, respectively. Leica TCS-SE Confocal equipment was used to measure the volume loss of the wear tracks and to recreate the wear path. Dry abrasive tests (ASTM G65-00 standard) were carried out using a rubber wheel system with a rotation of 139 rpm, a load of 50 N, and a SiO_2 flux of between 250 and 310 g/min [3]. Material loss was measured by weighing the samples every 1 min during the first 10 min, and then every 5 min until the end of the test (45 min).

The resistance of the samples to corrosion was evaluated by performing electrochemical measurements in 80 ml of an aerated and unstirred 3.4% NaCl solution. The open-circuit potential (E_{OC} vs. time) and polarization curve (CP) were measured using EG&G Parc-273 equipment. Polarization experiments were carried out in a potential range of −100 to +350 mV. All electrochemical experiments were performed at room temperature.

3. Results and discussion

3.1. Structural characterization of WC-17 and 12Co powders

Both powders have a micrometric particle size in the range of −32 to 10 μm according to the provider. Near nanosized WC particles are found embedded in the particles. The WC–17Co powder shows a spheroid and rather uniform morphology as well as a narrow particle size distribution (Fig. 1) as confirmed by the LS analysis (Fig. 2). In Fig. 4 two different SEM micrographs of the WC–12Co experimental powder are depicted and represent the free surface of this powder. A representative XRD analysis of the WC-17 and 12Co powders showed no other phases of WC or Co such as W_2C, W, Co_6W_6C or Co_3W_3C (Fig. 3).

3.2. Structural characterization of the WC-17 and 12Co coatings by HVOF and CGS

Fig. 5 depicts representative SEM cross-section micrographs at different magnifications of the obtained coatings onto Al7075-T6 substrates, by HVOF (a) and CGS (b), respectively, using the experimental WC–17Co powder. Those obtained using the WC–12Co powder by HVOF (a) and CGS (b) onto Al7075-T6 are shown in Fig. 6.

3.2.1. WC–17Co coatings

WC–17Co coatings obtained by HVOF onto Al7075-T6 present a uniform thickness and hardness with values of 113 ± 8 μm and 1379 ± 75HV_{300}, respectively, without any cracks or delamination and with a homogeneous and defect-free interface with the substrate. In previous studies with WC-17 and 12Co powders sprayed onto Al7075-T6 by CGS, M. Couto et al. [5] reported thickness values of 129 ± 5 μm and Vickers hardness values of 1223 ± 59HV_{300} (an example of a WC–17Co coating sprayed onto Al7075-T6 by CGS is depicted in Fig. 5b). During Cold Gas Spraying the effect of decarburization or formation of fragile η phases is not present, i.e., the microstructure of the initially sprayed material will not suffer any changes [6]. On the other hand, during HVOF spraying this occurs [7]. Therefore the produced coatings by HVOF will cause a decomposition of the WC–Co powders and hence a hardening effect due to the presence of these fragile phases. Besides the higher hardness values obtained due to the hard phases formed during the spraying process using HVOF the coatings will also be more brittle than those sprayed by CGS due to the lower content in ductile elemental Co matrix.

3.2.2. WC–12Co coatings

The coatings obtained using a WC–12Co depicted in Fig. 6a also presented a rather uniform thickness, 119 ± 10 μm, and HV_{300} values of 1536 ± 42 as well as a clean interface with the substrate. As expected and owing to the privileged percentage of hard phase in this cermet the obtained HV values are higher in approximately 21% than those obtained from WC–17Co coatings.

In the same study referred in the previous paragraph [5] the authors presented, for the deposition of the same studied WC–12Co cermet powder by CGS, uniform coatings, well adhered to the substrate, without any cracks or inter-layer delamination, with thickness values of 93 ± 8 μm and hardness values of 1419 ± 93HV_{300} (Fig. 6b).

The obtained WC-17 and 12Co coatings showed in Figs. 5a and 6a show some porosity when compared to Figs. 5b and 6b. During the CGS process there is a compressive effect of the impinging particles during spraying which allows the production of virtually non-porous coatings as the ones presented in the compared study [4].

On the other side the deposition efficiency (D.E.) is an issue when spraying hard materials by CGS as shown by these results: D.E. of WC–17Co by CGS = 11.9%; D.E. of WC–17Co by HVOF = 67%. The deposition efficiencies for the deposition of WC–12Co onto Al7075-T6 by HVOF and CGS were of 40 and 14.2%, respectively. This is one of the major disadvantages of the CGS process for the deposition of WC–Co cermets. CGS is a solid-state deposition process where no melting of the powder particles occurs. For this reason it is influenced by different parameters than conventional thermal spraying techniques. The particles are injected into a supersonic jet of compressed gas which deposits

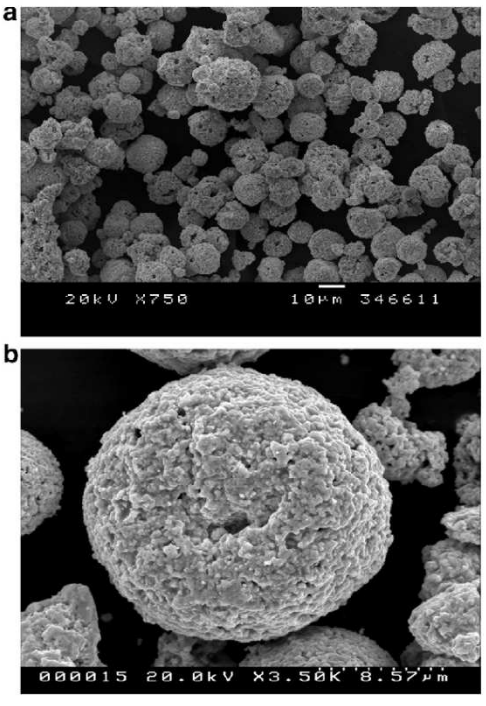

Fig. 1. SEM micrographs at 750× and 3500×, respectively, of the free surface of the studied experimental WC–17Co cermet powder.

Please cite this article as: M. Couto, et al., Surf. Coat. Technol. (2014), http://dx.doi.org/10.1016/j.surfcoat.2014.04.034

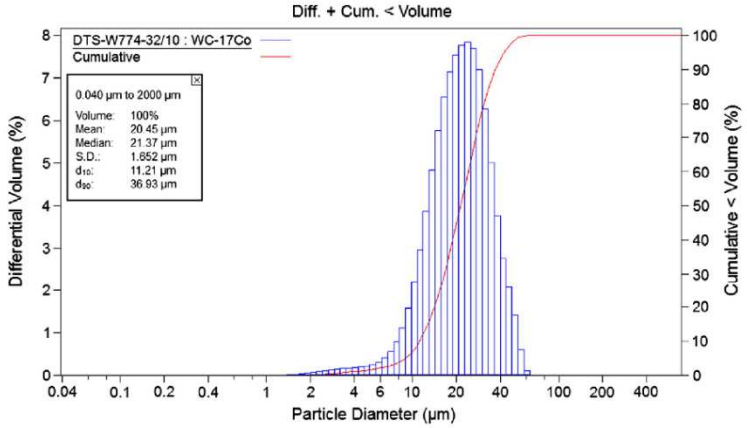

Fig. 2. Representative LS particle size distribution analysis graph.

them onto a substrate, deforming these incoming particles and thus building a layer of material [5,9]. The ductility of the spraying powder and the substrates, and the critical velocity are main parameters in CGS. In HVOF the powder is heated due to the elevated combustion temperatures produced in the mixing chamber, causing the formation of molten or semi-molten particles of the sprayed powder. These droplets hit the substrate and consequently flatten and solidify meaning that most of the injected spraying material arriving on the substrate will adhere to it, or to the previously deposited material layers [1]. In CGS, if not all the particles achieve a certain acceleration (critical velocity), due to its being a solid-state deposition process where it is entirely dependent on kinetic energy and none on thermal energy, they will not adhere or, furthermore, if they achieve extremely high velocities, erode the substrate/layers of coatings [7,10].

In Fig. 5a$_2$ a SEM micrograph of an obtained coating onto Al7075-T6 by HVOF shows the dissolution of the Co matrix originated during the spraying process. The light gray areas can be seen spread out throughout (Fig. 5a$_2$) the bands of dissolution of the WC into the Co matrix. This means that there are few free carbides in the final coating, resulting in a decrease in some mechanical properties, for example, fracture toughness, as a direct consequence of the formation of Co_6W_6C and Co_3W_3C hard phases [2,3]. Initially, a partial dissolution of WC grains in the liquid matrix happens. This decomposition leads to a hardened matrix holding the submicronic partially dissolved WC particles in place surrounded by W_2C. This sub-carbide formation is due to the carbon diffusion towards the outside of the grains [2,10,11]. During CGS there is no dissolution of the carbides into the matrix therefore allowing the coating to enhance the powder's original properties (Fig. 3).

An XRD analysis of the obtained WC–17Co coatings was performed to confirm the presence of brittle W_2C phase as well as fragile Co_6W_6C

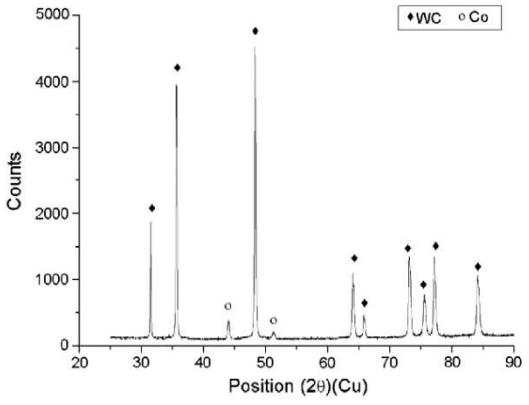

Fig. 3. Representative XRD analysis of the WC–17Co powder.

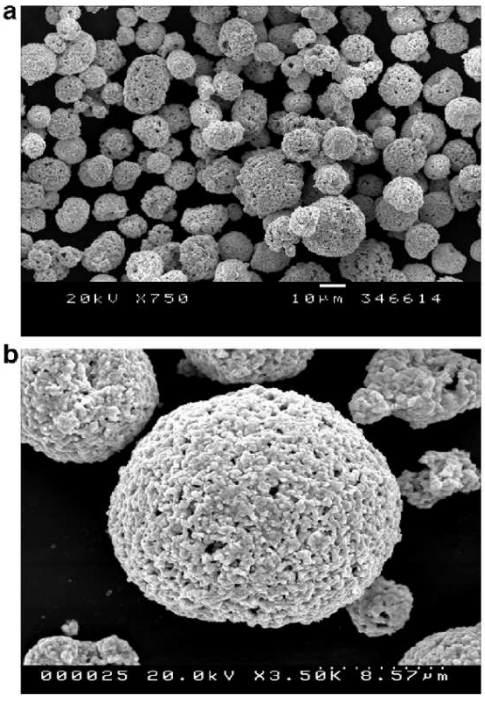

Fig. 4. SEM micrographs at 750× and 3500×, respectively, of the free surface of the studied experimental WC–12Co cermet powder.

Please cite this article as: M. Couto, et al., Surf. Coat. Technol. (2014), http://dx.doi.org/10.1016/j.surfcoat.2014.04.034

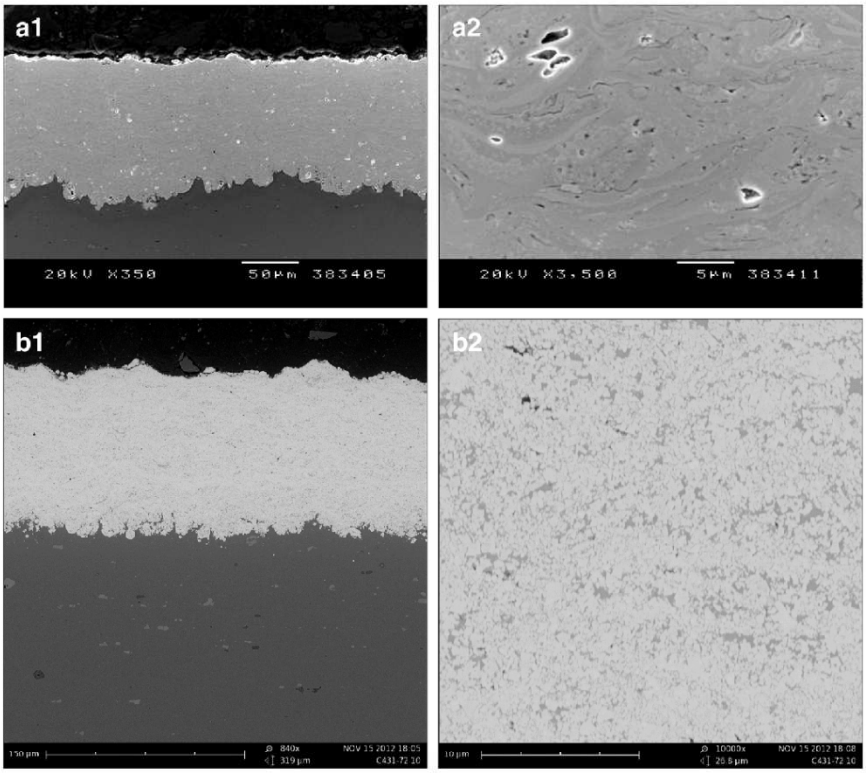

Fig. 5. SEM micrographs of the obtained coatings by HVOF (a) and CGS (b) onto Al7075-T6 using WC–17Co cermet powder.

or Co_3W_3C η (eta) phases and an example is shown in Fig. 7a whereas the XRD analysis results for CGS coatings are shown as an example in Fig. 7b — where no impurity phases are evidenced, just the presence of WC and Co. This was verified in both WC-17 and 12Co spraying by HVOF and CGS.

3.3. Abrasive wear tests (rubber-wheel)

Testing of samples of the optimum coatings obtained onto Al7075-T6 by HVOF and CGS resulted in wear rates of $2.1 \times 10^{-5} \pm 1.6 \times 10^{-6}$ and $1.3 \times 10^{-5} \pm 2.4 \times 10^{-6}$ $mm^3/N.m^{-1}$, respectively (Fig. 8). The initial decrease in the wear rate is due to the coating initial roughness. Even though during the HVOF spraying process there is the formation of brittle and hard phases the abrasive wear resistance of CGS coatings proved to be higher than HVOF coatings. So, in this case, there is another enhanced feature of CGS's advantage of not producing decarburization or dissolution during the process. These results show that with no depletion of the WC carbides and no hardness effect due to the production of brittle phase during deposition, CGS can produce better results than when spraying with HVOF.

Shown in Fig. 9 is the average result of the WC–12Co coatings obtained by each of the spraying techniques, HVOF and CGS with respective wear rates of $2.0 \times 10^{-5} \pm 9.2 \times 10^{-6}$ and $8.7 \times 10^{-6} \pm 7 \times 10^{-7}$ $mm^3/N.m^{-1}$.

A comparative summary of the abrasive wear rate in $mm^3/N.m^{-1}$ for both WC-17 and 12Co coatings – obtained by CGS and HVOF – after testing is shown in Fig. 10.

3.4. Sliding wear tests (ball-on-disk)

The friction wear resistance of the obtained coatings was performed under a load of 25 N and its best results were compared with the best obtained using the same system by CGS. The WC–17Co coatings produced by HVOF had a friction coefficient of 0.350 ± 0.076 (Fig. 11) and a lost volume of approximately 0.03041 mm^3 while those produced by CGS [5] ended with a friction coefficient of 0.470 ± 0.03 and lost volume of approximately 0.0086 mm^3.

In Fig. 12 the evolution of the friction coefficient for the WC–12Co coatings by HVOF and CGS can be seen. The WC–12Co coatings produced by HVOF had a friction coefficient of 0.355 ± 0.015 and a lost volume of approximately 0.00929 mm^3 while those produced by CGS [5] ended with a friction coefficient of 0.41 ± 0.01 and lost volume of approximately 0.0038 mm^3.

In both cases the wear resistance during testing proved to be quite high, with CGS showing better results especially in terms of lost volume with an improvement of approximately 72% for the WC–17Co coatings and 60% for the WC–12Co ones. In previous studies of WC–Co coatings produced by HVOF spraying Shipway et al. reported that the wear rate of the sprayed coatings increases with an increase in decomposition products, especially W_2C [11], which are formed due to the high temperatures during spraying. In this case, this did not happen and the fact that CGS produced coatings with no decomposition of the free WC carbides in the matrix had a better outcome behavior under such wear testing conditions.

Fig. 13 represents a wear track reconstruction using Confocal equipment of a WC–17Co coating by HVOF after BoD testing.

Please cite this article as: M. Couto, et al., Surf. Coat. Technol. (2014), http://dx.doi.org/10.1016/j.surfcoat.2014.04.034

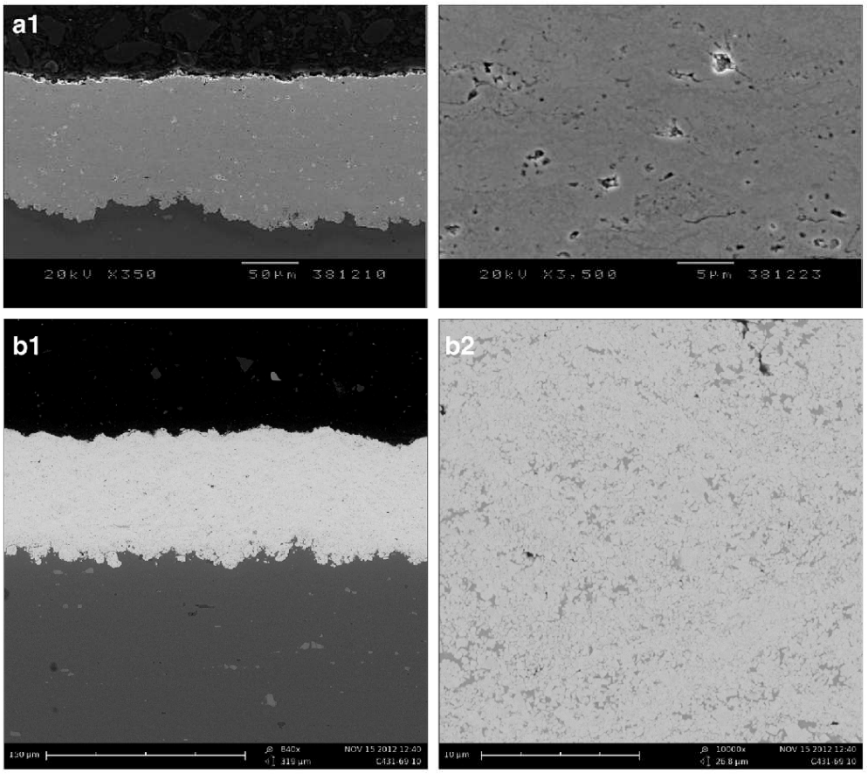

Fig. 6. SEM micrographs of the obtained coatings by HVOF (a) and CGS (b) onto Al7075-T6 using WC–12Co cermet powder.

A comparative summary of the lost volume in mm^3 for both WC–17 and 12Co coatings – obtained by CGS and HVOF – after testing is shown in Fig. 14.

3.5. Electrochemical tests

Electrochemical tests were run to determine the coating resistance in a corrosive environment. The initial decrease in the curve is a consequence of the dissolution of oxides on the surface of the coating samples and initial penetration of the electrolyte [12]. After 20 h of testing the potential was -0.539 ± 0.009 V for the WC–17Co coatings by HVOF and -0.394 ± 0.009 V by CGS obtained onto Al7075-T6 (Fig. 15). After 20 h of testing the potential was -0.420 ± 0.009 V for the WC–12Co coatings by HVOF and -0.387 ± 0.004 V by CGS obtained onto Al7075-T6.

A constant behavior is evidenced and a stabilization of the potential happens after 10 h of testing, where the potential is approximately the same as that after 20 h of testing. The electrolyte did not reach the substrate, meaning that both coatings, after 20 h, successfully protected the substrate from electrochemical corrosion. This is concluded after having submitted Al7075-T6 substrate samples to the same testing conditions: its open circuit potential is -0.687 V, after 20 h of testing, which is a considerably more negative potential than the ones obtained after testing over the HVOF and CGS sprayed WC–Co coatings. The WC/Co interface is a preferable path for the electrolyte to enter and corrode the coatings, meaning that the lower the ductile binder content the less the available ways for corrosion to take place and the higher the corrosion resistance, thus the higher resistance of the WC–12Co against the WC–17Co ones.

This slight improvement in electrochemical corrosion resistance showed by CGS vs HVOF coatings is attributed to the compressive effect of the particles during CGS, which produces less porous coatings and therefore less ways for the electrolyte to penetrate and reach the substrate.

4. Conclusions

- Dense, thick and well bonded WC–17 and 12Co coatings were obtained onto Al7075-T6 by HVOF and CGS using N_2 as process gas;
- No microstructural changes, decarburization or formation of fragile η phases while spraying with CGS; Microstructural changes, namely the formation of W_2C and W_xCo_xC phases, were present using HVOF;
- Higher HV_{300} hardness values were obtained by HVOF due to the formation of W_2C and Co_xW_xC phases, with a depletion of the ductility provided by the Co matrix due to the high decarburization and dissolution caused during the deposition process by the HVOF flame;
- There was an improvement of approximately 62% during rubber-wheel abrasive testing for WC–17Co coatings and approximately 130% for WC–12Co coatings. CGS showed better results and did not form strange brittle phases during the process;
- CGS coatings showed higher coefficient of friction than those produced by HVOF. WC–17Co coatings and WC–12Co coatings showed approximately 34% and 15% higher friction coefficient than HVOF coatings;

Please cite this article as: M. Couto, et al., Surf. Coat. Technol. (2014), http://dx.doi.org/10.1016/j.surfcoat.2014.04.034

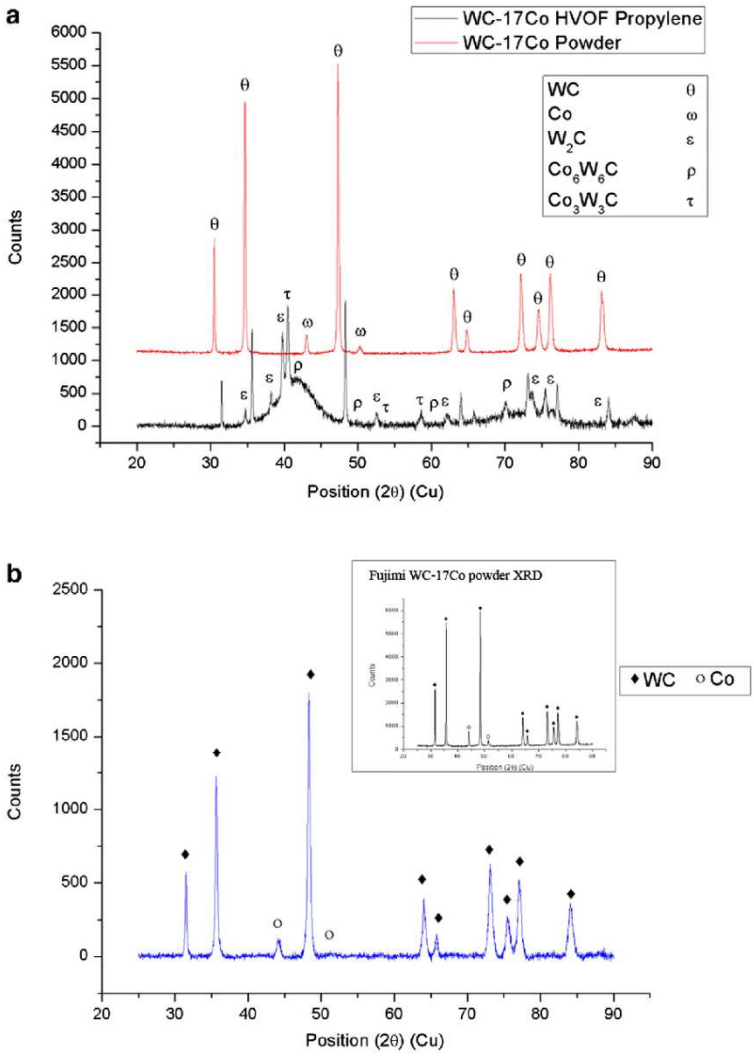

Fig. 7. a. XRD example of the obtained HVOF coatings and a comparison with XRD analysis of the experimental powder. b. XRD example of the obtained CGS coatings and a comparison with XRD analysis of the experimental powder.

- CGS coatings lost less volume than HVOF coatings and WC–12Co showed a higher wear resistance than WC–17Co coatings due to the higher content in hard WC phase. WC–17Co coatings by CGS lost ≈64% less volume than HVOF and WC–12Co ≈144% less.
- CGS produced compact and non-degraded coatings compared to HVOF and therefore a slight enhancement of the coating electrochemical resistance. There was ≈37% E_{OC} reduction on CGS WC–17Co coatings and ≈8% E_{OC} on WC–12Co coatings when compared to HVOF ones;
- Cold spray gas technology can clearly compete in terms of mechanical and electrochemical behavior with conventional deposition techniques to spray the studied WC-17 and 12Co powders. Nevertheless, CGS deposition efficiency has to be improved due to deposition efficiency by HVOF being higher (approximately 70%) while spraying WC–Co cermets when compared to CGS.

Conflict of interest

None.

Acknowledgments

The authors wish to thank the University of Barcelona (57CM201106001) for financial support for this research and the Generalitat de Catalunya for funding Project 2009 SGR-00390. Thanks also go to Fujimi Inc. for providing the WC–Co powders.

References

[1] V.V. Sobolev, J.M. Guilemany, J. Nutting, High Velocity Oxy-fuel Spraying, Maney, 2004.

Please cite this article as: M. Couto, et al., Surf. Coat. Technol. (2014), http://dx.doi.org/10.1016/j.surfcoat.2014.04.034

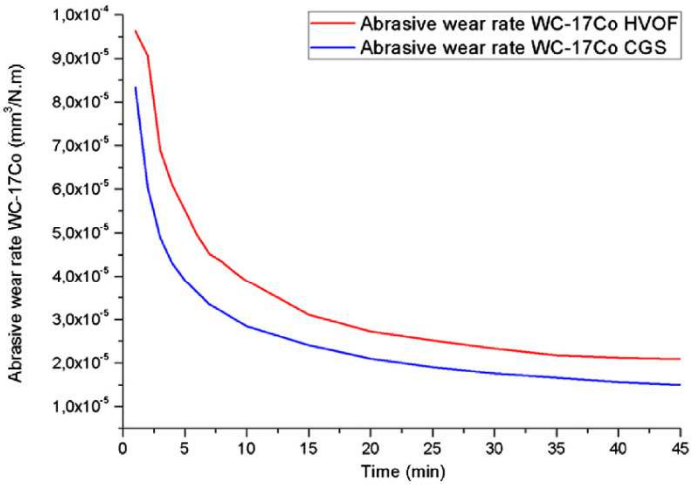

Fig. 8. Abrasive (rubber-wheel) wear rate vs. time (min) comparison curves for the WC–17Co coatings obtained by HVOF and CGS.

[2] J.M. Guilemany, S. Dosta, J.R. Miguel, Surf. Coat. Technol. 201 (2006) 1180–1190.
[3] J.M. Guilemany, S. Dosta, J. Nin, J.R. Miguel, J. Therm. Spray Technol. 14 (3) (2005) 405–413.
[4] S. Dosta, M. Couto, J.M. Guilemany, Acta Mater. 61 (2) (2013) 643–652.
[5] M. Couto, S. Dosta, M. Torrell, J. Fernández, J.M. Guilemany, Surf. Coat. Technol. 235 (2013) 54–61.
[6] M. Yandouzi, E. Sansoucy, P. Richer, B. Jodoin, L. Ajdelsztajn, Deposition and characterization of WC–Co coatings prepared by continuous- and pulsed-cold spray processes, Proceedings of The International Thermal Spray ConferenceASM International(OH), Beijing, China, 2007.
[7] V.K. Champagne, The Cold Spray Materials Deposition Process: Fundamentals and Applications, 2007. (Boca Raton).
[8] J. Kawakita, H. Katanoda, M. Watanabe, K. Yokoyama, S. Kuroda, Surf. Coat. Technol. 202 (2008) 4369–4373.
[9] N. Cinca, M. Barbosa, S. Dosta, J.M. Guilemany, Surf. Coat. Technol. 205 (2010) 1096–1102.
[10] A. Papyrin, V. Kosarev, S. Klinkov, A. Alkimov, V. Fomin, Chapter 5 — Current status of the cold spray process, Cold Spray Technology, 2007. 248–323.
[11] D.A. Stewart, P.H. Shipway, D.G. McCartney, Wear 225–229 (1999) p789–p798.
[12] R.G. Kelly, J.R. Scully, D.W. Shoesmith, R.G. Buchheit, Electrochemical Techniques in Corrosion Science and Engineering, Marcel Dekker, Inc., 2002. 236 (Chapter 7).

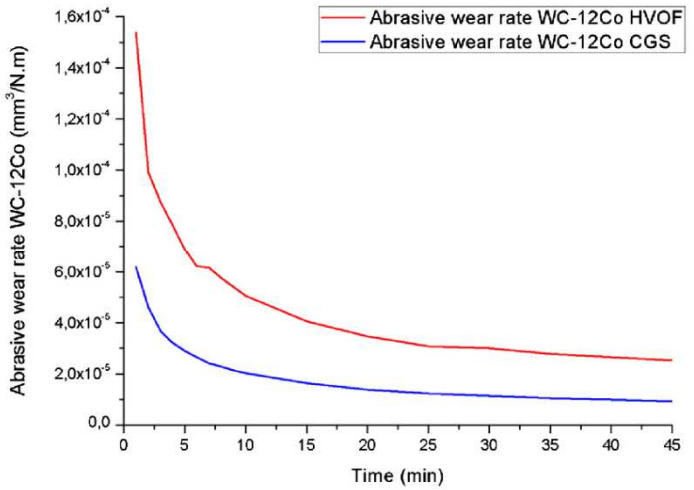

Fig. 9. Abrasive (rubber-wheel) wear rate vs. time (min) comparison curves for the WC–12Co coatings obtained by HVOF and CGS.

Please cite this article as: M. Couto, et al., Surf. Coat. Technol. (2014), http://dx.doi.org/10.1016/j.surfcoat.2014.04.034

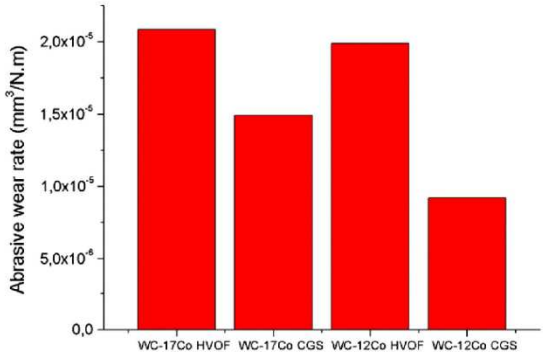

Fig. 10. Abrasive (rubber-wheel) wear rate versus time comparison of the optimum WC-17 and 12Co coating results obtained onto Al7075-T6 by HVOF and CGS.

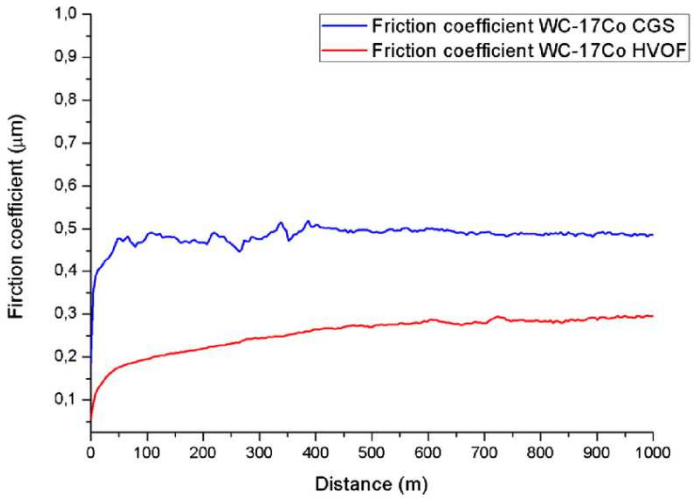

Fig. 11. Evolution of the friction coefficient for the WC–17Co coatings by HVOF and CGS obtained onto Al7075-T6 with a testing force of 25 N and a WC–Co counter-part.

Please cite this article as: M. Couto, et al., Surf. Coat. Technol. (2014), http://dx.doi.org/10.1016/j.surfcoat.2014.04.034

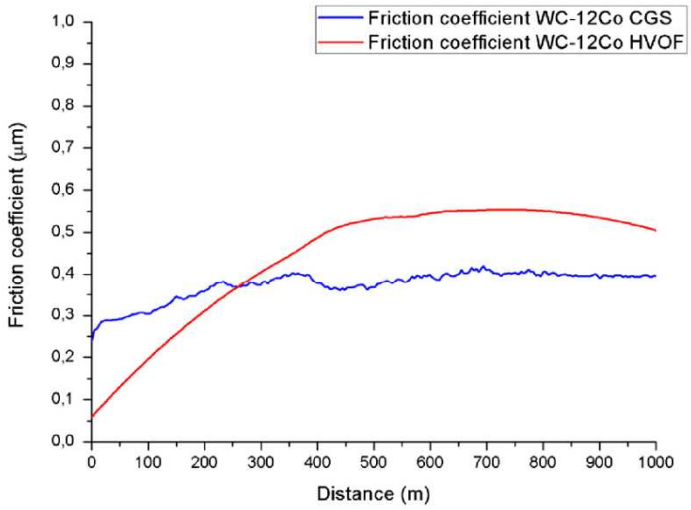

Fig. 12. Evolution of the friction coefficient for the WC–12Co coatings by HVOF and CGS.

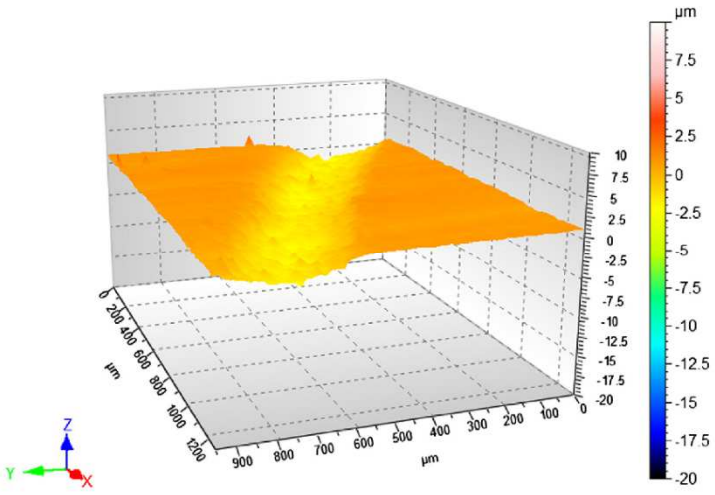

Fig. 13. Wear track reconstruction of WC–17Co HVOF coating after testing.

Please cite this article as: M. Couto, et al., Surf. Coat. Technol. (2014), http://dx.doi.org/10.1016/j.surfcoat.2014.04.034

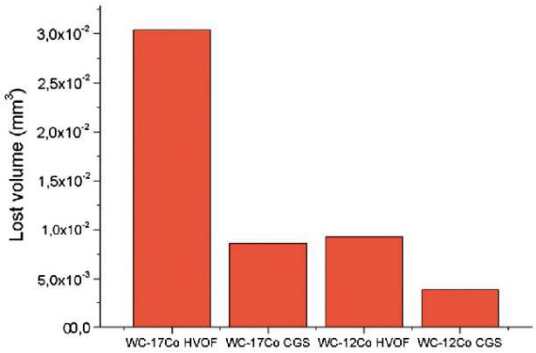

Fig. 14. Lost volume during ball-on-disk testing.

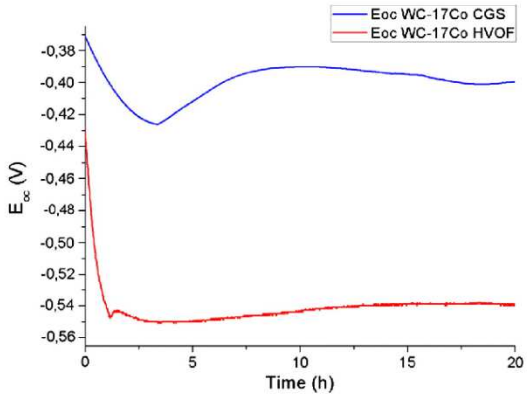

Fig. 15. Open circuit potential (E_{OC}) vs. time (h) curves for the WC–17Co coatings obtained by HVOF and CGS.

Please cite this article as: M. Couto, et al., Surf. Coat. Technol. (2014), http://dx.doi.org/10.1016/j.surfcoat.2014.04.034

7 OVERALL DISCUSSION

Chapter 6 compiled in published scientific papers all the results regarding Cold Gas Spraying of the three different WC-Co cermets (Papers 1 and 2) and the comparison of their mechanical and electrochemical properties with High Velocity Oxy-Fuel WC-Co coatings (Papers 3 and 4). In this chapter the above examined topics will not be mentioned in a detailed way again but instead approach some general concerns and relevant points as well as some gaps that were not explained in a proper way.

7.1 Starting considerations

In the beginning of this Thesis a deep theoretical study was done to understand:

- The application of WC-Co cermets in the heavy industry (automotive, aerospace, naval, mining, petrol and drilling, etc.);
- Which thermal spray technologies are used to obtain WC-Co coatings;
- The advantages/limitations of HVOF and CGS and future trend;
- CGS process parameters and bonding mechanism to allow an optimization of the spraying parameters.

The corrosion, erosion and wear resistance of WC-Co cermets makes them a widely used material for coatings using thermal spraying technologies. The state-

of-the-art indicated that HVOF is being used as the main technology for spraying cermets, so this lead to an increase effort in produce equally, or better, coatings by CGS than those produced nowadays by the conventional thermal spray techniques.

Heat generated during the spraying processes of these techniques leads to the formation of undesirable phase transformation and grain size growth. This effect causes the depletion of the original microstructure of the feedstock powders and therefore a reduction in specific mechanical and electrochemical properties. Usually the formation of these brittle eta (ŋ) phases – $Co_3W_3C_3$ and $Co_6W_6C_6$ – as well as W_2C and elemental W, leads not only to a reduction of the mechanical properties but also to false hardness values of the coatings, since the brittle phases will be harder than the initial cermet (Figure 22). Furthermore, the depletion of the cobalt in the matrix makes the coating less resistant to impact energy absorption and reduces the fracture toughness. When it comes to corrosion resistance the decarburization and oxidation reactions that lead to the formation of undesired phases such as the brittle ŋ phases make the coatings less resistant to corrosion. The formation of nobler than Co ceramic phases such as the referred $Co_3W_3C_3$ and $Co_6W_6C_6$ phases should provide an extra protection against corrosion but instead the compaction effect of the WC-Co particles between one another is reduced giving haze to the formation of extra porosity. So, this dissolution generates a lower cohesion between particles and thus more favourable ways for the electrolyte to penetrate and corrode the coatings and substrates.

Cold Gas Spraying as a technology for the production of WC-Co cermets is not widely spread. The fact that CGS does not use temperature to melt the powder particles, its dependence on kinetic energy and plastic deformation of the feedstock powders, makes it a more challenging process when it comes to the deposition of cermets. There is a need for ductility of the spraying materials to allow enough plastic deformation of the powder particles, binding to the substrate and growth of a coating without delamination and with good adhesion to the substrates.

The questions that arose were:

1st: Will it be possible to obtain WC-Co coatings by CGS, considering the limitations inherent to the process?

2nd: If so, will these coatings have enough quality to replace and improve the actual WC-Co being produced by conventional thermal spray techniques?

This data motivated the present research line and the obtained results proved that these findings were in fact useful in the successful deposition of WC-Co both onto low carbon steel and Al7075-T6 substrates by Cold Gas Spraying.

7.2 Cold Gas Spray

7.2.1. WC-25Co

The production of WC-25Co coatings as the first objective of this Thesis implied an extra effort in the understanding of the CGS process and its parameters. First of all, after the initial design of a pre-experiment for the WC-25Co feedstock powder onto both substrates (low carbon steel and Al7075-T6), series of coatings showed bad adhesion to the substrates, delamination of the few layers that had been deposited and even cracking of the coating itself when performing micro-hardness tests. The optimization of the spraying conditions led to what was desired at first: coatings onto low carbon steel and Al7075-T6 with excellent adhesion to the substrates (74 ± 6MPa and 60 ± 5MPa, respectively), no delamination between sprayed layers, uniformity, no porosity and high thicknesses. Added to this, an unaltered microstructure in the final coatings - representing one of the advantages of the CGS process – was also evidenced.

It was the first time such cermet was being produced using nitrogen as process gas in CGS. Automatically the cost of the process was reduced since nitrogen is a cheaper gas than helium or any other mixtures. This was due to an extensive understanding, research and optimization of the spraying conditions that allowed reaching the needed critical velocity, gas temperatures and pressures, for the

impinging particles to plastically deform and bind themselves to the substrates. Spraying distance was also a critical parameter that needed to be optimized and the optimum values were chosen between a wide range of pre-experimented distances.

These findings allowed for a series of coatings to be reproduced in order to perform different mechanical (micro-hardness and adhesion), tribological (abrasive and adhesive resistance) and electrochemical (corrosion and salt fog spray resistance) tests on them. All the obtained results were compared to the HVOF available ones at the time. WC-12Co cermets are the ones that are most widely used in industrial applications due to their high wear resistance and hardness. In this paper a comparison between CGS WC-25Co coatings, with lower content in hard carbide particles thenceforth a theoretically lower wear resistance and hardness values but higher fracture toughness and erosion resistance, and HVOF WC-12Co coatings was made. CGS coatings presented a lower hardness, as expected, but when it came to wear resistance values the difference was not as high as expected (this comparison is detailed in Paper 3). This was due to a good distribution of the WC hard particles in the ductile matrix, the homogeneous and sub-micrometric carbide particle size and the fact that no brittle/fragile phases were produced during the spraying process. Furthermore, in CGS there is a compressive effect of the impinging particles over the first deposited layers of coating material during spraying. This effect produces less porous coatings, and hence fewer paths for the electrolyte to penetrate and reach the substrate than those seen in conventional thermal spraying techniques such as HVOF; aided by the fact that no cobalt is dissolute from the grain boundaries, provided these coatings an excellent corrosion and salt fog spray resistance.

When the first extremely motivating results for spraying WC-25Co coatings were obtained and their properties characterized the results pointed in a direction that, in theory, with a reduction of the cobalt matrix one could obtain higher hardness values and wear resistance using CGS than HVOF. This enclosed two problems:

- the extra difficulty of producing WC-17 and 12Co cermets which had lower plasticity and therefore less chance that a thick and dense coating would build-up;

- that their tribological properties were in fact higher than the state-of-the-art HVOF coatings.

The mentioned problematic led to research **Paper 2** presented in the following chapter.

7.2.2. WC-17 and 12Co onto Al7075-T6

The same approach was made for the production of both these coatings. A large pre-experiment was planned and the optimum spraying conditions were achieved after characterization of all the coatings involved in both pre-experimental studies for WC-17 and 12Co. One other variable was added to the pre experiment: the use of a longer pre-chamber where the powders are heated for a longer time giving them an added plasticity. This made the pre-experiment larger but allowed for better final results. The obtained optimum coatings showed once again excellent adhesion to the substrates, homogeneity, density and no interlayer delamination.

This time just one kind of substrate was chosen: Al7075-T6. This was because since WC-17Co and WC-12Co are harder than WC-25Co a softer substrate would be easier to deform and build-up a coating of harder cermets.

In cold spraying, a certain degree of ductility of the particles and hardness of the substrate are needed to obtain sufficient localized plastic deformation to build up a dense coating. This and the adiabatic shear instabilities resulting from high strain rate deformation upon impact are the phenomena believed to play a major role in particle/substrate bonding — influenced by spraying conditions and powder characteristics — during cold spraying. This was the main reason why WC-25Co performed better under tensile tests than WC-17Co which performed better than WC-12Co ones (Ref 39, 40). Nevertheless all the sets of coatings showed an excellent adherence to the substrates and this did not appear to be a problem when it came to different tribological and electrochemical testing. In fact, considering wear resistance testing, WC-17Co coatings behaved approximately the same as the literature HVOF WC-12Co coatings and, as expected, CGS WC-12Co showed a higher abrasive and adhesive resistance as well as a better behaviour when exposed to aggressive corrosion environments (detailed results in **Paper 2**).

7.2.3. Properties comparison between WC-Co CGS and HVOF coatings

After successfully having obtained the three different WC-Co cermets with excellent results, a needed extra accurate comparison between these and HVOF WC-Co ones had to be studied. From this decision derived another two research papers (**Papers 3 and 4**) which compiled the optimization, production and full characterization of the same sprayed feedstock powders with a conventional thermal spray technique, namely High Velocity Oxy-Fuel.

7.2.3.1. WC-25Co CGS vs. HVOF

Having optimized and tested the WC-25Co CGS coatings onto carbon steel and Al7075-T6 the next step was comparing them with the same feedstock powder material sprayed by HVOF. This is a high temperature process (up to ≈3000ºC) that, in order to deposit the material onto a substrate uses the flame chemical heat to melt the powder particles. Due to the high temperatures used in this process, decarburization and formation of brittle phases happen.

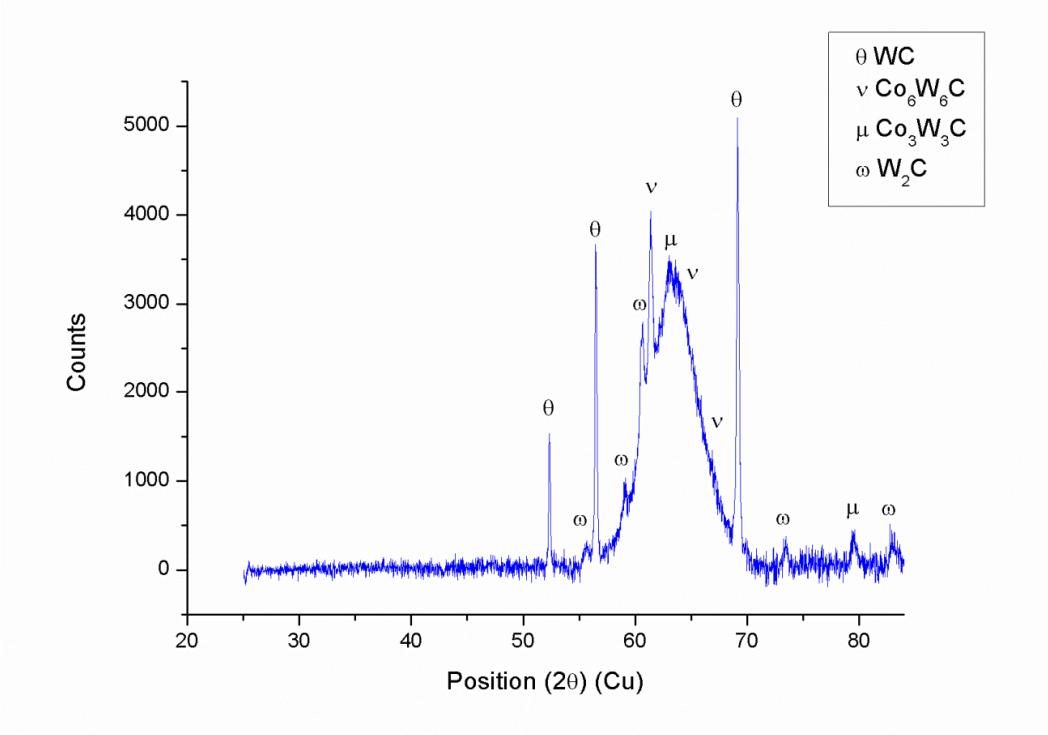

Figure 22. XRD X-Ray Diffraction of a HVOF WC-Co sprayed powder.

With this fact in mind, the fracture toughness of both CGS and HVOF coatings was tested to measure the impact of the formation of the mentioned brittle phases in HVOF and how much was the gain in ductility when spraying the same material by CGS.

To study the fracture toughness of brittle materials the application of the Vickers indentation technique is the most used method chosen because it can determine this property in a specific zone of a coating and therefore determine the fracture toughness as a function of the material microstructure. The elastic modulus was estimated using a *Knoop* indentation technique by performing 10 *Knoop* indentations at a load of 9.80N. Crack models used for predicting the fracture toughness are function of the indenter, crack geometries and indentation loads: the *Palmqvist* model is used for low indentation loads and the Half-Penny model for high indentation loads. The *Half-Penny* (Eq. 8) cracks are typically observed in brittle ceramics at high indentation loads. In order to measure the fracture toughness Vickers indentations at 9,80 N were performed on polished coating cross-sections, and its diagonals and crack lengths measured using an optical microscope. An average of 10 indentations was made and the total crack length was estimated by using Equation 8, where $2d_{II}$ and $2d_{\perp}$ are the parallel and perpendicular Vickers diagonals to the coating surface produced in the indentation, and a_l and a_r are the left and right crack lengths; to determine the fracture toughness Equation 9 was used, where Hv and E are the Vickers hardness and elastic modulus, respectively:

$$c = {(2d_{II} + 2d_{\perp})}/{4} + {(a_l + a_r)}/{2} \qquad \text{(Eq 8)}$$

$$K_c = 0.0711\left(H_v d^{1/2}\right)\left[{E}/{H_v}\right]^{2/5}\left[{c}/{d}\right]^{-3/2} \qquad \text{(Eq 9)}$$

This equation is only valid for a Half-Penny crack regime that occurs when c/d ≥ 2.5 where d is the Vickers half-diagonal.

HVOF coatings were optimized at first, followed by a characterization of the optimum coatings and finally mechanical and electrochemical tests were performed on a set of the optimum WC-25Co coatings. HVOF coatings presented higher hardness values than CGS mainly because of decomposition of the WC-25Co powder during the spray process and therefore hardening effect due to the presence of the η phases. Besides a higher hardness, these coatings will also be more brittle than those sprayed by CGS due to the lower content in elemental ductile Co matrix and the presence of fragile and hard Co_6W_6C or Co_3W_3C η phases formed during the HVOF spraying process (Figure 22). The temperatures achieved during this process cause a depletion of the ductile Co matrix thus forming a more brittle coating as well as bands of dissolution of the WC into the Co matrix. There is a hardening of the matrix due to dissolution resulting in fewer free carbides in the final coating henceforth a decrease in some mechanical properties such as fracture toughness, as a direct consequence of the formation of ŋ hard phases. This considered fracture toughness tests were run performed and the results were according to what was expected: CGS coatings showed higher fracture toughness than HVOF coatings. This is attributed to the fact that during spraying the powder is not subjected to phase changes and no draining of the ductile free metallic matrix in the microstructure happens. The cobalt present in the coatings is kept and acts as a ductile element hence improving the fracture toughness of the CGS coatings.

Abrasive and adhesive wear resistances were also compared. CGS and HVOF found to have approximately the same abrasive resistance values and behavior showing that without depletion of the WC carbides and no hardness effect due to the production of fragile phases during deposition, CGS can produce coatings with approximately the same abrasive wear properties as HVOF coatings. Testing of the friction wear resistance proved to be high for both coatings, with an improvement in CGS coatings. These produced a much narrower wear track and lost 5 times less material than HVOF coatings under the same testing conditions. The fact that during Cold Gas Spraying process there is no decomposition of the free WC carbides gave haze to a higher adhesive resistance behaviour since all the initial powder hard particles were fully performing their function.

The improvement in electrochemical corrosion resistance of the CGS coatings was attributed to the compressive effect of the particles during CGS, which produces less porous coatings and therefore less ways for the electrolyte to penetrate and reach the substrate. There was a reduction of approximately 15% of the CGS open circuit potential.

To complement the corrosion resistance studies also the corrosion rates of the sprayed coatings were measured. The *Tafel* anodic and cathodic curves were calculated (Figures 23 to 25) and from there each of the coatings' respective intensity of corrosion was determined.

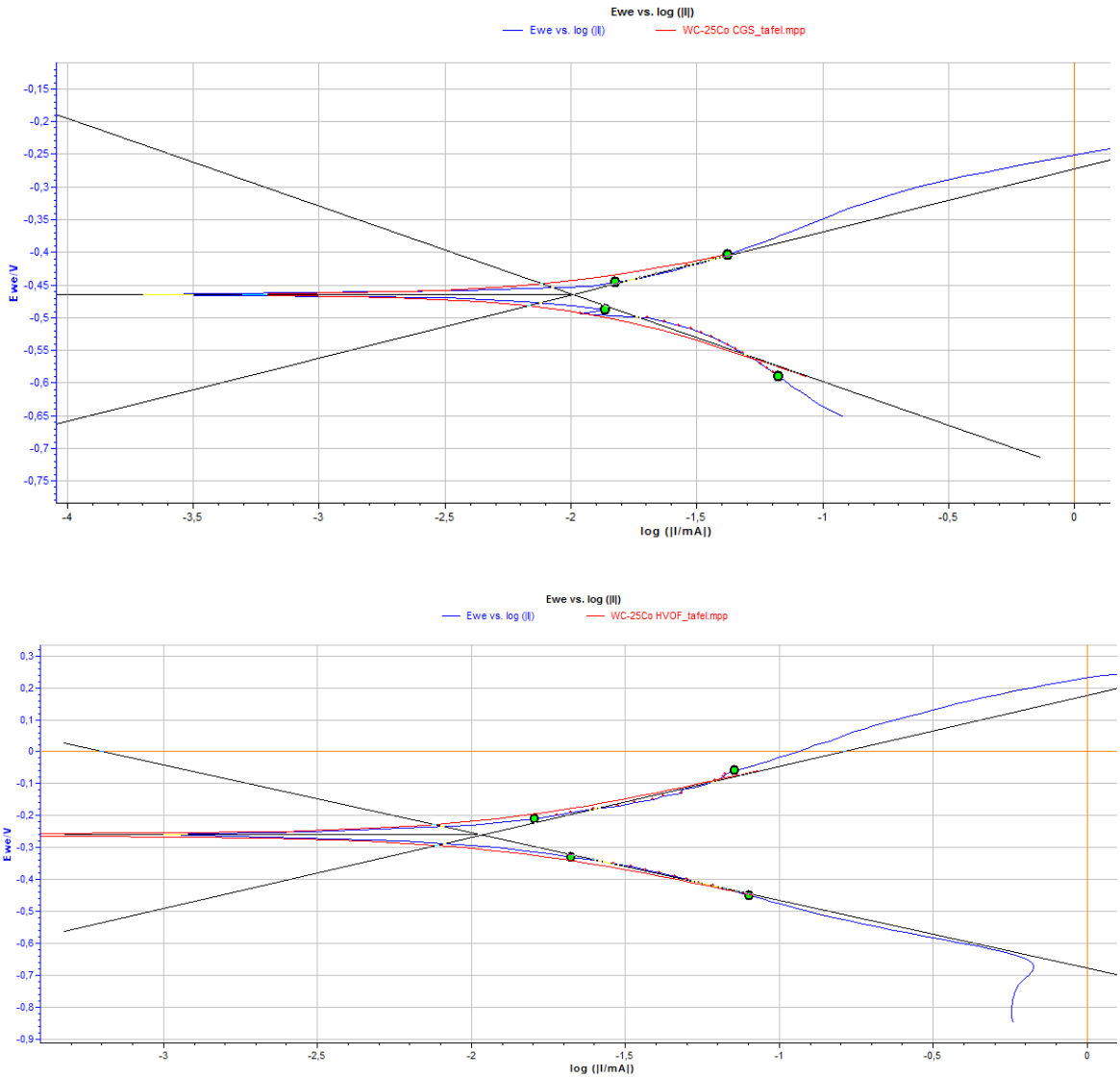

Figure 23. WC-25Co CGS (first) and HVOF (second) *Tafel* potential curves.

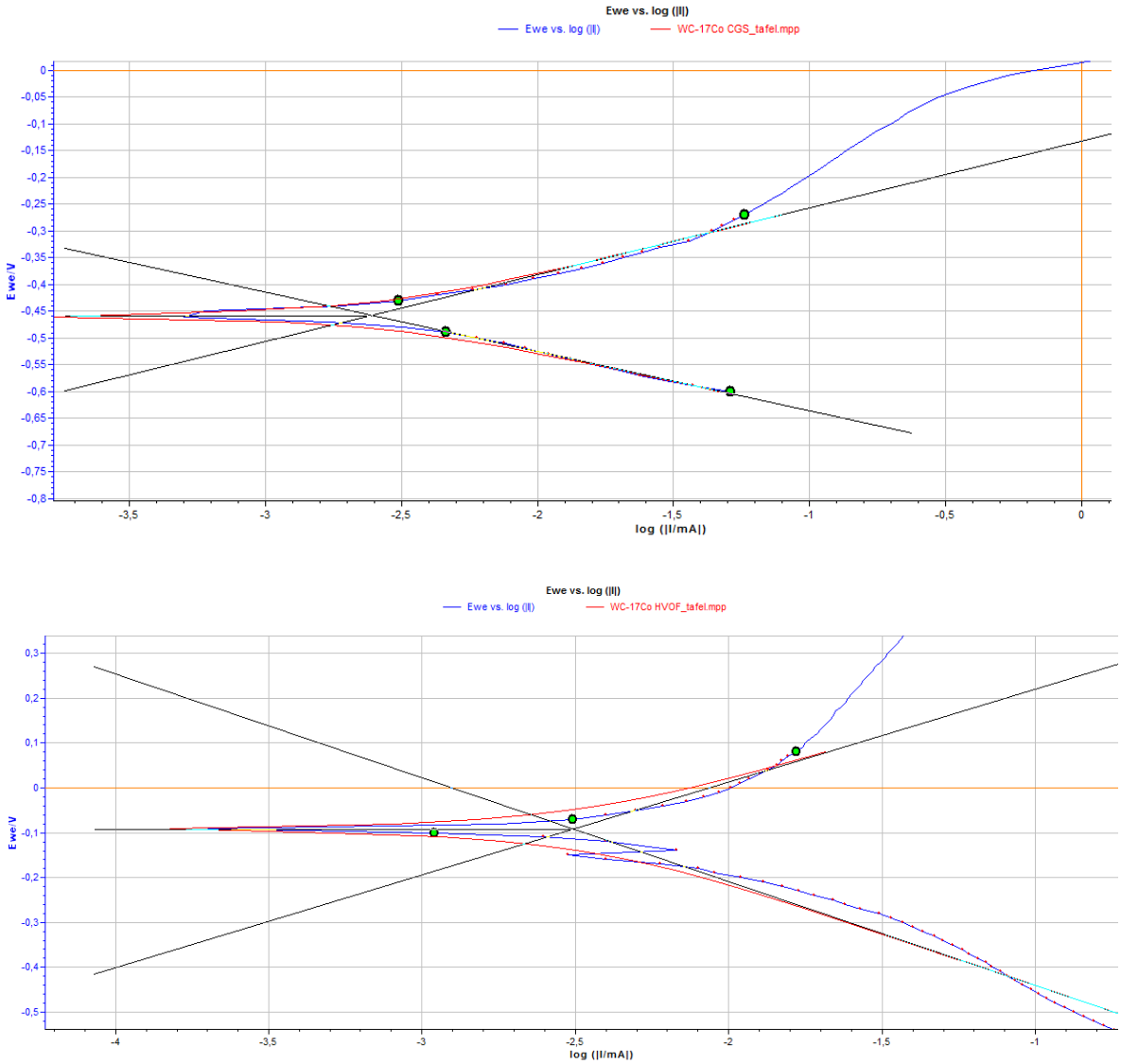

Figure 24. WC-17Co CGS (first) and HVOF (second) *Tafel* potential curves.

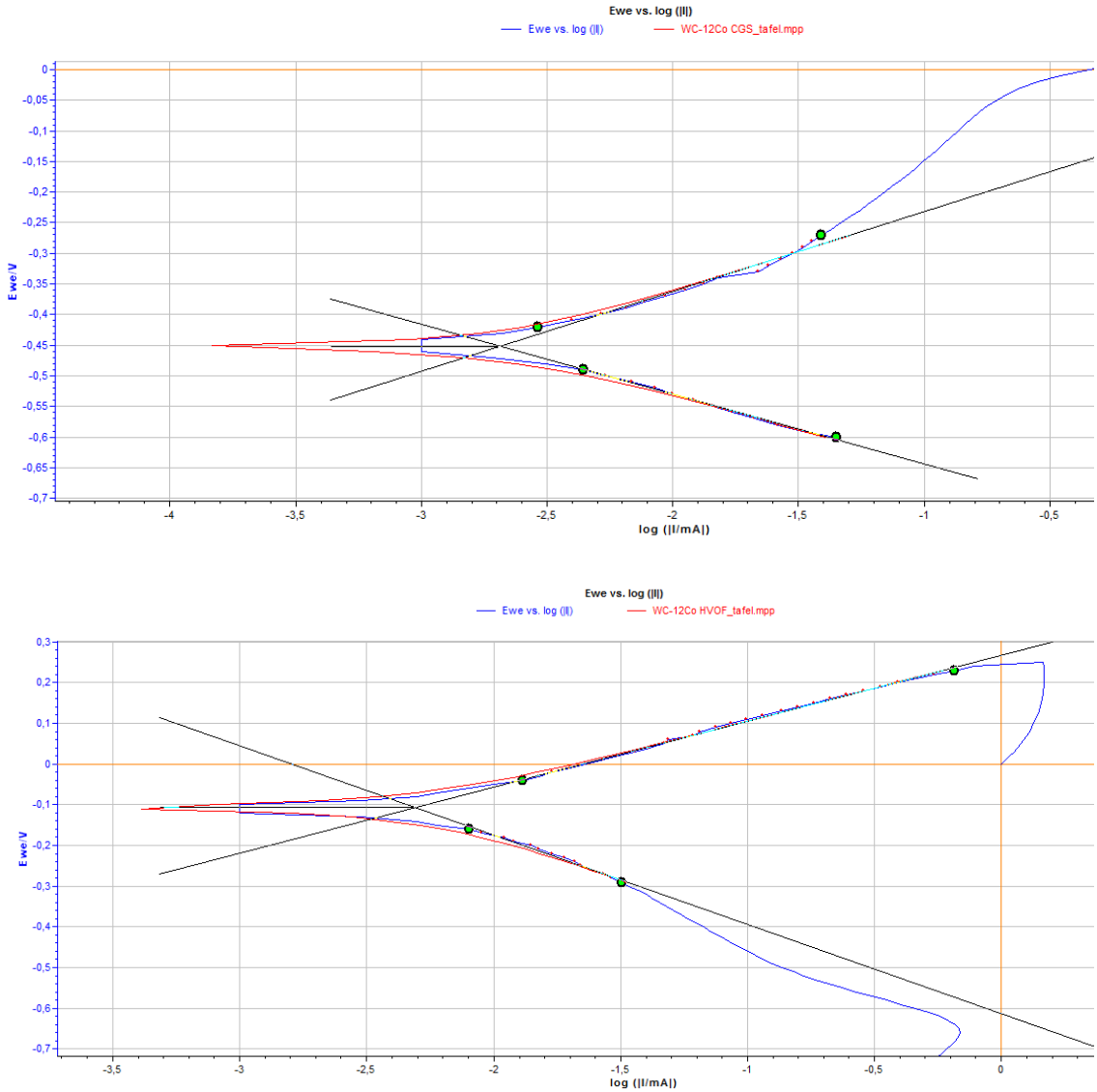

Figure 25. WC-12Co CGS (first) and HVOF (second) *Tafel* potential curves.

The i_{corr} values for each of the Cold Gas Spray and High Velocity Oxy-Fuel are shown in Table 5.

Table 5. i_{corr} values for CGS and HVOF WC-25/17/12Co coatings.

Techonology/i_{corr} (µA)	WC-25Co	WC-17Co	WC-12Co
CGS	10.154	2.456	2.050
HVOF	11.602	3.111	4.926

The analysis of the *Tafel* potential curves allowed understanding the kinetic side of the electrochemical corrosion testing. The higher the i_{corr} the higher the corrosion rate of the coatings, therefore all CGS coatings were confirmed to have better electrochemical corrosion protection when compared to HVOF coatings under the same corrosion testing conditions. This can be explained with the compressive effect that the kinetically accelerated particles cause on the CGS sprayed coatings, making the coatings less porous. Also, since there is no dissolution of the matrix during the spraying process there is no decohesion inter particles due to the formation of other phases, and therefore less ways for the electrolyte to penetrate and faster corrode the coating.

Salt fog spray tests were also carried out on samples of WC-25, 17 and 12Co. These coatings were tested for more than 500h and remained unaltered – with no visible results of superficial corrosion. The state of the art cites that for a conventional WC-12Co coating sprayed by HVOF, after 130h of salt fog spray testing the first signs of corrosion start to appear which confirms a better resistance, of approximately 380%, for all of the CGS sprayed coatings, with different metallic matrix contents, during this Thesis. The state of the art also cites the testing of a nanostructured WC-12Co coating sprayed by HVOF where after 590h the first signs of corrosion started to appear (Ref 9, 10).

7.2.3.2. WC-17 and 12Co CGS vs HVOF

After optimization and characterization of HVOF WC-17Co and WC-12Co the same procedure as the one used for CGS vs HVOF comparison in **Paper 3** was performed and resulted in the publication of **Paper 4**. All the results followed the same line as the ones mentioned in Chapter 7.2.3.1 to a larger extent in the improvement of hardness, wear and electrochemical resistance. The difference in the content of ductile Co binder (17 and 12Co) of these powders affects their final mechanical and electrochemical properties. A decrease in Co content provides greater coating specific properties (abrasive and friction wear resistance, hardness values, corrosion resistance) while fracture toughness, adhesion and deposition efficiency (Ref 41) show the opposite behaviour.

In the following chapter a summary of CGS coatings' mechanical and electrochemical properties is shown as well as a comparison between the most relevant results obtained while spraying the studied WC-25, 17 and 12Co feedstock powders by Cold Gas Spray and High Velocity Oxy-Fuel.

7.2.4. Summary of CGS and CGS vs. HVOF properties

A graphical summary of the main wear and corrosion resistance properties for the three studied WC-Co powders sprayed by CGS is shown in the following figures. Following these results, also a graphical comparison between these results and those obtained by HVOF is shown to understand the improvements achieved using Cold Gas Spray.

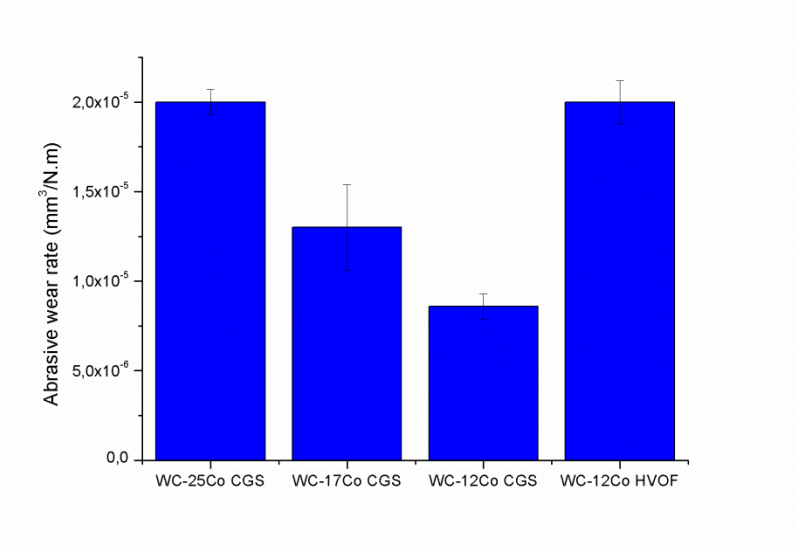

Figure 26. Abrasive (Rubber-wheel) wear rate of the optimum CGS coatings obtained onto Al7075-T6.

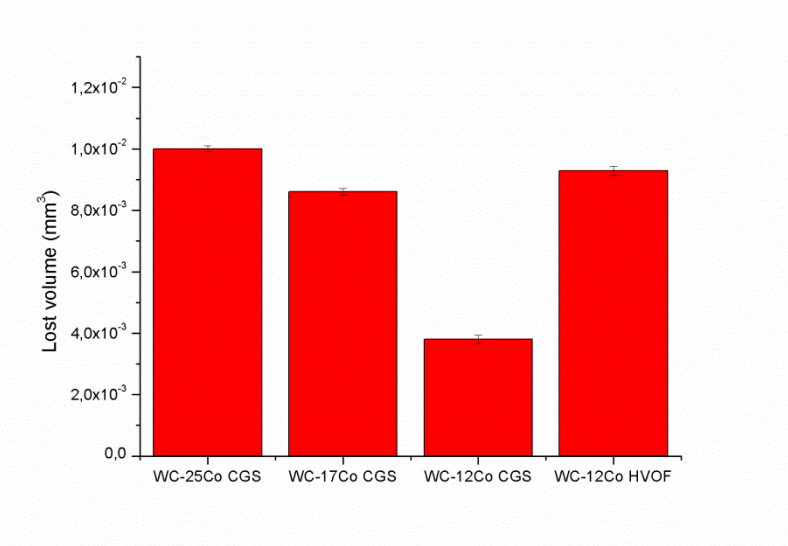

Figure 27. Friction wear lost volume after testing of the optimum CGS coatings obtained onto Al7075-T6.

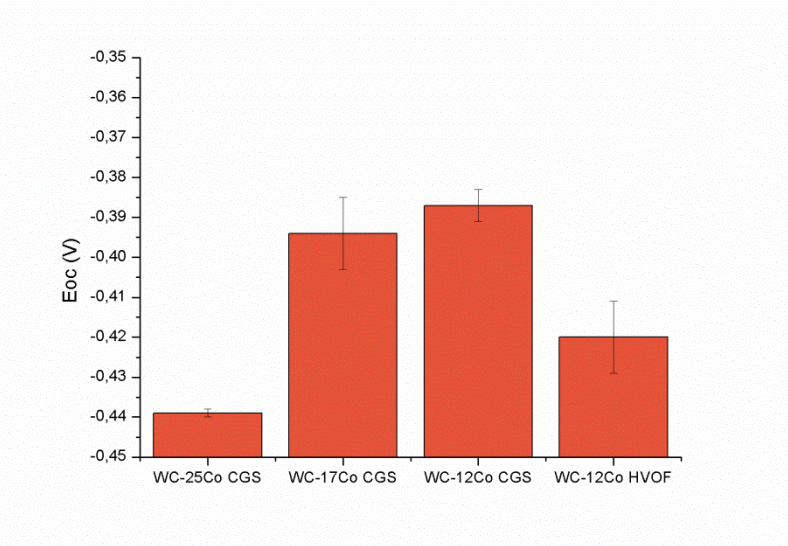

Figure 28. Open-circuit potential (Eoc) for WC25-17-12-Co coatings onto Al7075-T6 in aerated and unstirred 3.5%NaCl aqueous solution, after 16h of testing.

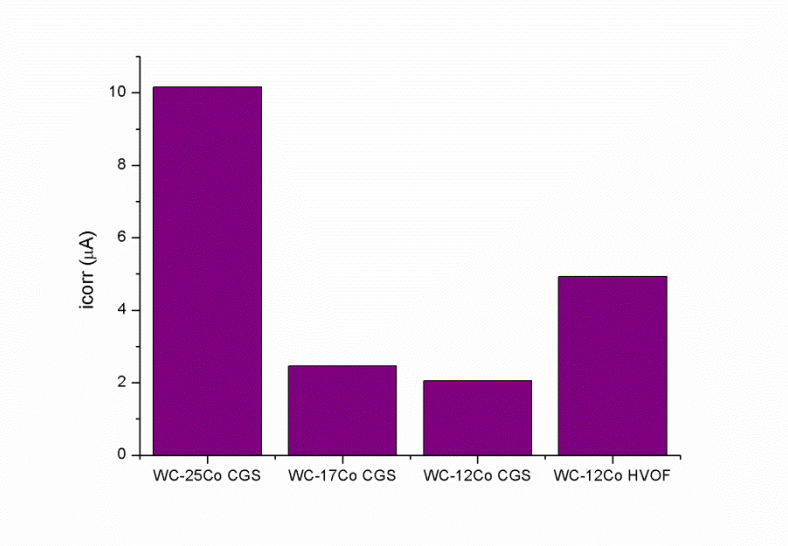

Figure 29. Intensity of corrosion of CGS WC25/17 and 12Co coatings vs. HVOF WC-12Co sprayed coating.

As expected, and mentioned in the previous paragraphs, with an increase of hard WC particles there is an increase in both abrasive and adhesive/friction wear resistance and electrochemical corrosion resistance. In the following figures a comparison between these and the wear and electrochemical corrosion results for the HVOF coatings is depicted.

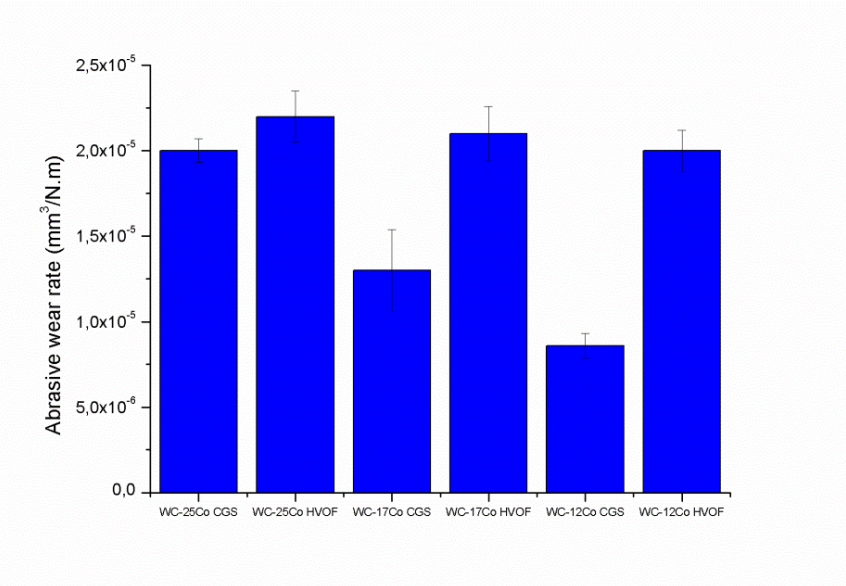

Figure 30. Abrasive wear rate comparison between the obtained WC-25/17/12Co coatings by CGS and HVOF onto Al7075-T6.

Considering the coatings' resistance to abrasive wear there was an improvement of 10% for WC-25Co by CGS, 62% for WC-17Co and 133% for WC-12Co coatings by CGS. CGS WC-25Co coatings show similar abrasive wear rate results than WC-12Co coatings by HVOF.

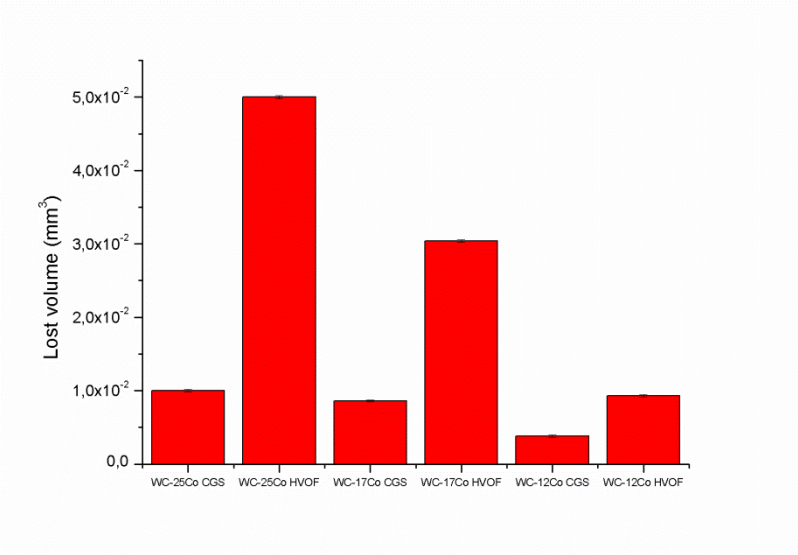

Figure 31. Friction wear lost volume comparison between the obtained WC-25/17/12Co coatings by CGS and HVOF onto Al7075-T6.

Considering the coatings' lost volume after wear friction (ball-on-disk) testing WC-25Co, WC-17Co and WC-12Co CGS coatings lost 4, 2.5 and 2.4 times less than the respective HVOF coatings. WC-25Co coatings by CGS lost only approximately 0.1 times more than WC-12Co coatings by HVOF.

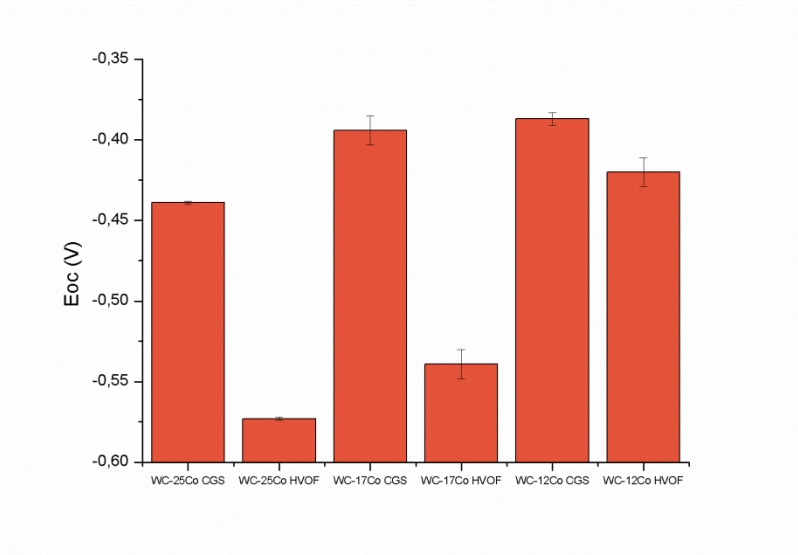

Figure 32. Open-circuit potential (Eoc) comparison between WC25-17-12-Co coatings onto Al7075-T6 by CGS and HVOF.

In neither case the electrolyte reached the substrates as indicated by the open circuit potential obtained after testing. This means that the coatings are resisting electrochemical corrosion and the coatings are protecting the substrate.

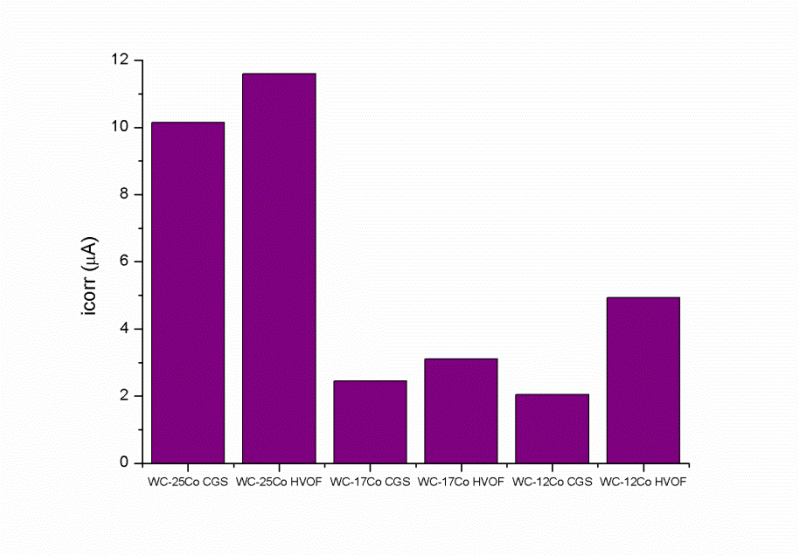

Figure 33. Intensity of corrosion (i_{corr}) comparison between WC25-17-12-Co coatings onto Al7075-T6 by CGS and HVOF.

As depicted in the graphic of Figure 33, CGS coatings showed – when compared to the same coatings sprayed by HVOF – less intensity of corrosion after the kinetic

electrochemical tests meaning that their corrosion rates are slower and therefore will resist for a longer period of time to extreme corrosion environments.

7.2.5. Deposition efficiency

Deposition efficiency (D.E.) is an issue when spraying hard materials by CGS as shown by these results of CGS coatings onto Al7075-T6: D.E. $_{WC\text{-}25Co}$ = 24%; D.E. $_{WC\text{–}17Co}$ = 14%; D.E. $_{WC\text{–}12Co}$ = 14%. The deposition efficiencies for the deposition of WC-25, 17 and 12Co onto Al7075-T6 by HVOF were of 69, 67 and 40%, respectively. The deposition efficiency of WC-25Co by CGS and HVOF onto carbon steel substrates were 17 and 66%, respectively, while WC-17Co and WC-12Co coatings onto carbon steel by CGS showed D.E. values of 17 and 16%. This is one of the major disadvantages of the CGS process for the deposition of WC–Co cermets. Despite the low deposition efficiency values they represent the highest values of deposition efficiency accomplished until the day while spraying this material by CGS. CGS is a solid-state deposition process where no melting of the powder particles occurs and this is the reason why it is influenced by so many different parameters when compared to conventional thermal spraying techniques, making it extra difficult to obtain cermet coatings by CGS. The particles are injected into a supersonic jet of compressed gas which deposits them onto a substrate, deforming these incoming particles and thus building a layer of material. The ductility of the spraying powder and the substrates, and the critical velocity are main parameters in CGS. In HVOF the powder is heated due to the elevated combustion temperatures produced in the mixing chamber, causing the formation of molten or semi-molten particles of the sprayed powder. These droplets hit the substrate and consequently flatten and solidify meaning that most of the injected spraying material arriving on the substrate will adhere to it, or to the previously deposited material layers. In CGS, if not all the particles achieve a certain acceleration (critical velocity), due to its being a solid-state deposition process where it is entirely dependent on kinetic energy and none on thermal energy, they will not adhere or, furthermore, if they achieve extremely high velocities, erode the substrate or layers of coatings.

The loss of material during CGS process makes it a rather expensive alternative to conventional thermal spraying techniques. For this reason several trials were made using the optimum spraying conditions of the WC-17Co powder onto Al7075-T6 substrates (except trials number 3, where a WC-25Co powder onto carbon steel, and 4, where carbon steel substrates, were used) to improve the deposition efficiency of the process when it comes to spraying hard materials such as cermets or even ceramics. Different approaches were studied, here listed:

Trial 1: Substrate heating while spraying using an industrial air ventilator and an infra-red lamp;

These two experiments offered no increase in the deposition efficiency of the process mainly because a poor heating of the substrates was achieved using both the industrial air ventilator and the infra-red lamp. Nevertheless, if a proper heating of the substrates could be achieved, an added ductility and bonding of the cermet powder particles could be expected to increase the deposition efficiency.

Trial 2: Designing a new pre-experiment of different conditions per coating layer recurring to samples of sprayed powder splats to analyse their interaction with the substrate;

The second trial consisted of producing two layers of WC-Co material with different spraying conditions to improve the adhesion of the first layer to the substrate and hence the adhesion of the second layer to the WC-Co coating. Firstly, to better understand the adhesion of these particles to the substrate, a pre-experiment of sprayed splats of the feedstock powder was made. This pre-experiment consisted of the fixing specific parameters, such as the spraying distance and gas pressure, and changing the gas temperatures. These temperatures varied from 500 to 800ºC. The particles did not seem to have enough plasticity to deform and adhere to the substrate when the temperatures were inferior to 700ºC. After characterization and analysis of the obtained splats at 700 and 800ºC it appeared to exist a much higher percentage of adhered particles to the substrates at 700 than 800ºC (Figure 34). This led to producing WC-17Co coatings with two different layers: the first one with the optimum conditions at 700ºC, and the

second with the previously defined optimum conditions. A total improvement of about 3% was achieved.

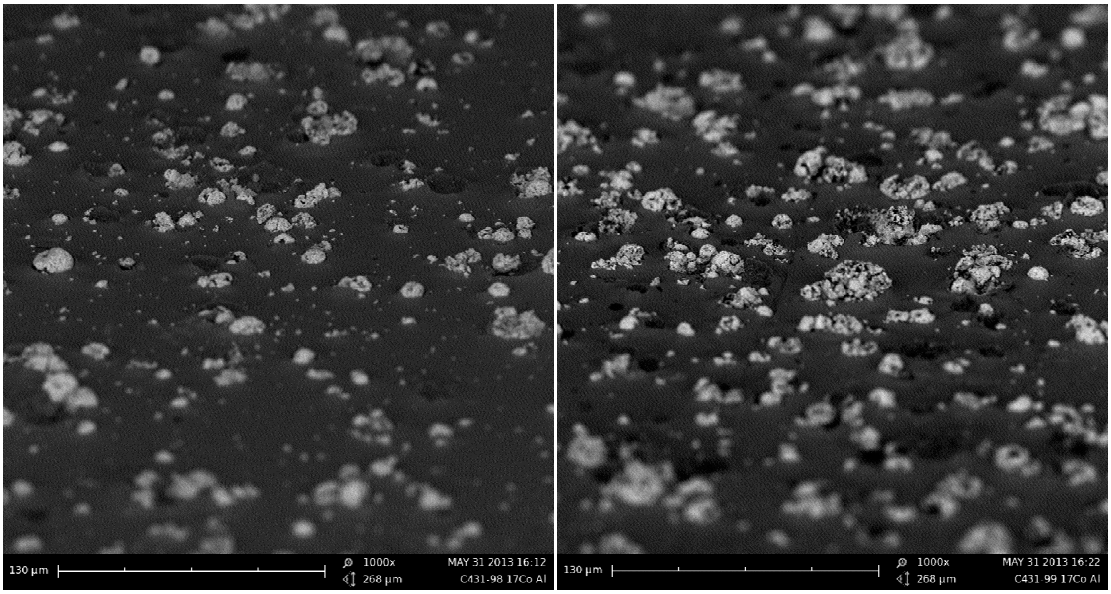

Figure 34. Splats of WC-17Co sprayed powder at 800ºC (left) and 700ºC (right).

Furthermore, this trial allowed at the same time a deeper analysis on the bonding mechanism of the three different powders onto Al7075-T6 substrate. Using SEM microscopy the particles splats' were observed and the different behaviour of each powder at the moment of impact on the substrate helped understand with further detail the diminishing deposition efficiency of the coatings with the lower metallic matrix. On the following figures sole particles of each powder are shown in detail with a brief explanation of its bonding mechanism to the substrate.

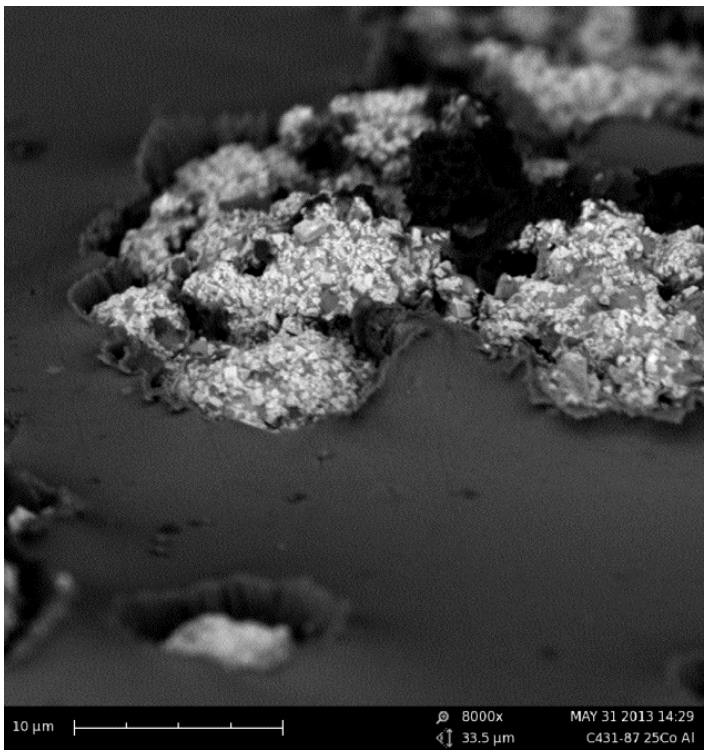

Figure 35. Splat WC-25Co particle onto Al7075-T6 at 8000x.

Figure 35 depicts a typical WC-25Co particle sprayed onto Al7075-T6 after hitting the substrate. The particle is well embedded into the substrate; besides, after impacting, the particle did not break into smaller pieces and there is some visible jetting occurring on the borders of it.

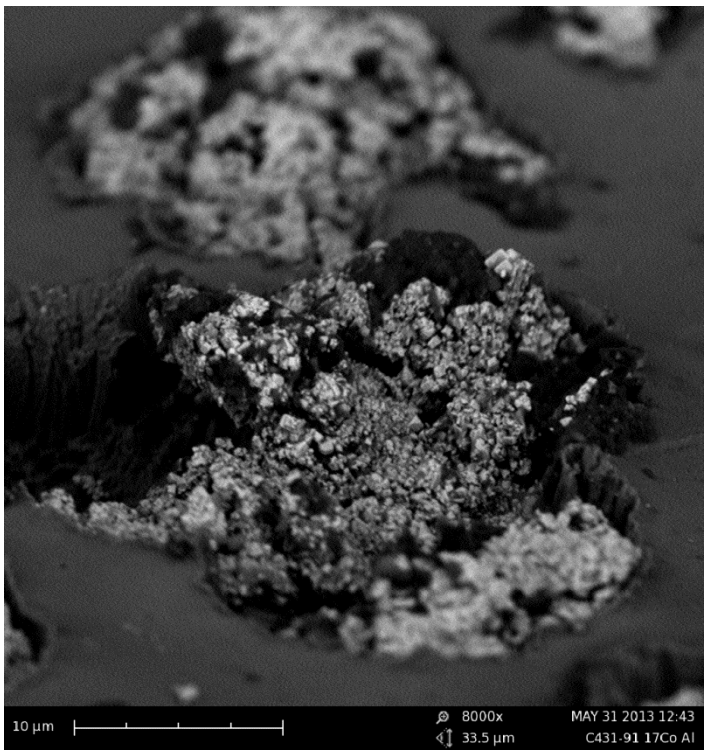

Figure 36. Splat WC-17Co particle onto Al7075-T6 at 8000x.

The decrease of the Co content in the particles accompanies a decrease in ductility and plastic deformation. When spraying a WC-17Co powder onto the same substrate as the previous powder it is possible to observe not only the adhesion of some particles to the substrate but also the adverse effect of erosion of the substrate by some other particles that were not able to successfully adhere. Figure 36 shows a well adhered particle next to a hole created by the excess of kinetic energy of one another particle; Figure 37 is showing the deformation of one WC-17Co particle, which possesses less ability to plastically deform than an average WC-25Co particle, next to a hole of a unadhered particle where some small pieces of the impinging of the latter can be seen (after having hit the substrate and probably break up).

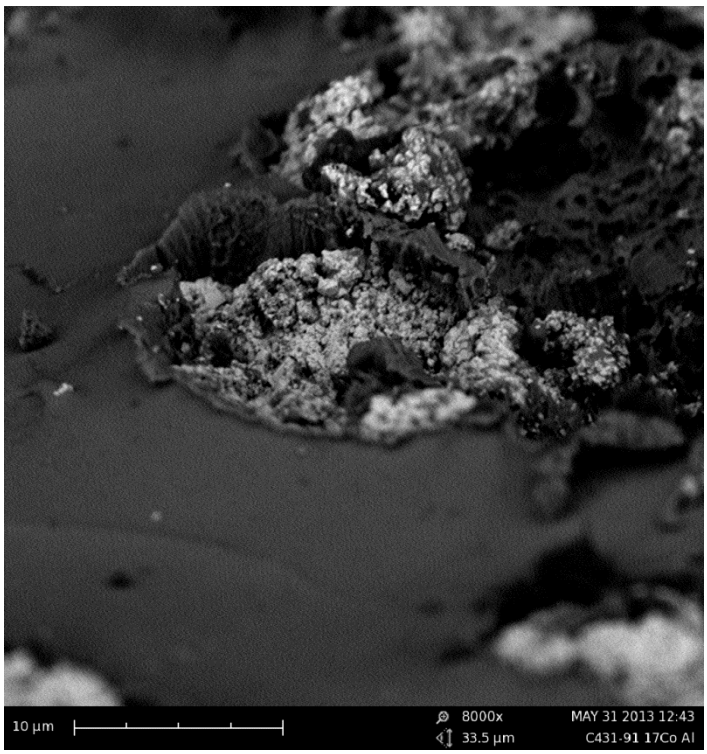

Figure 37. Splat of a broken WC-17Co particle onto Al7075-T6 at 8000x.

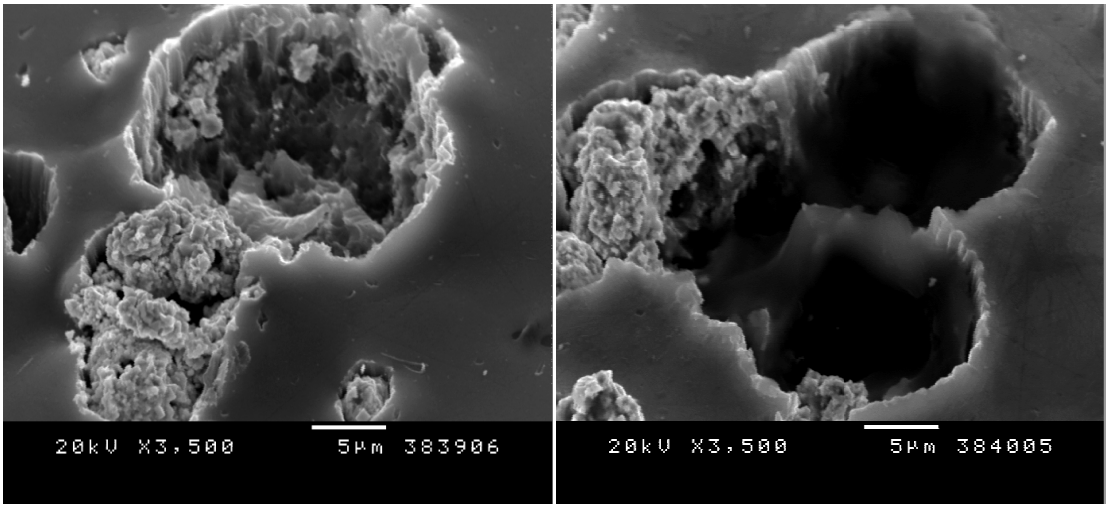

Figure 38. Splat of WC-12Co particles onto Al7075-T6 at 3500x.

The same adverse effect is happening when spraying WC-12Co particles as depicted in Figure 38. Fewer particles seem to adhere to the substrate with an increased number of holes, gaps and exploded particles being evidenced all around the substrate.

These facts confirm that a sufficient ductility of the sprayed particles is needed in order to increase the number of adhered particles and hence the deposition

efficiency of the process. With a decrease of the Co content in the particles it seems to exist a higher number of particles that are not adhering to the substrate, creating small holes in it, as well as some particles that are somewhat adhering and breaking up at the same time leaving some debris spread around the substrate. The advantages of being able to spray cermet particles – which usually have a low ability to deform – by CGS are well stated in this Thesis and the splat analysis show the increasing difficulty of spraying cermets with a low content in metallic matrix, especially WC-17Co and WC-12Co powders.

Trial 3: Designing a new pre-experiment with higher gas temperatures (900 – 1100ºC) and gas pressures (40 – 50bar);

There was an initial limitation of gas temperature and pressure with the KINETICS® 4000 of a maximum of 800ºC and 40bar, respectively. Later in this Thesis an opportunity of making a few trials using a CGS KINETICS® 8000 – which operates up to 1100ºC and 50bar – came up. Nevertheless, after designing an extensive pre-experiment the results appeared to be not as reasonable as those obtained using KINETICS® 4000. The kinetic energy given to the particles with the mentioned sprayed conditions was too extreme making them collide against the substrate and erode it instead of adhering to it. Most of the particles produced an effect of erosion and poor coatings with unsatisfying adhesion were produced as seen in Figure 39.

The initial investment for producing these coatings can be made with an actual cheaper model than the KINETICS® 8000 as a conclusion of this trial.

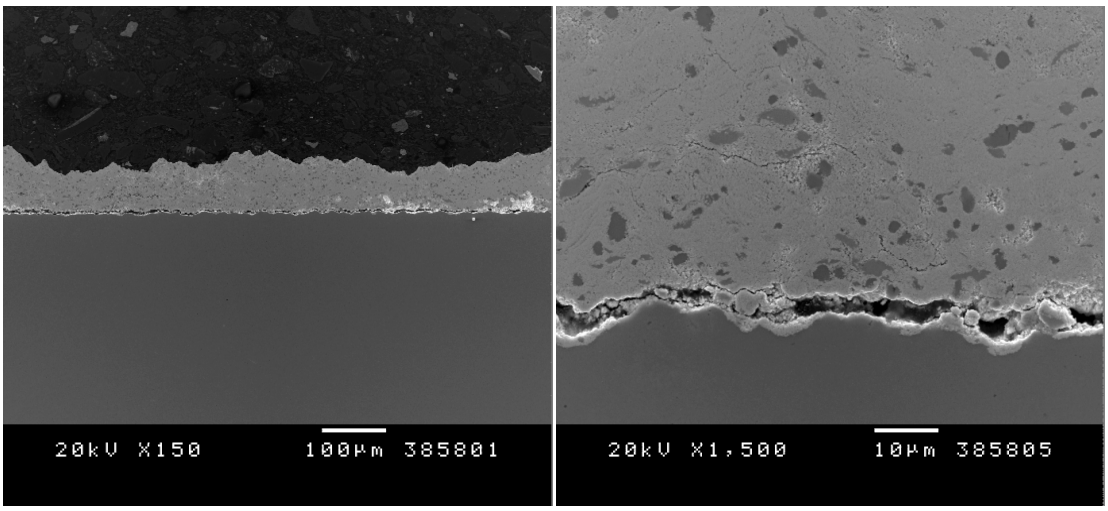

Figure 39. WC-17Co onto Al7075-T6 at 45bar of gas pressure and 1000ºC of gas temperature.

Trial 4: Activation of the substrates surface prior to spraying.

Activation of the surface was made to improve the preparation of the substrates in terms of roughness since an increase of the latter helps the deformation and bonding of the impinging particles. *Nital 2%* was used as the chemical reactive solution at 5 different attack times: 0, 20, 40, 60 and 90 seconds. In fact an improvement was evidenced when the substrates were attacked for 20 seconds achieving an increase of about 3% (from 20 to 23%). When the substrates were attacked for more than 20s a continuously decreasing efficiency was evidenced.

Trial 5: Spraying a CGS layer over a WC-12Co HVOF coating

It was possible to achieve a deposition efficiency of 18,5% when spraying a WC-12Co powder over a previously optimized and sprayed sample of WC-12Co by HVOF onto a low carbon steel substrate. Besides this value of deposition efficiency, the most noteworthy of this innovative idea is to spend as less powder possible during the CGS process, by spraying solely one layer of coating, in order to provide the WC-12Co by HVOF coating that lies below it to have those better erosion, abrasive and adhesive wear and corrosion properties provided in general by the CGS coatings. In Figure 40 the difference in density between the HVOF and CGS layers is evident with the HVOF one showing much more porosity.

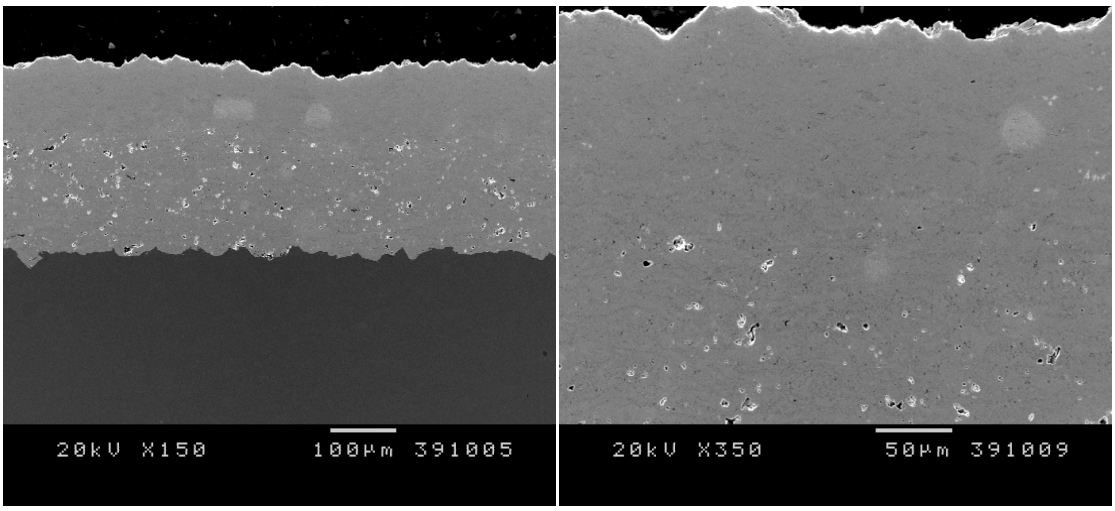

Figure 40. WC-12Co coating with the first layers sprayed by HVOF and the last layer by CGS.

The good adherence between the different layers is depicted in Figure 41 along with the difference in microstructures. The lower HVOF layer shows dissolution of the matrix while the CGS layer shows an intact microstructure after spraying.

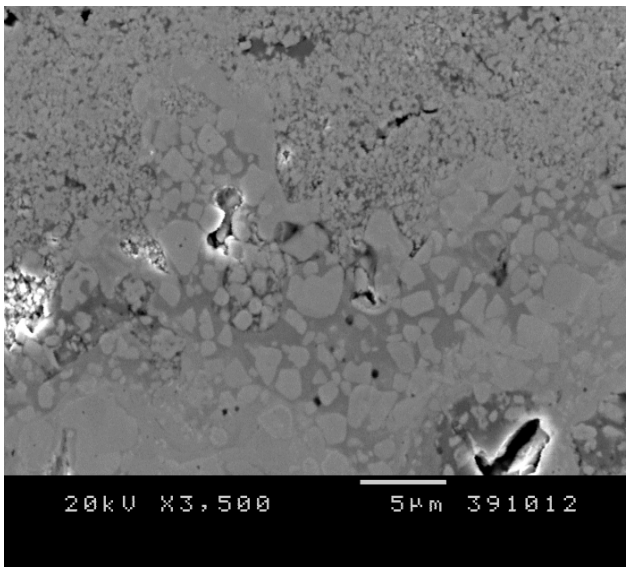

Figure 41. WC-12Co coating with the first layers sprayed by HVOF and the last layer by CGS.

After these trials it is evident that there is a chance of improving the deposition efficiency - while maintaining the exceptional properties of the CGS coatings - of the process even though there is a low limit related to the fact that the particles

don’t melt during CGS and also to the fact that CGS is a process that relies on kinetic energy to plastically deform particles, which, in this case, have a small percentage in ductile matrix making them harder to efficiently deposit by this technology.

8 CONCLUSIONS

In the end of this Thesis, all the objectives were accomplished. WC-Co cermets were produced using the novel Cold Gas Spraying technique and High Velocity Oxy-Fuel is a very recent subject, being these one the first works written about its deposition onto aluminium and low carbon steel substrates. After gathering and analyses of research data it can be concluded:

8.1 With regard to general juncture

1. It is possible to obtain dense, thick and well bonded WC-Co coatings by Cold Gas Spray both onto aluminium and low carbon steel substrates;

2. After spraying, there aren't any microstructural changes, decarburization or formation of fragile η phases, meaning that the powder's bulk properties are kept, when using Cold Gas Spray;

3. The effects of temperature, gas pressure and distance were studied and the best set of spraying conditions were chosen after doing several pre-experiments, where it was found that for a spraying distance of 40mm the quality of the coatings was

not good. All the obtained coatings were characterized in terms of their density, thickness, deposition efficiency and hardness;

4. For the deposition of WC-Co, higher temperatures result in denser and thicker coatings while spraying onto both aluminium and LCS substrates;

5. Gas pressure and distance were the studied parameter variables that affect the most the quality of the obtained coatings. The best pair of gas pressure/distance conditions for spraying onto aluminium substrates and LCS substrates were obtained;

8.2 With regard to CGS WC-25/17/12Co coatings

6. It is possible to obtain dense, thick and well bonded WC-Co coatings both onto aluminium and low carbon steel substrates;

7. Coatings showed highly satisfactory adhesive resistance, comparable with that achieved by HVOF spraying;

8. The good distribution of WC particles in the Co matrix led to high abrasion and friction resistance of both coatings;

9. After electrochemical corrosion testing the electrolyte did not reach the substrates of either coating. WC-12Co coatings showed the lowest rate of corrosion (i_{corr} = 2.1μA), followed by WC-17Co (i_{corr} = 2.5μA), and WC-25Co (i_{corr} = 10.2μA). Salt fog spray tests were also run on WC-Co coatings and after 500h neither sample showed signs of pitting corrosion;

10. Spraying distances equal or higher than 20 mm will result in poor quality results while sprayingWC-17/12Co powders onto Al7075-T6;

11. For the deposition of WC–Co, higher temperatures resulted in denser and thicker coatings on both coatings; in the case of WC–12Co using a pre-chamber provides better results;

12. The higher the content in ductile matrix, the better adherence results;

13. The higher the content in WC hard phase in the coatings, the better tribological and electrochemical properties;

14. CGS technology can clearly compete with conventional deposition techniques when used to spray WC-Co powders. This cold spraying technique allows thick, dense and hard WC-Co coatings to be deposited on Al7075-T6 and carbon steel substrates in a short time and with excellent tribological and electrochemical properties.

8.3 With regard to HVOF WC-25/17/12Co coatings

15. Higher HV300 hardness values were obtained by HVOF due to the formation of W_2C and Co_xW_xC phases, with a depletion of the ductility provided by the Co matrix due to the high decarburization and dissolution caused during the deposition process by the HVOF flame;

16. Microstructural changes, namely the formation of W_2C and W, were present;

17. Deposition efficiency was approximately 3 times higher while spraying WC-25Co by HVOF when compared to CGS nevertheless the obtained CGS deposition efficiency values still represent the highest for spraying WC-Co by CGS;

18. Rubber-Wheel tests produced abrasive wear rates in the magnitude of 10^{-5} sprayed both by HVOF and CGS, meaning that both processes can produce equally

wear resistant WC-25Co coatings; there was an improvement of approximately 62% during rubber-wheel abrasive testing for WC–17Co coatings and approximately 130% for WC–12Co coatings. CGS showed better results and did not form strange brittle phases during the process;

19. CGS WC-25Co coatings showed 5 times higher friction wear resistance and a gain of 71% in fracture toughness when compared to HVOF coatings; CGS coatings showed higher coefficient of friction than those produced by HVOF. WC–17Co coatings and WC–12Co coatings showed approximately 34% and 15% higher friction coefficient than HVOF coatings;

20. CGS coatings lost less volume than HVOF coatings and WC–12Co showed a higher wear resistance than WC–17 and 25Co coatings due to the higher content in hard WC phase. WC-25Co coatings by CGS lost 4 times less volume than HVOF ones, WC–17Co coatings by CGS lost 2.5 times less volume and WC–12Co 2.4 times less;

21. CGS produced compact and non-degraded coatings with less porosity than HVOF and therefore a slight enhancement of the coatings electrochemical resistance (≈15% E_{oc} reduction); there was ≈37% E_{oc} reduction on CGS WC–17Co coatings and ≈8% E_{oc} on WC–12Co coatings when compared to HVOF ones; CGS coatings' intensity of corrosion were also lower than those of HVOF coatings with a reduction of approximately 13, 21 and 58% for WC-25/17 and 12Co coatings, respectively; all CGS coatings showed an improvement of about 380% under salt fog spray testing conditions when compared to a WC-12Co HVOF coating;

22. It was shown trough this Thesis that Cold Spray Gas technology can clearly compete in terms of mechanical and electrochemical behaviour with conventional deposition techniques to spray the studied WC-Co powders.

9 FUTURE TRENDS

In the end of this Thesis several conclusions were drawn not only in terms of optimization and characterization of coatings and their properties but also in terms of their future development. It is clear that novel Cold Gas Spray is a promising technology for producing wear and corrosion resistance coatings without compromising the feedstock powders original microstructure, providing them an added advantage compared to conventional thermal spraying techniques; and as a novel technology there are still some problems related to cost-efficiency that should be solved before making it a wide used process in industry, namely, deposition efficiency.

Even though the deposition efficiency of the process is still lower than HVOF's there are some industries that are already producing their engineering parts using this technology as seen in Figure 42 where a after coating and after coating and machining piston sleeve is depicted. This means that when a top end application with top end properties is needed, CGS is the preferable technique to be used due to the better properties that the coatings' exhibit under work.

Figure 42. Specific automotive parts before (left) and after (right) coating by CGS; and after machining (down).

Next moves for this line of research should focus on:

- Increase of the deposition efficiency of the process by trying out new spraying conditions and equipments, as well as focusing on some of the trials presented in chapter 7 for an improvement of the efficiency;

- Production of nanostructured feedstock powders since CGS process does not use any temperature to melt the particles and therefore the original nano sized grains can be kept and the coatings' properties even more enhanced;

- Carry on the testing of the coatings' fracture toughness and compare them with HVOF WC-Co coatings;

- New mechanical tests such as four point bending, high temperature corrosion and fatigue tests;

- Nanoindentation of the powder particles and sprayed coatings should also be studied for a better understanding of the coatings' nanohardness and young modulus, where both low contact loads and high spatial precision can be advantageous;

- Optimization of spraying parameters and production of different types of carbides for specific applications, such as TiC, WC-Co-Cr, SiC;

- Selling and transferring the registered and protected know-how enclosed in Trade Secret 1 for the production of WC-Co cermets by Cold Gas Spray.

10 REFERENCES

10.1 Specific references

[1] D., W. (2007). *Materials science and engineering: an introduction*. Wiley.

[2] E., R, & J., R. (1999). *Modern physical metallurgy and materials engineering: science, process, applications*.

[3] Society, A, & International, A. (1992). *Metals Handbook Volume 2 – Properties and Selection: Nonferrous Alloys and Special-Purpose Materials.*

[4] Society, A, & International, A. (1998). *Metals handbook: desk edition*.

[5] Lassner, E, & Schubert, W. (1999). *Tungsten: properties, chemistry, technology of the element, alloys, and chemical compounds*. Springer Us.

[6] McCandlish, L.E., Kevorkian, V., Jia, K., & Fischer, T.E. (1994). *Nanostructured WC-Co composite powders* . Proceedings of the International conference and exhibition on powder metallurgy and particulate materials (pp. 329-337). Toronto, Ontario; Canada.

[7] Yandouzi, M., Sansoucy, E., Richer, P., Jodoin, B., & Ajdelsztajn, L. (2007). *Deposition and characterization of WC–Co coatings prepared by continuous- and pulsed-cold spray processes*. Proceedings of the The international thermal spray conference Beijing, China: ASM International(OH).

[8] B.H Kear, G Skandan, R.K Sadangi, *Factors controlling decarburization in HVOF sprayed nano-WC/Co hardcoating*, Scripta Materialia, 44 (2001), 1703-1707

[9] Guilemany, J.M., Dosta, S., Nin, J., & Miguel, J.R. (2005). *Study of the properties of wc-co nanostructured coatings sprayed by high-velocity oxyfuel*. JOURNAL OF THERMAL SPRAY TECHNOLOGY, 14(3), 405-413.

[10] Guilemany, J.M., Dosta, S., Miguel, J.R., *The enhancement of the properties of WC-Co HVOF coatings through the use of nanostructured and microstructured feedstock powders*, Surface & Coatings Technology, 2006, 201, 1180 - 1190

[11] Davis, J.R., & International., A. (2004). *Handbook of thermal spray technology*. Asm Intl.

[12] Framroze, R. (2001). *Handbook of hard coatings: deposition technologies, properties and applications*. William Andrew Publishing.

[13] Image obtained on 15th of July 2014 from http://www.bodycotemetallurgicalcoatings.com/technologies/plasma-spraying.aspx

[14] HVAF, High Velocity Air-Fuel, *Process Overview*, http://www.hvaf.com/, accessed on 2nd of September 2014

[15] I. A. Gorlach (2008), *The application of high velocity air fuel process for the deposition coatings*, R&D Journal, 24 (3)

[16] Champagne, V.K. (2007). *The cold spray materials deposition process: fundamentals and applications*. CRC.

[17] Converging-Diverging Nozzle, accessed on the 1st of July 2014, http://www.engapplets.vt.edu/fluids/CDnozzle/cdinfo.html

[18] Kim, H., Lee, C., & Hwang, S. (2005). *Superhard nano WC–12%Co coating by cold spray deposition*. Materials Science and Engineering A, 391(1-2), 243-248.

[19] Image obtained on the 11th of July 2014, http://en.wikipedia.org/wiki/De_Laval_nozzle.

[20] Klinkov, S.V., & Kosarev, V.F. (2006). *Measurements of cold spray deposition efficiency*. JOURNAL OF THERMAL SPRAY TECHNOLOGY, 15(3), 364-371

[21] Li, W., Zhang, C., Guo, X., Zhang, G., & Li, C. (2008). *Effect of standoff distance on coating deposition characteristics in cold spraying*. Materials & Design, 29(2), 297-304.

[22] Raletz, F., Vardelle, M., & Ezo'o, G. (2006). *Critical particle velocity under cold spray conditions*. Surface and Coatings Technology, 201(5), 1942-1947.

[23] Stoltenhoff, T., Kreye, H., & Richter, H.J. (2001). *An analysis of the cold spray process and its coatings*. JOURNAL OF THERMAL SPRAY TECHNOLOGY, 11(4), 542-550.

[24] Schmidt, T., Assadi, H., Gärtner, F., Richter, H., & Stoltenhoff, T.A. (2009). *From particle acceleration to impact and bonding in cold spraying*. JOURNAL OF THERMAL SPRAY TECHNOLOGY, 18(5-6), 794-808.

[25] Li, C., Li, W., & Liao, H. (2006). *Examination of the critical velocity for deposition of particles in cold spraying*. JOURNAL OF THERMAL SPRAY TECHNOLOGY, 15(2), 212-222.

[26] Schmidt, T., Gärtner, F., & Assadi, H. (2006). *Development of a generalized parameter window for cold spray deposition*. Acta Materialia, 54, 729–742.

[27] Jodoin, B., Ajdelsztajn, L., Sansoucy, E., Zúñiga, A., & Richer, P. (2006). *Effect of particle size, morphology, and hardness on cold gas dynamic sprayed aluminum alloy coatings*. Surface and Coatings Technology, 201(6), 3422-3429.

[28] Gilmore, D.L., Dykhuizen, R.C., Neiser, R.A., Smith, M.F., & Roemer, T.J. (1999). *Particle velocity and deposition efficiency in the cold spray process*. JOURNAL OF THERMAL SPRAY TECHNOLOGY, 8(4), 576-582.

[29] Li, Y., Li, W., Wang, Y., & Fukanuma, H. (2003). *Effect of spray angle on deposition characteristics in cold spraying*. Proceedings of the Thermal spray 2003: advancing the science and applying the technology Ohio, USA: ASM International(OH).

[30] Pattison, J., Celotto, S., Khan, A., & O'Neill, W. (2008). *Standoff distance and bow shock phenomena in the cold spray process*. Surface and Coatings Technology, 202(8), 1443-1454.

[31] Richer, P., Jodoin, B., Taylor, K., Sansoucy, E., & Johnson, M. (2005). *Effect of particle geometry and substrate preparation in cold spray*. Proceedings of the Thermal spray connects: explore its surfacing potential! Basel, Switzerland: ASM International.

[32] Klinkov, S.V. , Kosarev, V.F., & Rein, M. (2005). *Cold spray deposition: significance of particle impact phenomena*. Aerospace Science and Technology, 9(7), 582-591.

[33] Assadi, H., Gartner, F., Stoltenhoff, T., & Kreye, H. (2003). *Bonding mechanism in cold gas spraying*. Acta Materialia, 51, 4379–4394.

[34] Wright, T. (2002). *The physics and mathematics of adiabatic shear bands.* Cambridge Univ Pr.

[35] Hussain, T., McCartney, D.G., Shipway, P.H., & Zhang, D. (2008). *Bonding mechanisms in cold spraying: the contributions of metallurgical and mechanical components*. JOURNAL OF THERMAL SPRAY TECHNOLOGY, 18(3), 364-379.

[36] N. Cinca, J.M. Rebled, S. Estradé, F. Peiró, J. Fernández, J.M. Guilemany, *Influence of the particle morphology on the Cold Gas Spray deposition behaviour of titanium on aluminum light alloys*, Journal of Alloys and Compounds, 554 (2013), 89-96

[37] M., Douglas. (2005). *Diseño y análisis de experimentos*. Editorial Limusa S.A. De C.V.

[38] R. E., Kirk (1994), *Experimental designs*, Wadsworth Publishing

[39] H. Wang, X. Chen, X. Bai, G. Ji, Z. Dong, D. Yi, *Microstructure and properties of cold-sprayed multimodal WC-17Co deposits*, International Journal of Refractory Metals and Hard Metals, 45 (2014), 196-203

[40] P. Gao, C. Li, G. Yang, Y. Li, C. Li, *Influence of substrate hardness on deposition behaviour of single porous WC-12Co particle in cold spraying*, Surface and Coatings Technology, 203, 3-4 (2008), 384-390

[41] A. Ang, C. Berndt, P. Cheang, *Deposition effects of WC particle size on cold-sprayed WC-Co coatings*, Surface and Coatings Technology, 205, 10 (2014), 3260-3267

10.2 General references

Paper 1: References from [1] to [20]

Paper 2: References from [1] to [18]

Paper 3: References from [1] to [16]

Paper 4: References from [1] to [12]

11 RESUMEN

Deposición de *cermets* de WC-Co por Proyección Fria

11.1 Consideraciones iniciales

En primer lugar, el objetivo principal de este trabajo de investigación fue proporcionar un nuevo método de deposición para depositar *cermets* de WC-Co. Esta nueva tecnología proporcionó nuevos recubrimientos sin ninguna descomposición de la microestructura del polvo inicial y por lo tanto la mejora de las presentes aplicaciones de WC-Co en la gran industria.

La deposición de *cermets* de WC-Co resistentes al desgaste ha sido siempre una de las principales aplicaciones de las técnicas de proyección térmica convencionales como por ejemplo *High Velocity Oxy-Fuel* (HVOF). Las demandas de la industria en términos de producción y la necesidad y constante búsqueda de mejores propiedades mecánicas y electroquímicas conducen al objetivo principal y la motivación de esta tesis: la producción de nuevos y mejores recubrimientos de WC-Co sobre varios sustratos utilizando una técnica de deposición nueva, *Cold Gas Spraying* (CGS).

El hecho de que antes de la publicación del primer artículo que nació de este trabajo de investigación no se había depositado previamente con éxito este tipo de materiales por CGS fue también uno de los principales puntos de motivación. Por esta razón, el lector encontrará, en la integridad del documento, los trabajos de investigación que fueron publicados durante estos años de programa de doctorado y cumplen los objetivos principales de esta tesis titulada "Deposición de *cermets* de WC-Co por Proyección Fría".

11.2 Objetivos de la tesis

El objetivo principal de esta tesis fue producir con éxito *cermets* de WC-25, 17 y 12Co sobre dos sustratos diferentes usando la tecnología de *Cold Gas Spraying* utilizando nitrógeno como gas de proceso y comparar sus propiedades mecánicas, tribológicas y electroquímicas con los mismos *cermets* producidos por HVOF. Un objetivo secundario era aumentar sus propiedades utilizando la novedosa técnica de CGS y, por lo tanto, aplicar los conocimientos a las aplicaciones de la vida real, sobre todo en piezas resistentes al desgaste y la corrosión para ayudar a aumentar su vida en trabajo. El tercer objetivo era generar suficiente conocimiento y

transferirlo a la industria. Para lograr estos objetivos, se alcanzaron los siguientes puntos clave:

- Comprender el estado del arte de los revestimientos de WC-Co obtenidos por *Cold Gas Spray* y *High Velocity Oxy-Fuel*, ventajas y limitaciones de los procesos, y determinar nuevas oportunidades para la producción de recubrimientos de WC-Co por *CGS*;

- Estudio de los mecanismos de adherencia de las partículas de WC-Co de *cermets*, con diferentes contenidos en la matriz dúctil, en diferentes tipos de sustratos a fin de lograr recubrimientos de buena calidad;

- Producir recubrimientos de WC-Co por CGS y estudiar su microestructura antes y después de la deposición;

- Optimizar las condiciones de proyección por CGS condiciones para todos los polvos de WC-Co;

- Medir las propiedades mecánicas y electroquímicas de los recubrimientos de CGS obtenidos;

- Producir recubrimientos de WC-Co por HVOF utilizando los mismos polvos que en CGS;

- Medir y comparar propiedades mecánicas y electroquímicas por HVOF y CGS;

- Mejorar las propiedades de los recubrimientos de CGS en comparación con HVOF;

- Transferencia de las condiciones óptimas de proyección de CGS para los polvos de WC-25, 17 y 12Co sobre sustratos de acero de bajo carbono y Al7075-T6;

- Ensayos de los recubrimientos obtenidos en aplicaciones de la industria para mejorar el desgaste y la resistencia a la corrosión.

11.3 Introducción

A medida que los requisitos para las aplicaciones de ingeniería se hacen más exigentes, la demanda de mejores propiedades también se incrementan para los recubrimientos compuestos. Estos recubrimientos protegen el sustrato para retener sus propiedades mecánicas al tiempo que aumenta la resistencia al desgaste y la corrosión. En esta Tesis se prestó especial atención a los recubrimientos obtenidos en acero de bajo carbono y una aleación de aluminio, Al7075-T6.

11.4 Deposición de *cermets* de WC-Co

Metales duros, o carburos cementados, son un grupo de materiales compuestos duros, muy resistentes al desgaste y a la degradación, en el que partículas de carburo duro se encuentran "cementados" por una matriz dúctil a través de la sinterización en fase líquida. Estas propiedades del compuesto se logran combinando tanto la dureza y plasticidad de la matriz de Co metálico y la alta dureza y resistencia del carburo de WC. En materia de consumo y aplicabilidad el grupo WC-Co es considerado como el *cermet* más importante, representando con un presupuesto de más de 80% en aplicaciones de corte y resistencia al desgaste, especialmente para la industria de la maquinaria pesada. Estas aplicaciones para herramientas de corte y aplicaciones de resistencia al desgaste surgen debido a su combinación única de propiedades mecánicas, físicas y químicas.

Los carburos de tungsteno son comercialmente uno de los productos de polvo-metalurgia más antiguos y exitosos y los recubrimientos de WC han sido ampliamente utilizados por su excepcional dureza, resistencia al desgaste y erosión y resistencia a la corrosión. Matrices de metales dúctiles, tales como cobalto, mejoran considerablemente su tenacidad así que la fractura por fragilidad se puede evitar, y aún más, permite la sinterización a temperaturas razonables. Los *cermets* de WC-Co son los materiales de recubrimiento resistentes al desgaste más importantes que se emplean hoy en día para las técnicas de deposición. Su alta resistencia (dos a tres veces mayor que la de acero), una excelente conductividad térmica, baja expansión térmica, y una excelente adhesión, hacen de este el material de recubrimiento ideal.

Además, estas propiedades pueden ser controladas por la composición y microestructura, con el fin de mejorar ciertas propiedades para aplicaciones específicas. Por ejemplo, la dureza del *cermet* disminuirá con la disminución del contenido en Co y el aumento de tamaño de partículas de WC, con una pérdida asociada de resistencia a la rotura y la tenacidad a la fractura.

Al utilizar estos polvos por técnicas de proyección térmica convencionales hay algunos efectos de descarburación y oxidación no deseados debido a las altas temperaturas de la llama.

11.5 Técnicas de deposición de proyección térmica

En la actualidad existen tres principales técnicas de deposición de WC-Co: *Plasma Spraying*, HVOF y CGS. Limitaciones asociadas con la formación de fases frágiles, más la descarburación observada cuando se calienta a altas temperaturas fueron el principal precursor en la búsqueda y desarrollo de nuevos y más eficientes procesos de deposición, tales como el *Cold Gas Spraying*.

11.6 Técnicas de proyección térmica

El proceso de *Cold Gas Spraying* como una tecnología de deposición fue desarrollado por un grupo de científicos rusos de la Academia de Ciencias de Rusia a mediados de los años 80. Este grupo, dirigido por el profesor Anatolii Papyrin,

podía depositar una amplia variedad de materiales, tales como metales puros, aleaciones metálicas, polímeros y materiales compuestos sobre distintos tipos de sustratos obteniendo tasas de deposición muy altas utilizando este novedoso proceso de deposición. A través del estudio de los modelos sometidos a un flujo supersónico de dos fases (gas + partículas) en un túnel de viento se verificó que sería posible depositar una amplia gama de materiales sobre diversos sustratos sin el uso de la temperatura para fundir y depositar el material de proyección, como se suele hacer en los procesos de proyección térmica más comunes.

A diferencia de las técnicas de deposición convencionales, que requieren tanto energía cinética (velocidad de las partículas) como energía térmica (temperatura) con el fin de promover la formación de un recubrimiento sobre un sustrato, el proceso de *Cold Gas Spraying* utiliza simplemente la energía cinética de las partículas de polvo para la formación del dicho recubrimiento. La energía cinética de las partículas que inciden es suficiente para producir deformación plástica y altas presiones y temperaturas interfaciales. Esto significa que es, casi por completo, un proceso en el estado sólido. Además, debido a ser un proceso de baja temperatura, es decir, no utiliza energía térmica, produce recubrimientos menos porosos, con menos oxidación y mayor dureza.

En el proceso de *Cold Gas Spraying* es necesario producir una corriente de alta velocidad del gas con el fin de dar a las partículas de polvo suficiente energía cinética para permitir la deposición sobre el sustrato. Las partículas de polvo de metal que varían en tamaño de partícula de 5 a 50 micras son alimentadas centralmente, por una corriente de gas separada, en una cámara convergente-divergente de *de Laval* donde un gas precalentado (normalmente aire, helio, nitrógeno, o una mezcla, en función del material de deposición y temperatura del gas) en el intervalo de 300-800ºC es comprimido y se expandirá hasta la velocidad supersónica mientras que ocurre una disminución de la presión y la temperatura.

11.7 Ventajas

Como la tecnología de *Cold Gas Spraying* es un proceso en estado sólido y no requiere altas temperaturas para promover la adhesión entre el recubrimiento y el material de sustrato se proporcionan un gran número de ventajas asociadas con

este proceso en comparación con los procesos convencionales de proyección térmica. Esta es una ventaja muy importante si se desea una porosidad baja y bajo contenido en óxido en el recubrimiento. Estas son dos de las mayores ventajas cuando se producen recubrimientos con CGS: baja porosidad y bajo contenido en óxidos. La baja porosidad resultado del hecho de que el CGS es, como se dijo antes, un proceso en estado sólido así que no hay partículas de polvo que se funden sobre el sustrato además de haber un efecto de *peening* resultante del impacto de las partículas presentes en el flujo de alta velocidad que tienden a cerrar los pequeños poros y vacíos en el material de recubrimiento subyacente que también dará lugar a una densidad muy alta. Como se procesa a bajas temperaturas, las reacciones de los metales con el oxígeno son reducidas o eliminadas en gran medida. Además, como estos dos "defectos" se reducen habrá una mejora de las propiedades mecánicas, eléctricas y térmicas.

En CGS, la composición de la fase, el cristal (tamaño de grano) y la estructura de la materia prima en polvo se conservan en el recubrimiento final; esto significa que se retienen las propiedades del material inicial y en el producto final se muestran las mismas propiedades como las que se demuestran en el polvo del material a proyectar. La baja temperatura es una vez más el principal precursor de estas ventajas porque evita la vaporización de los elementos más volátiles en el proceso de deposición, también los procesos de fusión y de solidificación son inhibidos por lo que la composición de la fase y de la estructura del cristal permanecen inalterados. Esto puede ser una ventaja increíble si alguien desea trabajar con polvos nanocristalinos ya que sus propiedades únicas no se cambiarán por el crecimiento del grano causado por la energía térmica.

La alta densidad, la pureza de fase y microestructura homogénea también promueven las características de corrosión excepcionales.

Dado que las partículas durante el proceso de CGS frío se depositan a temperaturas relativamente bajas hay poco cambio dimensional (contracción térmica). Añadiendo el efecto de *peening* a esto resulta que los recubrimientos de CGS se encuentren típicamente en un estado de tensión residual de compresión que evitará el agrietamiento y separación de recubrimiento. Esto también puede ser una ventaja para producir recubrimientos con mayor espesor. Este proceso también produce una muy alta adhesión de los recubrimientos sobre muchos tipos

de sustratos (metales, aleaciones, compuestos, etc), permitiendo trabajar con materiales altamente disímiles debido a que en CGS el material de recubrimiento no se calienta ni funde y la formación de las interfaces débiles se evita. Además, en este proceso, hay un *input* térmico mínimo para el sustrato (recibido por la entalpía de las partículas que impactan), lo que permite también trabajar sobre sustratos hechos de materiales sensibles a la temperatura.

También es posible depositar materiales de recubrimiento en áreas muy localizadas sin la necesidad de operaciones de enmascaramiento costosas. Además, este proceso tiene una tasa de deposición elevada debido a su haz de proyección estrecho y bien definido.

Teniendo en cuenta todas las ventajas anteriores y las tasas de deposición del polvo altas también se espera que los altos valores de eficiencia de deposición (DE) sean elevados para la mayoría de los materiales.

La ausencia de chorros de gas de alta temperatura, la radiación y gases explosivos aumenta la seguridad operacional.

11.8 Limitaciones

El proceso de CGS, a diferencia de los procesos de proyección térmica tradicionales, se limita esencialmente a materiales que presentan una buena ductilidad para producir enlaces de calidad entre el recubrimiento y el material de sustrato. El hecho de que es un proceso de estado sólido y las partículas de polvo no se funden antes del impacto, haz con que estos últimos deban tener al menos una ductilidad limitada a fin de deformar plásticamente y crear unión entre las partículas y el material subyacente. Al mismo tiempo, el material del sustrato debe ser lo suficientemente duro para permitir que las partículas dúctiles se deformen el momento del impacto. Así, en CGS, materiales más duros y más frágiles no se pueden utilizar como material de revestimiento, así como materiales más blandos que no pueden ser utilizados como sustratos; aunque esto es muy limitativo, compuestos que tienen una matriz dúctil, tales como WC-Co se pueden depositar. Además, esta extensa deformación plástica sufrida por las partículas que inciden sobre el sustrato proporcionará un efecto de endurecimiento en el revestimiento. Para algunas aplicaciones puede ser un problema mientras que en otras, tales como en componentes para resistencia al desgaste, puede ser una ventaja.

Otro inconveniente del proceso de *Cold Gas Spraying* es que consume mucho más gas de proceso que las técnicas de deposición térmicos tradicionales, en el orden de 1-2m^3/min. Si a esto le sumamos que algunos materiales de deposición tales como el titanio, que tienen alta velocidad crítica de partículas individuales, requieren el uso de gases muy caros (He) para alcanzar la velocidad de impacto y el recubrimiento de la calidad necesaria, entonces puede convertirse en un proceso costoso y convertirse en un gran inconveniente. Una solución podría estar en utilizar temperaturas de precalentamiento más altas (~800ºC) del nitrógeno con el fin de lograr velocidades del chorro superiores, y por lo tanto, proporcionar la velocidad mínima necesaria para los materiales de deposición que requieren mayores valores de velocidad crítica.

Como esta tecnología produce un haz muy fino y bien definido hace que el proceso no sea adecuado para recubrir superficies muy grandes. Al igual que en otros procesos la pulverización de formas complejas y superficies internas es algo difícil sin el uso de una amplia planificación y programación del robot.

11.9 Mecanismo de adherencia

En el proceso de CGS, la unión del recubrimiento al sustrato se produce cuando la velocidad de impacto de las partículas de polvo es igual o superior a su valor crítico de velocidad, pasando por una deformación localizada e inestabilidad de cizalla adiabática al mismo tiempo. La adhesión de las partículas al sustrato en este proceso se debe únicamente a su energía cinética en caso de impacto a pesar de que el mecanismo real por el cual las partículas sólidas se deforma durante el proceso todavía no está bien entendido. Durante la deposición en frío hay dos etapas muy diferentes. Durante la etapa inicial, una película delgada de material de partículas (monocapa) se deposita sobre el sustrato. Esta etapa se caracteriza por una interacción directa de las partículas con el sustrato y depende en gran medida del grado de preparación de la superficie y de las propiedades del material del sustrato. La etapa inicial incluye el tiempo de activación de la superficie, es decir, el tiempo de incubación, durante el cual puede ocurrir erosión en lugar de deposición. En la segunda etapa de una capa de revestimiento de espesor finito se

produce. En esta etapa las partículas interactúan con una superficie formada por las propias partículas.

Se sabe que el sustrato o el material depositado (dependiendo si ya se ha depositado una capa de material de recubrimiento), y las partículas de polvo se someten a una extensa deformación localizada durante el impacto, por lo tanto hay que proporcionar las condiciones necesarias para que la partícula / sustrato y partículas / material de unión depositado, por medio de una superficie de contacto limpia y presiones altas.

11.10 Procedimiento experimental

Cold Gas Spraying y *High Velocity Oxy-Fuel* se utilizaron como principales tecnologías para producir los recubrimientos mostrados en esta Tesis.

El equipo de CGS utilizado fue un Kinetics® 4000 (Cold Gas Technology, Ampfing, Alemania), con una presión máxima de servicio de 40 bar, temperatura de 800 °C y se utilizó nitrógeno como gas de proceso. Además, la Kinetics® 4000 tiene la posibilidad de utilizar una pre-cámara de 120 mm de longitud conectado a la boquilla de la pistola, donde los polvos se calientan durante un tiempo más largo. El equipo utilizado de HVOF es un Sulzer (Winterthur, Suiza) DJH con dos cabezas diferentes: DJH 2700 de propileno y DJH 2600 para el hidrógeno.

Como se explicó anteriormente, CGS es un proceso que se ve afectado por varios parámetros. Durante esta Tesis y después de estudiarlos, la presión del gas y la distancia fueron elegidas como los principales parámetros variables. Por este motivo se realizó un diseño factorial de experimentos para cada uno de los tres polvos estudiado diferentes, a fin de optimizar las condiciones de proyección.

Un diseño experimental es un plan de asignación de unidades experimentales a niveles de tratamiento y el análisis estadístico asociado con el plan. Identifica las variables independientes y dependientes del proceso estudiado y nos dice la forma en que la asignación al azar y los aspectos estadísticos de un experimento deben ser llevadas a cabo; el objetivo principal de un diseño experimental consiste en

establecer conexiones causales entre las variables independientes y dependientes y extraer la máxima información con el mínimo gasto de recursos. En el diseño experimental hay tres tipos de variables:

- Factor controlable: este factor puede ser manipulado y su manejo afectará a la variable de respuesta. Su manejo ayuda a sacar conclusiones;

- Factor incontrolable: este factor no puede ser manipulado y puede afectar a la variable de respuesta por lo que uno tiene que predecir su influencia en esto;

- Variable de respuesta: tanto los factores controlables e incontrolables actúan sobre esta variable que se utiliza para sacar conclusiones y, por tanto, la variable principal para estudiar.

Estas variables y factores pueden ser dependientes o independientes con el fin de inter-relacionarse entre ellos y eliminar algunos de los parámetros del proceso estudiado.

El diseño factorial es un tipo de diseño experimental en la que el experimento tendrá dos o más factores para ser estudiados a dos o más niveles, de modo que esto significa que, esas unidades experimentales toman todas las posibles combinaciones de estos niveles a través de todos estos factores. La mayoría de los experimentos factoriales cada factor tiene sólo dos niveles.

Teniendo en cuenta todos los diferentes parámetros del proceso mediante la recopilación y el análisis de datos experimentales para mejorar el rendimiento del proceso de proyección, una tabla de datos estructurada que contiene datos sustancialmente importantes acerca de las interacciones estructuradas fue generada para permitir una mayor comprensión del proceso a partir de un menor número de experimentos. Una vez definidos los parámetros fijos y variables, se seleccionaron un total de 3 niveles para cada factor (parámetro variable). El diseño

fue compuesto por de tres niveles (bajo, medio y alto) de cada uno de dos factores. Esto significa que hubo un total de $3^2 = 9$ posibles combinaciones de tratamiento. Valores de distancia variaron de 10 a 40 mm y la presión de gas de 30 a 40 bar.

11.11 Discusión general

En el principio de esta tesis un estudio teórico profundo se hizo para comprender:

- La aplicación de los *cermets* de WC-Co en la industria pesada (automoción, aeronáutica, naval, minería, petróleo y perforación, etc);

- ¿Qué tecnologías de proyección térmica se utilizan para obtener recubrimientos de WC-Co?;

- Las ventajas / limitaciones de los procesos de HVOF y CGS y tendencia futura;

- Parámetros del proceso de CGS y mecanismo de unión para permitir una optimización de los parámetros de proyección.

La producción de recubrimientos de WC-25Co como el primer objetivo de esta Tesis implicaba un esfuerzo adicional en la comprensión del proceso de CGS y sus parámetros. En primer lugar, después de que el diseño inicial de un pre-experimento fue diseñado para el polvo de WC-25Co sobre ambos sustratos (acero de bajo carbono y Al7075-T6), una serie de recubrimientos mostró mala adhesión a los sustratos, la delaminación de las pocas capas que habían sido depositadas e incluso la rotura del mismo recubrimiento al realizar pruebas de microdureza. La optimización de las condiciones de proyección dio lugar a lo que se deseaba en primer lugar: recubrimientos sobre acero bajo en carbono y Al7075-T6 con una excelente adhesión a los sustratos (74 ± 6 MPa y 60 ± 5 MPa, respectivamente), sin delaminación entre las capas, uniformidad, sin porosidad y altos espesores. Añadido a esto, una microestructura inalterada en los recubrimientos finales - que representa una de las ventajas del proceso de CGS - también se evidenció.

Fue la primera vez que tal *cermet* se producía utilizando nitrógeno como gas de proceso en CGS. Automáticamente el coste del proceso se redujo ya que el nitrógeno es un gas más barato que el helio o cualquier otra mezcla. Esto se debió a una comprensión extensa, investigación y optimización de las condiciones de proyección que permitían alcanzar la velocidad crítica necesaria, temperaturas y presiones de gas, para que las partículas se deformen plásticamente y se unan a los sustratos. La distancia de proyección era también un parámetro crítico que necesitó ser optimizado y los valores óptimos fueron elegidos entre una amplia gama de distancias pre-experimentadas.

Estos hallazgos permitieron reproducir una serie de revestimientos con el fin de realizar diferentes ensayos mecánicos (micro-dureza y adhesión), tribológicos (resistencia a la abrasión y adhesión) y electroquímicos (corrosión y la resistencia de niebla salina) en ellos. Todos los resultados obtenidos se compararon con los que están disponibles en la bibliografía para HVOF en el momento. Los *cermets* de WC-12Co son los que más se utilizan en aplicaciones industriales debido a su alta resistencia al desgaste y dureza. En este trabajo se realizó una comparación entre los recubrimientos de WC-25Co por CGS y recubrimientos de WC-12Co por HVOF, por lo tanto con menor contenido en partículas de carburo duro y una resistencia al desgaste y dureza teóricamente inferior pero al tiempo una mayor resistencia a la fractura y resistencia a la erosión. Los recubrimientos de CGS presentan una dureza inferior, como se esperaba, pero cuando se trata de la resistencia al desgaste la diferencia no fue tan alta como se esperaba. Esto se debió a una buena distribución de las partículas duras WC en la matriz dúctil, la dispersión homogénea y el tamaño sub-micrométrico de las partículas de carburo y el hecho de que no hay fases frágiles. Además, en CGS hay un efecto de compresión de las partículas que inciden sobre las primeras capas depositadas de material de recubrimiento durante la pulverización. Este efecto produce recubrimientos menos porosos, y por lo tanto, un menor número de caminos para el electrolito penetrar y llegar al sustrato, que las observadas en las técnicas de proyección térmica convencionales, tales como HVOF. Esto proporciona a los recubrimientos de CGS una excelente resistencia a la corrosión y a la niebla salina.

Cuando se obtuvieron los primeros resultados muy motivadores después de proyectar y medir las propiedades de los recubrimientos de WC-25Co apuntan en

una dirección que, en teoría, con una reducción de la matriz de cobalto se podría obtener valores de dureza y resistencia al desgaste más altos utilizando CGS en lugar de HVOF. Sin embargo, esto trajo dos problemas:

- la dificultad adicional de la producción de cermets de WC-17 y 12Co que tenían menor plasticidad y, por tanto, menor posibilidades de obtener una capa suficientemente espesa y densa para usar como aplicación;

- producir efectivamente recubrimientos con un contenido de 12Co con mejores propiedades tribológicas que las presentadas en el estado de arte de los recubrimientos de WC-12Co por HVOF.